

AD736984

Office of Naval Research  
Contract N00014-67-A-0200-0005 NR-371-010

Microwave Physics Branch  
Ballistic Research Laboratories  
U.S. Army Aberdeen Proving Ground

**THE PROXIMITY EFFECT IN SYSTEMS OF  
PARALLEL CONDUCTORS AND ELECTRICALLY  
SMALL MULTITURN LOOP ANTENNAS**

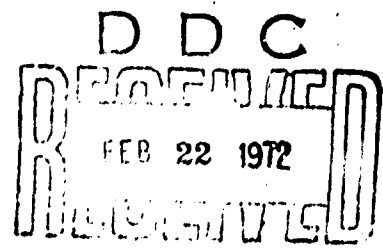


By  
Glenn Smith

December 1971

Technical Report No. 624

Reproduced by  
NATIONAL TECHNICAL  
INFORMATION SERVICE  
Springfield, Va 22151



This document has been approved for public  
release and sale; its distribution is unlimited.

Division of Engineering and Applied Physics  
Harvard University - Cambridge, Massachusetts

Unclassified

Security Classification

DOCUMENT CONTROL DATA - R & D

Security classification of title, body of abstract and indexing annotation must be entered when the overall report is classified

1. ORIGINATING ACTIVITY (Corporate author)

2a. REPORT SECURITY CLASSIFICATION

Division of Engineering and Applied Physics  
Harvard University  
Cambridge, Massachusetts 02138

2b. GROUP

3. REPORT TITLE

THE PROXIMITY EFFECT IN SYSTEMS OF PARALLEL CONDUCTORS AND ELECTRICALLY SMALL MULTITURN LOOP ANTENNAS

4. DESCRIPTIVE NOTES (Type of report and inclusive dates)

Interim technical report

5. AUTHOR(S) (First name, middle initial, last name)

Glenn Smith

6. REPORT DATE

December 1971

7a. TOTAL NO. OF PAGES

116

7b. NO. OF REFS

38

8a. CONTRACT OR GRANT NO

N00014-67-A-0298-0005

8b. PROJECT NO.

9a. ORIGINATOR'S REPORT NUMBER(S)

624

9b. OTHER REPORT NO(S) (Any other numbers that may be assigned this report)

10. DISTRIBUTION STATEMENT

This document has been approved for public release and sale; its distribution is unlimited.

11. SUPPLEMENTARY NOTES

12. SPONSORING MILITARY ACTIVITY

"Joint Services Electronics Program through (Adm. Service - Office of Naval Research, Air Force Office of Scientific Research or U. S. Army Elect. Command)"

13. ABSTRACT

In this report losses in systems of parallel sound conductors are studied. Both the normal skin effect loss and the additional loss due to the close proximity of adjacent conductors are considered. The results obtained for the parallel conductors are used to evaluate the radiation efficiency of electrically small multi-turn loop antennas.

Office of Naval Research

Contract N00014-67-A-0298-0005 NR-371-016

Microwave Physics Branch  
Ballistic Research Laboratories  
U. S. Army Aberdeen Proving Ground

THE PROXIMITY EFFECT IN SYSTEMS OF  
PARALLEL CONDUCTORS AND ELECTRICALLY  
SMALL MULTITURN LOOP ANTENNAS

By

Glenn Smith

Technical Report No. 624

This document has been approved for public  
release and sale; its distribution is unlimited

December 1971

The research reported in this document was made possible through support extended the Division of Engineering and Applied Physics, Harvard University by the U. S. Army Research Office, the U. S. Air Force Office of Scientific Research and the U. S. Office of Naval Research under the Joint Services Electronics Program by Contracts N00014-67-A-0298-0006, 0005, and 0008.

Division of Engineering and Applied Physics  
Harvard University · Cambridge, Massachusetts

**THE PROXIMITY EFFECT IN SYSTEMS OF  
PARALLEL CONDUCTORS AND ELECTRICALLY  
SMALL MULTITURN LOOP ANTENNAS**

**By**

**Glenn Smith**

**Division of Engineering and Applied Physics  
Harvard University · Cambridge, Massachusetts**

**ABSTRACT**

**In this report losses in systems of parallel round conductors are studied. Both the normal skin effect loss and the additional loss due to the close proximity of adjacent conductors are considered. The results obtained for the parallel conductors are used to evaluate the radiation efficiency of electrically small multiturn loop antennas.**

**SECTION I**  
**ANALYSIS OF SYSTEMS OF PARALLEL**  
**ROUND CONDUCTORS**

**1. Introduction**

In a system of parallel conductors the distribution of current over the conductor cross section is determined by two effects--the normal skin effect and a proximity effect. Both are the result of the same phenomenon, eddy currents in the conductors. The former is usually considered to be the result of the net current in a single conductor while the latter is due to the currents in neighboring conductors. For close conductor spacings, the distribution of current due to the proximity effect can cause an increase in the ohmic resistance which is larger than the skin effect resistance alone, i. e. larger than the ohmic resistance of the isolated conductors.

The skin effect in round conductors is discussed in most texts on electromagnetic theory [1], [2], [3]. The proximity effect has received much less attention. Most of the theoretical and experimental works on the proximity effect deal with two wire systems where the wires carry equal currents in opposite directions. For examples, see the work of Kennelly [4], [5], Carson [6], and Dwight [7], [8]. This geometry has a direct application in the problem of wave propagation along parallel wire transmission lines.

The only investigations of the proximity effect in systems with more than two conductors appear to be those done in conjunction with

determining ohmic resistance and Q of inductance coils. Of the theoretical treatments, Butterworth's discussion of the alternating current resistance of cylindrical conductors and solenoidal coils is the most thorough [9], [10], [11]. His work is considered the standard theoretical approach and is summarized in several places [12], [13], [14]. The experimental work of Medhurst, however, indicates that Butterworth's calculations of the radio frequency resistance of coils are not valid over as large a range of parameters as expected; for certain dimensions, errors as large as 190% were observed [15].

In the remainder of this chapter, systems composed of various numbers of in-line, parallel conductors are analyzed. All the conductors have the same circular cross section and carry equal currents in the same direction. Only the high frequency case where the currents are confined to a thin layer near the surface of the wires is considered. This report is an extension of the investigation of the two turn loop antenna reported in [16].

## 2. The Nature of the Current Distributions in a System of Parallel Conductors

### A. Proximity and Skin Effects

In the system of parallel conductors illustrated in Fig. 1-1 there are two factors which determine the distribution of current over the cross section. The first is the normal skin effect which, for high frequencies, causes a concentration of the current near the outer surfaces of the conductor. This is depicted in Fig. 1-2a for a single, isolated,

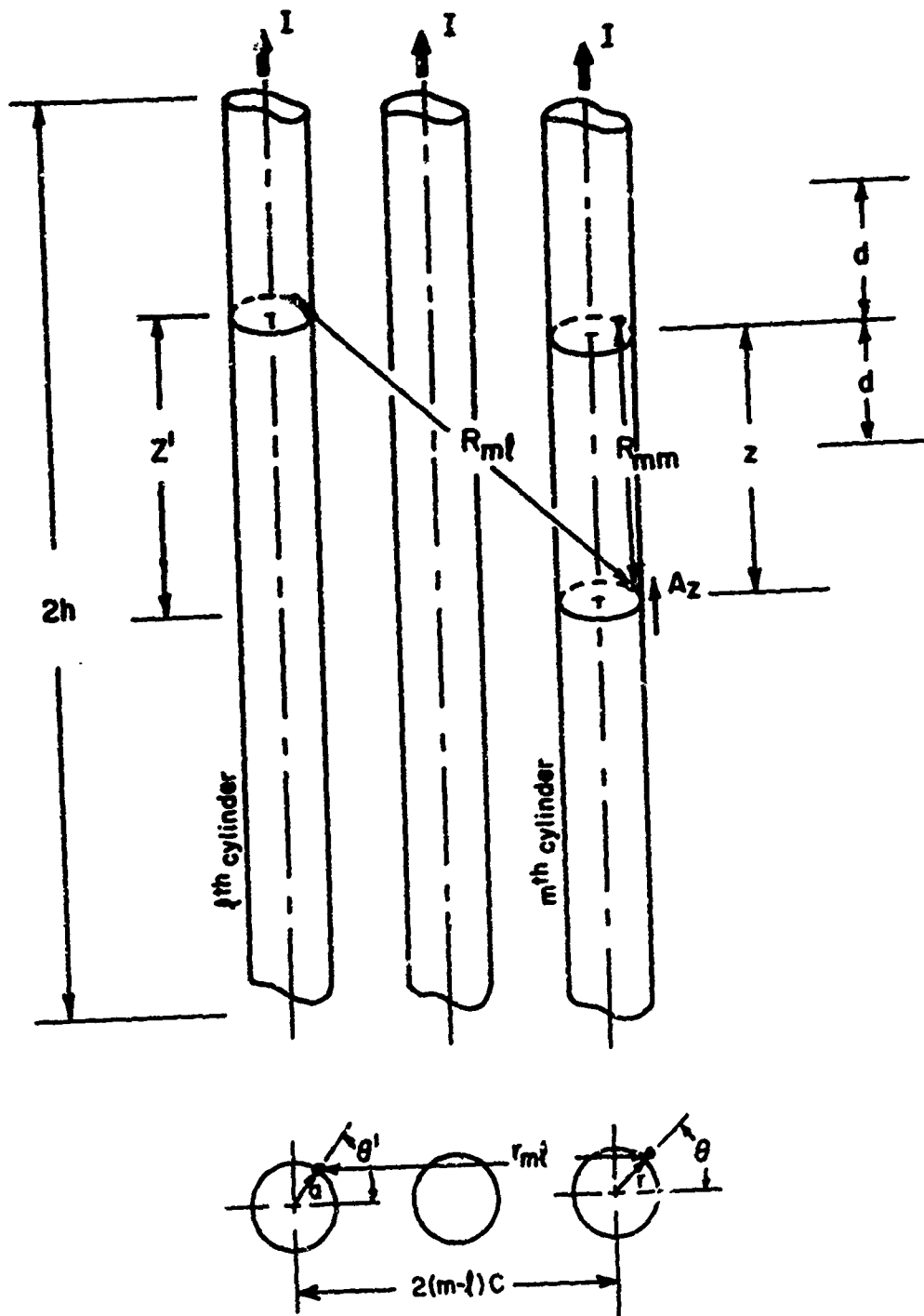
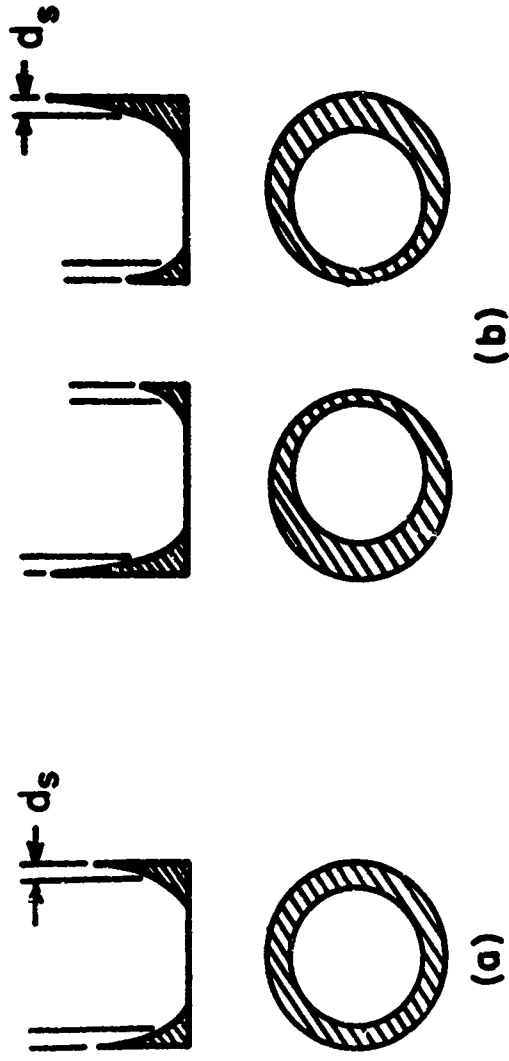


FIG. 1-1 PARALLEL WIRES OF CIRCULAR CROSS-SECTION CARRYING EQUAL CURRENTS IN THE SAME DIRECTION.



(a) THE SKIN EFFECT IN A SINGLE CONDUCTOR  
(b) A COMBINATION OF SKIN EFFECT AND PROXIMITY EFFECT IN A SYSTEM OF TWO CONDUCTORS  
THE SHADED AREA REPRESENTS THE DISTRIBUTION OF CURRENT ON THE SURFACE OF THE WIRE.

FIG. 1-2

round conductor. Secondly, there is an additional redistribution of the current due to the proximity effect. This is caused by the magnetic field present at any one conductor due to the currents in the other conductors of the system. The proximity effect for two parallel, round conductors carrying equal currents in the same direction is illustrated in Fig. 1-2b. In the two conductors, the proximity effect forces the current to the outside edges, much as the skin effect forces the current to the outside surface of the single conductor.

#### B. High Frequency Approximation for the Current Distribution and Resistance

At sufficiently high frequencies the skin depth  $d_s$  for a good conductor is a small quantity compared to the cross sectional dimensions and most of the current in the conductor is confined to a thin layer near the surface. The magnetic field external to the conductor is approximately the same as the field of a perfect conductor of the same shape carrying an equivalent surface current. An expression for the time average power loss per unit surface area of the good conductor, in terms of the component of the magnetic field  $B_t$  tangent to the surface of the perfect conductor, is

$$P \doteq \frac{1}{2} R^s \left( \frac{|B_t|}{\mu_0} \right)^2 \text{ Watts/(meter)}^2 \quad (1-1)$$

In terms of the surface current  $K_s$  on the perfect conductor

$$P \doteq \frac{1}{2} R^s |K_s|^2 \text{ Watts/(meter)}^2 \quad (1-2)$$

where  $R^s$  is the surface resistance.

$$R^s = \frac{1}{\sigma d_s} \quad (1-3a)$$

$$d_s = \sqrt{\frac{2}{\omega \mu_0 \sigma}} \quad (1-3b)$$

If the conductor is cylindrical and  $K_s$  is an axial current density, the power loss per unit length of the conductor is

$$P = \frac{1}{2} R^s \oint |K_s|^2 dw \quad \text{Watts/meter} \quad (1-4)$$

where the integral is over the periphery of the conductor.

For the isolated, circular, cylindrical conductor of radius  $a$  carrying total current  $I$ , rotational symmetry applies. Equation (1-4) reduces to the familiar "Rayleigh formula" for the high frequency resistance per unit length of a circular conductor

$$P = \frac{R^s}{4\pi a} |I|^2 \quad \text{Watts/meter} \quad (1-5a)$$

$$R_{\text{Rayleigh}} = \frac{R^s}{2\pi a} = \frac{1}{2\pi a} \sqrt{\frac{\omega \mu_0}{2\sigma}} \quad \text{Ohms/meter} \quad (1-5b)$$

which is valid for

$$a/d_s \gg 1 \quad (1-6)$$

With more than one conductor present the current distribution and external fields for each conductor are no longer rotationally symmetric; therefore, equations (1-5) no longer apply. Further investigation

is necessary to determine conditions like (1-6) which insure that the high frequency approximation expressed in (1-4) is valid.

Consider a system of long, in-line, parallel conductors carrying equal currents in the same direction (Fig. 1-1) with parameters such that

$$a \ll h, \quad \beta_0 a \ll 1 \quad (1-7)$$

$$n^2 c^2 \ll h^2, \quad \beta_0 n c \ll 1$$

$$c > a \quad (1-8)$$

Neglecting displacement currents as compared to conduction currents, the axial component of the volume current density  $J_{mz}$  interior to the  $m^{\text{th}}$  cylinder must satisfy the following partial differential equation in cylindrical coordinates  $(r, \theta, z)$ .

$$r \frac{\partial}{\partial r} \left( r \frac{\partial J_{mz}}{\partial r} \right) + \frac{\partial^2 J_{mz}}{\partial \theta^2} + i\omega\mu_0 \sigma r^2 J_{mz} = 0$$

$$r \leq a \quad (1-9)$$

An  $e^{-i\omega t}$  time dependence is used. The solution to (1-9), obtained by the method of separation of variables, which has the desired symmetry and remains finite at the origin is

$$J_{mz}(r, \theta, z) = \sum_{P=0}^{\infty} (-1)^P C_{mp} M_p \left( \sqrt{2} \frac{r}{d_s} \right) e^{i\Theta_p \left( \sqrt{2} \frac{z}{d_s} \right)} \cos(P\theta) \quad (1-10)$$

where  $M_p$  and  $\Theta_p$  are the modulus and phase of the Kelvin functions  $(\text{ber}_p + i \text{bei}_p)$  [17, p. 379]. The  $C_p$  are functions of  $z$  only. The total

current at a given cross section of the conductor is  $I_m(z)$ ; therefore

$$I_m(z) = \int_{r=0}^a \int_{\theta=-\pi}^{\pi} J_{mz}(r, \theta, z) r d\theta dr = \frac{2\pi a d_s}{\sqrt{2}} C_{m0} M_1(\sqrt{2} \frac{a}{d_s}) e^{-i \Theta_1(\sqrt{2} \frac{a}{d_s})} \quad (1-11)$$

and

$$C_{m0} = \frac{I_m(z)}{\sqrt{2} \pi a d_s} \frac{e^{i \Theta_1(\sqrt{2} \frac{a}{d_s})}}{M_1(\sqrt{2} \frac{a}{d_s})} \quad (1-12)$$

The volume density of current extrapolated to the surface of the conductor is

$$J_{mz}(a, \theta, z) = \frac{I_m(z) M_0(\sqrt{2} \frac{a}{d_s})}{\sqrt{2} \pi a d_s M_1(\sqrt{2} \frac{a}{d_s})} e^{-i[\Theta_0(\sqrt{2} \frac{a}{d_s}) - \Theta_1(\sqrt{2} \frac{a}{d_s})]} [1 + \sum_{p=1}^{\infty} a'_{mp} \cos(p\theta)] \quad (1-13)$$

With (1-12) and (1-13) substituted in (1-10), the current density becomes

$$J_{mz}(r, \theta, z) = \frac{I_m(z) M_0(\sqrt{2} \frac{a-s}{d_s})}{\sqrt{2} \pi a d_s M_1(\sqrt{2} \frac{a}{d_s})} e^{-i[\Theta_0(\sqrt{2} \frac{a-s}{d_s}) - \Theta_1(\sqrt{2} \frac{a}{d_s})]} \left\{ 1 + \sum_{p=1}^{\infty} a'_{mp} \frac{M_0(\sqrt{2} \frac{a}{d_s}) M_p(\sqrt{2} \frac{a-s}{d_s})}{M_0(\sqrt{2} \frac{a-s}{d_s}) M_p(\sqrt{2} \frac{a}{d_s})} \cos(p\theta) \right. \\ \left. e^{-i[\Theta_p(\sqrt{2} \frac{a-s}{d_s}) - \Theta_p(\sqrt{2} \frac{a}{d_s}) + \Theta_0(\sqrt{2} \frac{a}{d_s}) - \Theta_0(\sqrt{2} \frac{a-s}{d_s})]} \right\} \quad (1-14)$$

Where  $s = a - r$  is the radial distance into the conductor from the surface. In the present analysis, the coefficients  $a'_{mp}$  are assumed to be complex numbers.

When the current distribution at the surface of the conductor is sufficiently smooth, a finite number  $q$  of the Fourier series terms in equation (1-14) are adequate to approximate the current density. If, in addition, the frequency and conductivity are high ( $a/d_s \gg 1$ ,  $\epsilon \ll a$ ) the large argument asymptotic formulas for  $M_p$  and  $\Theta_p$  apply [1?]. Inserting these into equation (1-14) yields

$$J_{mz}(r, \theta, z) \doteq \frac{I_m(z) e^{-\frac{s}{d_s}(1-i)}}{\sqrt{2} \pi a d_s \sqrt{1-s/a}} \left\{ 1 + \sum_{p=1}^q a'_{mp} \cos(p\theta) e^{-i0 \left[ \frac{\left(\frac{pd_s}{2a}\right)^2}{\left(1 - \left(\frac{p}{2}\right)^2 \frac{d_s}{a}\right)} + \dots \right]} + 0 \left[ \frac{\left(\frac{pd_s}{2a}\right)^2}{\left(1 - \left(\frac{p}{2}\right)^2 \frac{d_s}{a}\right)} + \dots \right] \right\} \quad (1-15)$$

which simplifies to

$$J_{mz}(r, \theta, z) \doteq \frac{I_m(z) e^{-\frac{s}{d_s}(1-i)}}{\sqrt{2} \pi a d_s \sqrt{1-s/a}} \left[ 1 + \sum_{p=1}^q a'_{mp} \cos(p\theta) \right] \quad (1-16)$$

for

$$\frac{\left(\frac{pd_s}{2a}\right)^2}{\left(1 - \left(\frac{p}{2}\right)^2 \frac{d_s}{a}\right)} \ll 1, \quad p = 1, 2, \dots, q \quad (1-17)$$

With these conditions satisfied, the current, although non-uniform in  $\theta$ , is confined to a thin layer near the surface much as in the case of an isolated cylinder. The power dissipated per unit length in the  $m^{\text{th}}$  conductor is then

$$P'_m = \frac{1}{\sigma} \int_{r=0}^a \int_{\theta=-\pi}^{\pi} |J_{mz}(r, \theta, z)|^2 r dr d\theta$$

$$\approx \frac{I_m^2(z) R^s}{4\pi a} \left[ 1 + \frac{1}{2} \sum_{p=1}^q |a'_{mp}|^2 \right] \text{ Watts/meter} \quad (1-18)$$

If the cylinders are now made perfectly conducting, the current on the  $m^{\text{th}}$  cylinder will be of the form.

$$K_{mz}(\theta, z) = \frac{I_m(z)}{2\pi a} g_m(\theta) \approx \frac{I_m(z)}{2\pi a} \left[ 1 + \sum_{p=1}^q a_{mp} \cos(p\theta) \right] \quad (1-19)$$

where  $g_m(\theta)$  is the normalized surface current density. Using the approximation expressed in equation (1-4), the power loss per unit length for a good conductor expressed in terms of the coefficients  $a_{mp}$  for the perfect conductor is

$$P_m \approx \frac{1}{2} \left( \frac{I_m(z)}{2\pi a} \right)^2 R^s \int_{\theta=-\pi}^{\pi} g_m^2(\theta) a d\theta \approx \frac{I_m^2(z) R^s}{4\pi a} \left[ 1 + \frac{1}{2} \sum_{p=1}^q |a_{mp}|^2 \right]$$

Watts/meter (1-20)

For large values of  $a/d_s$  this expression is a good approximation to the correct relation, equation (1-18), that is

$$\left. \begin{aligned} a_{mp} &\doteq a'_{mp} \\ P_m &\doteq P'_m \end{aligned} \right\} a/d_s \gg 1 \quad (1-21)$$

provided

$$\frac{\left(\frac{pd_s}{2a}\right)^2}{\left(1 - \left(\frac{p}{2}\right)^2 \frac{d_s}{a}\right)} \ll 1 \quad p = 1, 2, \dots, q \quad (1-22)$$

The first term in equation (1-20) is the power loss in the  $m^{\text{th}}$  conductor due to the net current  $I_m$  in that wire. This is the normal skin effect loss. The sum in (1-20) represents the loss due to nonuniform currents induced by other wires in the system. It is the additional loss in the  $m^{\text{th}}$  wire due to the proximity effect. Since the coefficients  $a_{mp}$  in the sum are a function of the net currents  $I_1$  in all wires of the system, the equation for  $P_m$  cannot be written as  $P_m = R_m \left(\frac{1}{2} I_m^2\right)$  if  $R_m$  is to be only a function of the physical parameters of the system. As a result, the usual circuit definition of the ohmic resistance of each wire ( $R_m = P_m / \left(\frac{1}{2} I_m^2\right)$ ) makes no sense.

When all conductors carry the same total current at each cross section the ohmic resistance per unit length of the system of wires is a useful quantity. Using the series definition of the current (1-19) the ohmic resistance per unit length of a system of  $n$  parallel wires is given by

$$R \doteq \frac{R^s}{2\pi a} \sum_{m=1}^n \left[ 1 + \frac{1}{2} \sum_{p=1}^q |a_{mp}|^2 \right] \text{ Ohms/meter} \quad (1-23)$$

If the separation between conductors is large enough that each can be considered as isolated from the others, (1-23) becomes

$$R_o \doteq \frac{R^s}{2\pi a} n = n R_{\text{Rayleigh}} \text{ Ohms/meter} \quad (1-24)$$

The additional ohmic resistance per unit length due to the proximity effect is then

$$R_p = R - R_o = \frac{R^s}{4\pi a} \sum_{m=1}^n \sum_{p=1}^q |a_{mp}|^2 \text{ Ohms/meter} \quad (1-25)$$

Normalized quantities are useful when comparing different configurations of conductors.

$$\frac{R}{R_o} = \sum_{m=1}^n \left[ 1 + \frac{1}{2} \sum_{p=1}^q |a_{mp}|^2 \right] \quad (1-26)$$

$$\frac{R_p}{R_o} = \frac{1}{2} \sum_{m=1}^n \sum_{p=1}^q |a_{mp}|^2 \quad (1-27)$$

In the present analysis a smooth conductor with a uniform surface resistance is assumed. Recent research by A. Sanderson [18] indicates that surface roughness in the form of scratches transverse to the direction of the current can significantly alter the equivalent surface

resistance. The type of wire used in practical applications is usually formed by a drawing process, such as drawn copper wire. Surface scratches are in the same direction as the current flow and are expected to increase the ohmic loss much less than equivalent transverse imperfections would. Calculations using Sanderson's theory indicates that surface roughness can be ignored at the frequencies of interest (< 100 MHz.) in this study.

### 3. Formulation of the Integral Equations for the Transverse Current Distributions

Consider each of the long, parallel cylinders in Fig. 1-1 as being perfectly conducting. The surface current density on the 1<sup>th</sup> conductor is then

$$K_{\ell}(\theta', z') = \frac{I}{2\pi a} g_{\ell}(\theta') f(z'), \quad \ell = 1, 2, \dots, n \quad (1-28)$$

The dimensionless quantity  $g_1(\theta')$  is the normalized surface current density. In (1-28) the same  $z'$  dependence  $f(z')$  is assumed for the current distributions on all cylinders. The conductors are composed of three sections; the length  $z-d \leq z' \leq z+d$  and the two end sections  $z+d \leq z' \leq h$ ,  $-h \leq z' \leq z-d$ . In addition to the inequalities presented in (1-7) and (1-8) the following constraints are placed on the length  $d$

$$\beta_0 d \ll 1 \quad (1-30a)$$

$$d^2 \gg n^2 c^2 \quad (1-30b)$$

This makes the current distributions at every cross section along the

length  $z-d \leq z' \leq z+d$  approximately the same.

$$K_f(\theta', z') = \frac{I}{2\pi a} g_f(\theta') f(z), \quad z-d \leq z' \leq z+d \quad (1-31)$$

The Helmholtz integral for the vector potential component  $\vec{A}_z(r, \theta, z)$  at a point just off the surface of the  $m^{\text{th}}$  conductor is

$$\begin{aligned} A_{mz}(r, \theta, z) = & \frac{\mu_0 I}{8\pi^2} \left\{ f(z) \int_{z'-z-d}^{z+d} \int_{\theta'=-\pi}^{\pi} \sum_{l=1}^n \left[ \frac{g_f(\theta') e^{i\beta_0 R_{mf}}}{R_{mf}} \right] d\theta' dz' \right. \\ & \left. + \left( \int_{z'=-h}^{z-d} \int_{z'-z+d}^h \right) \int_{\theta'=-\pi}^{\pi} \sum_{l=1}^n \left[ \frac{g_f(\theta') f(z') e^{i\beta_0 R_{mf}}}{R_{mf}} \right] d\theta' dz' \right\} \quad (1-32) \end{aligned}$$

where

$$\begin{aligned} R_{mf} = & [(z-z')^2 + r_{mf}^2]^{1/2} \quad [(z-z')^2 + 4(m-l)^2 c^2 + \\ & r^2 + a^2 - 2ar \cos(\theta - \theta') + 4(m-l)c(r \cos \theta - a \cos \theta')]^{1/2} \quad (1-33) \end{aligned}$$

If terms of order  $\beta_0 d$  or less are neglected in the first integral and setting

$$R_{mf} = [(z-z')^2 + 4(m-l)^2 c^2]^{1/2} \quad (1-34)$$

in the last two integrals, equation (1-33) reduces to

$$A_{mz}(r, \theta, z) \doteq \frac{\mu_0 I}{8\pi^2} \left\{ f(z) \int_{z'=z-d}^{z+d} \int_{\theta'=-\pi}^{\pi} \sum_{l=1}^n \left[ \frac{g_l(\theta')}{R_{ml}} \right] d\theta' dz' \right. \\ \left. + \left( \int_{z'=-h}^{z-d} \int_{z'=z+d}^h \right) 2\pi f(z') \sum_{l=1}^n \left[ \frac{e^{i\beta_0[(z-z')^2 + 4(m-l)^2 c^2]^{1/2}}}{[(z-z')^2 + 4(m-l)^2 c^2]^{1/2}} \right] dz' \right\} \quad (1-35)$$

The  $z'$  integration in the first integral can be evaluated directly [19, p. 50, 200.01]. The result is

$$\int_{z'=z-d}^{z+d} \frac{1}{R_{ml}} dz' = 2 \sinh^{-1} \left( \frac{d}{r_{ml}} \right) \doteq 2[\ln(r_{ml}) - \ln(2d)] \quad (1-36)$$

where terms of order  $n^2 c^2/d^2$  are dropped in the last expression.

With (1-36), equation (1-35) becomes

$$A_{mz}(r, \theta, z) \doteq \frac{\mu_0 I}{8\pi^2} \left\{ -2i(z) \int_{\theta'=-\pi}^{\pi} \sum_{l=1}^n [g_l(\theta') \ln(r_{ml})] d\theta' \right. \\ \left. + 4\pi n \ln(2d) + A'_{mz}(z) \right\} \quad (1-37)$$

The term  $A'_{mz}(z)$  represents the last two integrals in (1-35).

The normalized surface current density is given by the boundary condition

$$g_m(\theta) = \frac{-2\pi a}{\mu_0 I f(z)} \left. \frac{\partial A_{mz}(r, \theta, z)}{\partial r} \right|_{r=a} \quad (1-38)$$

The next step is to substitute the approximate expression for the vector potential (1-37) into (1-38) to obtain

$$g_m(\theta) = \frac{1}{2\pi} \left\{ \lim_{\tau \rightarrow 1} \int_{\theta' = -\pi}^{\pi} \frac{g_m^{(l')}(\theta - \theta') (\tau - \cos(\theta - \theta'))}{\tau^2 + 1 - 2\tau \cos(\theta - \theta')} d\theta' \right. \\ \left. + \int_{\theta' = -\pi}^{\pi} \sum_{\substack{l=1 \\ l \neq m}}^n \frac{[1 + 2(m-l)(c/a)\cos\theta - \cos(\theta - \theta')] g_l^{(l')}(\theta')}{(r'_{ml})^2} d\theta' \right\} \quad (1-39)$$

where

$$\tau = r/a \quad (1-40)$$

and

$$r'_{ml} = [4(m-l)^2(c/a)^2 + 2 - 2\cos(\theta - \theta') + 4(m-l)(c/a)(\cos\theta - \cos\theta')]^{1/2} \quad (1-41)$$

The first integral, which represents the self term, is indefinite when  $\tau = 1$ ; therefore, the order of the limiting and integration processes are not interchangeable. For values of  $\tau$  near unity the integrand has the behavior

$$\text{Integrand} \sim \left[ \frac{\Delta}{\Delta^2 + \theta^2} + \frac{1}{2} \right] \quad (1-42)$$

where

$$\Delta = \tau - 1 \ll 1 \quad (1-43)$$

Comparing this with the following definition of the Dirac delta function

$$\delta(\theta) = \frac{1}{\pi} \lim_{\Delta \rightarrow 0} \left[ \frac{\Delta}{\Delta^2 + \theta^2} \right] \quad (1-44)$$

it is evident that in the limit the integrand becomes

$$\text{Integrand} = \left[ \pi \delta(\theta) + \frac{1}{2} \right] \quad (1-45)$$

Substituting (1-45) into (1-39) and rearranging yields

$$g_m(\theta) = 1 + \frac{1}{\pi} \int_{\theta' = -\pi}^{\pi} \sum_{\substack{\ell=1 \\ \ell \neq m}}^n K_{m,\ell}(\theta, \theta') g_\ell(\theta') d\theta' \quad (1-46)$$

where

$$K_{m,\ell}(\theta, \theta') = \frac{1 + 2(m-\ell) \frac{c}{a} \cos \theta - \cos(\theta - \theta')}{(r'_{m\ell})^2} \quad (1-47)$$

Symmetry about the center of the system of wires requires  $g_{n+1-m}(\theta) = g_m(\pi - \theta)$  which reduces the number of terms in (1-47) to  $n/2$  for  $n$  even or  $(n+1)/2$  for  $n$  odd.

$n$  even

$$g_m(\theta) = \frac{1}{\pi} \int_{\theta' = -\pi}^{\pi} K_{m, n+1-m}(\theta, \pi - \theta') g_m(\theta') d\theta' + \left\{ 1 + \frac{1}{\pi} \sum_{\substack{\ell=1 \\ \ell \neq m}}^{n/2} \int_{\theta' = -\pi}^{\pi} [K_{m,\ell}(\theta, \theta') + K_{m, n+1-\ell}(\theta, \pi - \theta')] g_\ell(\theta') d\theta' \right\}, \quad m = 1, 2 \dots n/2 \quad (1-48)$$

n odd

$$g_m(\theta) = \frac{h(m)}{\pi} \int_{\theta'=-\pi}^{\pi} K_{m, n+1-m}(\theta, \pi-\theta') g_m(\theta') d\theta' : \left\{ 1 + \frac{1}{\pi} \sum_{\substack{l=1 \\ l \neq m}}^{(n-1)/2} \int_{\theta'=-\pi}^{\pi} \right.$$

$$\left. [K_{m, l}(\theta, \theta') + K_{m, n+1-l}(\theta, \pi-\theta')] g_l(\theta') d\theta' + \frac{h(m)}{\pi} \int_{\theta'=-\pi}^{\pi} K_{m, (n+1)/2}(\theta, \theta') g_{(n+1)/2}(\theta') d\theta' \right\}$$

(1-49)

where

$$\begin{aligned} h(m) &= 1 & m \neq (n+1)/2 \\ &= 0 & m = (n+1)/2 \end{aligned} \tag{1-50}$$

Equations (1-48) and (1-49) represent, respectively, a system of  $n/2$  and  $(n+1)/2$  coupled integral equations whose solutions are the desired surface current densities,  $g_m(\theta)$ .

#### 4. Solution for Two Conductors

The simplest geometry for examining the proximity effect is two parallel circular conductors carrying equal currents. Exact expressions for the current distribution and ohmic resistance for this simple case are given in Technical Report No. 612 [16]. The normalized current distribution on the two wire system is graphed in Fig. 1-3 for various conductor spacings  $c/a$ . The distributions will prove useful in developing approximate solutions for systems with two or more conductors.

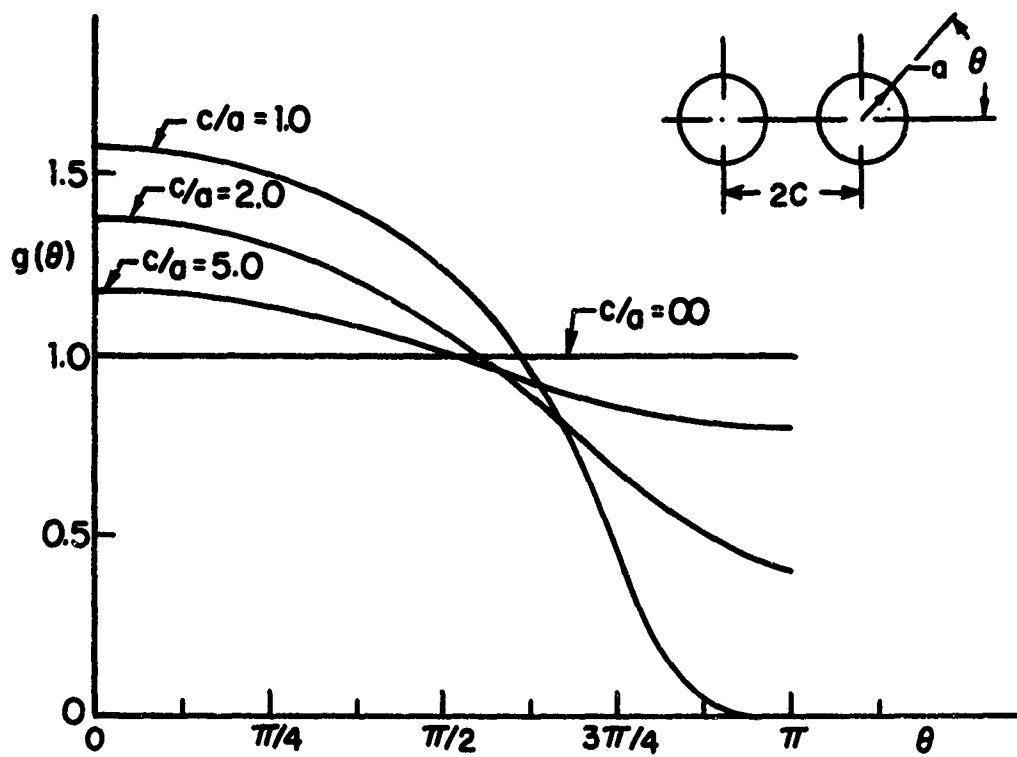


FIG. 1-3 THE NORMALIZED SURFACE CURRENT DISTRIBUTION ON TWO WIRES VARIOUS WIRE SPACINGS  $c/a$

5. Approximate Solution of the Integral Equations for Two or More Conductors

A. The Method of Undetermined Coefficients

1. Reduction to a Set of Algebraic Equations

For systems with more than two circular conductors approximate methods must be used to obtain the current distribution and resulting ohmic resistance per unit length of the system. In this section one such method, undetermined coefficients, is applied to the previously derived system of integral equations (1-48), (1-49).

As the previous analysis suggests, a trigonometric series is the natural choice for an expansion to represent the normalized surface current density.

$$g_m(\theta) = 1 + \sum_{p=1}^q a_{mp} \cos(p\theta) \quad (1-51)$$

Further evidence for this selection is found by examining the exact solution for the two wire case. A Fourier analysis of the current distribution (Fig. 1-3), for the limiting case  $c/a = 1$ , indicates that the first two cosine terms in the series are adequate to predict the correct value of the additional loss due to proximity  $R_p/R_o$  to within 1%. For large spacings,  $c/a \gg 1$ , the current distribution is of the form  $1 + a_1 \cos \theta$  as is evident from Fig. 1-3. This last statement is also true for systems with more than two wires and is easily understood if the magnetic field due to external currents is considered a constant over the cross section of each conductor. The magnetic field  $B_{my}$  normal to the

axis of the  $m^{\text{th}}$  conductor in a system of  $n$  conductors would be

$$B_{my} \doteq \frac{\mu_0 I}{4\pi c} \sum_{\substack{l=1 \\ l \neq m}}^n \frac{1}{(m-l)} \quad (1-52)$$

and the resulting current distribution becomes

$$g_m(\theta) \doteq 1 + \left(\frac{a}{c}\right) \sum_{\substack{l=1 \\ l \neq m}}^n \frac{1}{(m-l)} \cos \theta \quad (1-53)$$

Substituting (1-51) into the integral equations (1-48), (1-49), one obtains

$n$  even

$$\begin{aligned} & \sum_{p=1}^q a_{mp} \left[ -\cos(p\theta) + \frac{(-1)^p}{\pi} \int_{\theta'=-\pi}^{\pi} K_{m, n+1-m}(\theta, \theta') \cos(p\theta') d\theta' \right] \\ & + \sum_{\substack{l=1 \\ l \neq m}}^{n/2} \sum_{p=1}^q a_{lp} \left\{ \frac{1}{\pi} \int_{\theta'=-\pi}^{\pi} [K_{m, l}(\theta, \theta') + (-1)^p K_{m, n+1-l}(\theta, \theta')] \cos(p\theta') d\theta' \right\} = \\ & - \frac{1}{\pi} \int_{\theta'=-\pi}^{\pi} \left\{ K_{m, n+1-m}(\theta, \theta') + \sum_{\substack{l=1 \\ l \neq m}}^{n/2} [K_{m, l}(\theta, \theta') + K_{m, n+1-l}(\theta, \theta')] \right\} d\theta' \end{aligned} \quad (1-54)$$

$$m = 1, 2, \dots, n/2$$

n odd

$$\begin{aligned}
 & \sum_{p=1}^q a_{mp} [-\cos \left\{ \begin{matrix} p\theta & m \neq (n+1)/2 \\ 2p\theta & m = (n+1)/2 \end{matrix} \right\} + \frac{(-1)^p}{\pi} h(m) \int_{\theta'=-\pi}^{\pi} K_{m, n-1-m}(\theta, \theta') \cos(p\theta') d\theta'] \\
 & + \sum_{\substack{\ell=1 \\ \ell/m}}^{(n-1)/2} \sum_{p=1}^q a_{\ell p} \left\{ \frac{1}{\pi} \int_{\theta'=-\pi}^{\pi} [K_{m, \ell}(\theta, \theta') + (-1)^p K_{m, n+1-\ell}(\theta, \theta')] \cos(p\theta') d\theta' \right\} \\
 & + \sum_{p=1}^q a_{\frac{n+1}{2}, 2p} \left[ \frac{h(m)}{\pi} \int_{\theta'=-\pi}^{\pi} K_{m, (n+1)/2}(\theta, \theta') \cos(2p\theta') d\theta' \right] = -\frac{1}{\pi} \int_{\theta'=-\pi}^{\pi} h(m) K_{m, n+1-m}(\theta, \theta') \\
 & + \sum_{\substack{\ell=1 \\ \ell/m}}^{(n-1)/2} [K_{m, \ell}(\theta, \theta') + K_{m, n+1-\ell}(\theta, \theta')] \left. \right\} d\theta \quad m = 1, 2, \dots, (n+1)/2 \quad (1-55)
 \end{aligned}$$

where the same number of harmonic terms  $q$  is used to represent the surface current on all conductors. Due to symmetry about  $\theta = \pi/2$ , only even harmonics appear on the center conductor of a system with an odd number of conductors.

The definite integrals in equation (1-54) and (1-55) are of the form

$$\begin{aligned}
 I(\theta, m-\ell, p) &= \frac{1}{\pi} \int_{\theta'=-\pi}^{\pi} \frac{[1+2(m-\ell)(c/a)\cos\theta - (\cos\theta \cos\theta')] }{[4(m-\ell)^2(c/a)^2 + 2 + 4(m-\ell)(c/a)\cos\theta]} \\
 & \quad \frac{[ \sin\theta \sin\theta' ] \cos(p\theta') d\theta'}{[4(m-\ell)(c/a) + 2 \cos(\theta')] \cos[\theta' - 2 \sin\theta \sin\theta']} \quad (1-56)
 \end{aligned}$$

Appendix A contains a detailed evaluation of this integral, the results of which are

$$I(\theta, m-l, p) = \begin{cases} \frac{1}{(1-s^2)(-s)^{p+1}} [As^2 + Bs + C], & p = 1, 2, \dots, q \\ \frac{-1}{s(1-s^2)} [Bs + C], & p = 0 \end{cases} \quad (1-57a)$$

where

$$s = (4(m-l)^2 (c/a)^2 + 1 + 4(m-l) (c/a) \cos \theta)^{1/2} \quad (1-57b)$$

$$A = \cos (\theta - (p - 1) \psi) \quad (1-57c)$$

$$B = 2(1 + 2(m-l) (c/a) \cos \theta) \cos (p\psi) \quad (1-57d)$$

$$C = \cos (\theta + (p + 1) \psi) \quad (1-57e)$$

$$\psi = \begin{cases} \pi - \tan^{-1} \left( \frac{\sin \theta}{2(m-l)(c/a) + \cos \theta} \right), & (m-l) = 1, 2, \dots \\ \tan^{-1} \left( \frac{-\sin \theta}{2(m-l)(c/a) + \cos \theta} \right), & (m-l) = -1, -2, \dots \end{cases} \quad (1-57f)$$

The principle value of  $\tan^{-1}$  is used in (1-57f). For the case  $n$  even the system of equations (1-54) with (1-57) becomes

$$\sum_{p=1}^q a_{mp} [-\cos (p\theta) + (-1)^p I(\theta, 2m-n-1, p)] + \sum_{\substack{l=1 \\ l \neq m}}^{n/2} \sum_{p=1}^q a_{lp}$$

$$[I(\theta, m-l, p) + (-1)^p I(\theta, m+l-n-1, p)] = - \{ I(\theta, 2m-n-1, 0)$$

$$+ \sum_{\substack{l=1 \\ l \neq m}}^{n/2} [I(\theta, m-l, 0) + I(\theta, m+l-n-1, 0)] \}$$

$$m = 1, 2, \dots, n/2 \quad (1-58)$$

This is a set of  $n/2$  equations, one for each conductor, involving  $qn/2$  unknowns ( $a_{mp}$ ) the coefficients of which are functions of the variable  $\theta$ . In order to solve the system a set of  $qn/2$  conditions is necessary. Two procedures which yield such conditions were used, the methods of collocation and least squares [25].

## 2. Solution by the Methods of Collocation and Least Squares

In the method of collocation, the  $a_{mp}$  are chosen so that equation (1-77) is satisfied exactly at  $q$  points  $\theta_{mk}$  ( $0 \leq \theta_{mk} \leq \pi$ ,  $k = 1, 2, \dots, q$ ) on each conductor, more specifically for  $n$  even

$$\begin{aligned} & \sum_{p=1}^q a_{mp} [-\cos(p\theta_{mk}) + (-1)^p I(\theta_{mk}, 2m-n-1, p)] \\ & + \sum_{\substack{\ell=1 \\ \ell \neq m}}^n \sum_{p=1}^q a_{\ell p} [I(\theta_{mk}, m-\ell, p) + (-1)^p I(\theta_{mk}, m+\ell-n-1, p)] \\ & - \left\{ I(\theta_{mk}, 2m-n-1, 0) + \sum_{\substack{\ell=1 \\ \ell \neq m}}^{n/2} [I(\theta_{mk}, m-\ell, 0) + I(\theta_{mk}, m+\ell-n-1, 0)] \right\} \\ & \quad m = 1, 2, \dots, n/2 \\ & \quad k = 1, 2, \dots, q \end{aligned} \quad (1-59)$$

With the definition of the new variables  $t_{kp}^m$ ,  $t_{kp}^{m\ell}$ , and  $s_{mk}$ , equation (1-59) becomes

$$\sum_{p=1}^q a_{mp} t_{kp}^m + \sum_{\substack{\ell=1 \\ \ell \neq m}}^{n/2} \sum_{p=1}^q a_{\ell p} t_{kp}^{m\ell} = s_{mk} \quad (1-60)$$

In matrix form, the system of algebraic equations (1-59) is now

$$\begin{bmatrix} T_{11} & T_{12} & \dots & T_{1n/2} \\ T_{21} & T_{22} & \dots & T_{2n/2} \\ \dots & \dots & \dots & \dots \\ T_{\frac{n}{2}1} & T_{\frac{n}{2}2} & \dots & T_{\frac{n}{2}n/2} \end{bmatrix} \begin{bmatrix} A_1 \\ A_2 \\ \dots \\ A_{n/2} \end{bmatrix} = \begin{bmatrix} S_1 \\ S_2 \\ \dots \\ S_{n/2} \end{bmatrix} \quad (1-61)$$

where

$$T_{ii} = \begin{bmatrix} t_{11}^i & t_{12}^i & \dots & t_{1q}^i \\ t_{21}^i & t_{22}^i & \dots & t_{2q}^i \\ \dots & \dots & \dots & \dots \\ t_{q1}^i & t_{q2}^i & \dots & t_{qq}^i \end{bmatrix}, \quad T_{ij} = \begin{bmatrix} t_{11}^{ij} & t_{12}^{ij} & \dots & t_{1q}^{ij} \\ t_{21}^{ij} & t_{22}^{ij} & \dots & t_{2q}^{ij} \\ \dots & \dots & \dots & \dots \\ t_{q1}^{ij} & t_{q2}^{ij} & \dots & t_{qq}^{ij} \end{bmatrix} \quad (1-62a)$$

$$(1-62b)$$

$$A_i = \begin{bmatrix} a_{i1} \\ a_{i2} \\ \dots \\ a_{iq} \end{bmatrix}, \quad S_i = \begin{bmatrix} s_{i1} \\ s_{i2} \\ \dots \\ s_{iq} \end{bmatrix} \quad (1-62c)$$

$$(1-62d)$$

For the case  $n$  odd, a similar matrix equation results. All the elements of the  $S$  and  $T$  matrices are real; therefore, equation (1-61) can be written as two separate equations

$$[T] [A^r] = [S] \quad (1-63a)$$

$$[T][A^i] = 0 \quad (1-63b)$$

where  $A^r$  contains only the real part of the coefficients  $\text{Re}(a_{mp})$  and  $A^i$  contains only the imaginary part,  $\text{Im}(a_{mp})$ . For a unique solution of (1-63a), the T matrix must be nonsingular. A nonsingular T matrix indicates a trivial solution for the homogeneous equation (1-63b), i. e. all  $\text{Im}(a_{mp}) = 0$ . The normalized current distributions  $g_m(\theta)$  are therefore real quantities.

The method of least squares differs from collocation in that the  $a_{mp}$  are chosen in such a manner that equation (1-58) is satisfied in a least squares sense over the interval  $0 \leq \theta \leq \pi$  rather than satisfied exactly at specific points, namely

$$\int_{\theta=0}^{\pi} \left\{ \sum_{p=1}^q a_{mp} [-\cos(p\theta) + (-1)^p I(\theta, 2m-n-1, p)] + \sum_{\substack{\ell=1 \\ \ell \neq m}}^{n/2} \sum_{p=1}^q a_{\ell p} [I(\theta, m-\ell, p) + (-1)^p I(\theta, m+\ell-n-1, p)] + I(\theta, 2m-n-1, 0) + \sum_{\substack{\ell=1 \\ \ell \neq m}}^{n/2} [I(\theta, m-\ell, 0) + I(\theta, m+\ell-n-1, 0)] \right\}^2 d\theta$$

= minimum       $m = 1, 2, \dots, n/2$       (1-64)

Differentiating the left hand side with respect to each coefficient  $a_{mp}$  and setting the results equal to zero yields

$$\int_{\theta=0}^{\pi} [-\cos(k\theta) + (-1)^k I(\theta, 2m-n-1, k)] \left\{ \sum_{p=1}^q a_{mp} [-\cos(p\theta) + (-1)^p I(\theta, 2m-n-1, p)] + \sum_{\substack{\ell=1 \\ \ell \neq m}}^{n/2} \sum_{p=1}^q a_{\ell p} [I(\theta, m-\ell, p) + (-1)^p I(\theta, m+\ell-n-1, p)] + I(\theta, 2m-n-1, 0) \right\}$$

$$+ \sum_{\substack{\ell=1 \\ \ell \neq m}}^{n/2} [I(\theta, m-\ell, 0) + I(\theta, m+\ell-n-1, 0)] \Bigg\} d\theta = 0 \quad (1-65)$$

$$m = 1, 2, \dots, n/q$$

$$k = 1, 2, \dots, q$$

After rearranging terms and performing integrations, (1-65) becomes

$$\sum_{p=1}^q a_{mp} \left\{ \frac{\pi}{2} \delta(k, p) - \int_{\theta=0}^{\pi} [(-1)^p \cos(k\theta) I(\theta, 2m-n-1, p) + (-1)^k \cos(p\theta) I(\theta, 2m-n-1, k) - (-1)^{p+k} I(\theta, 2m-n-1, p) I(\theta, 2m-n-1, k)] d\theta \right\} + \sum_{\substack{\ell=1 \\ \ell \neq m}}^{n/2} \sum_{p=1}^q a_{\ell p} \left\{ - \int_{\theta=0}^{\pi} [\cos(k\theta) - (-1)^k I(\theta, 2m-n-1, k)] [I(\theta, m-\ell, p) + (-1)^p I(\theta, m+\ell-n-1, p)] d\theta \right\}$$

$$= \int_{\theta=0}^{\pi} [\cos(k\theta) - (-1)^k I(\theta, 2m-n-1, k)] \left\{ I(\theta, 2m-n-1, 0) + \sum_{\substack{\ell=1 \\ \ell \neq m}}^{n/2} [I(\theta, m-\ell, 0) + I(\theta, m+\ell-n-1, 0)] \right\} d\theta \quad (1-66)$$

$$m = 1, 2, \dots, n/2$$

$$k = 1, 2, \dots, q$$

which can be written as

$$\sum_{p=1}^q a_{mp} t_{kp}^m + \sum_{\substack{\ell=1 \\ \ell \neq m}}^{n/2} \sum_{p=1}^q a_{\ell p} t_{kp}^{m\ell} = s_{mk} \quad (1-67)$$

The variables  $t_{kp}^m$ ,  $t_{kp}^{ml}$  and  $s_{mk}$  enter the matrix equation (1-62) in the same manner as in the method of collocation.

## B. Numerical Results

### 1. Comparison of the Two Methods of Solution

For the collocation solution, the same matching points ( $\theta_{mk} = \theta_k$ ,  $0 \leq \theta_k \leq \pi$ ) were used on all cylinders except the center cylinder in a system with  $n$  odd. The current on the center cylinder has symmetry about  $\theta = \pi/2, \pi$ ; therefore only points in the first quadrant are needed. These were chosen to be  $\theta_k/2$ . Several different combinations of matching points were used in (1-59) and the resulting matrix equation (1-61) was solved for the coefficients  $a_{mp}$  using a standard Gaussian elimination algorithm [26]. The additional ohmic resistance due to the proximity effect  $R_p/R_o$  was calculated from (1-27) for various numbers of harmonic terms  $q$ . No particular distribution of points gave a best rate of convergence of  $R_p/R_o$  for all numbers of conductors and spacings. The final set of matching points settled on is

$$\theta_k = \left\{ \begin{array}{ll} k\left(\frac{\pi}{q+1}\right) & q \text{ even} \\ k\left(\frac{\pi}{q+2}\right) & k \leq \frac{q+1}{2} \\ (k+1)\left(\frac{\pi}{q+2}\right) & k > \frac{q+1}{2} \end{array} \right\} \quad q \text{ odd} \quad (1-68)$$

For an even number of harmonics, the points are equally spaced and internal to the region  $0 \leq \theta_k \leq \pi$ . With an odd number of harmonics, a slightly better rate of convergence was found when the set of matching points did not include  $\theta_k = \pi/2$ .

The least squares procedure requires the evaluation of the definite integrals in equation (1-66). Due to the complexity of the  $I(\theta, m-l, p)$  functions in the integrand, an exact evaluation was unobtainable and approximate numerical integration necessary. A typical integration from (1-66) was performed using three different numerical integration routines: Romberg, Simpson's rule, and Gauss quadrature. The six-point Gauss quadrature formula [27] required the least time for the desired accuracy. The interval  $0 \leq \theta \leq \pi$  was divided into  $k+1$  or  $p+1$  panels, whichever was larger, and the six-point formula applied to each panel. With the integrals evaluated, the resulting matrix equation (1-61) was solved using the same algorithm as for the collocation solution.

A comparison of the two methods is presented in Fig. 1-4, where  $R_p/R_o$  and the computation time for the I. B. M. 360/65 computer are graphed as a function of the number of harmonic terms used in the solution. The results are for 4 cylinders with a spacing  $c/a = 1.10$ . Least squares is the more elegant of the two procedures, converging to the limiting value of  $R_p/R_o$  when the number of harmonic terms is less than half that required in the collocation solution. In terms of computation time the collocation method is much faster--roughly 6q times faster for a given number of harmonic terms. Thus the limiting value of  $R_p/R_o$  is obtained in about one-tenth the computation time needed for the least squares solution. Similar time savings are found for other numbers of cylinders and spacings. For this reason, the majority of the calculations for this work were done by the method of

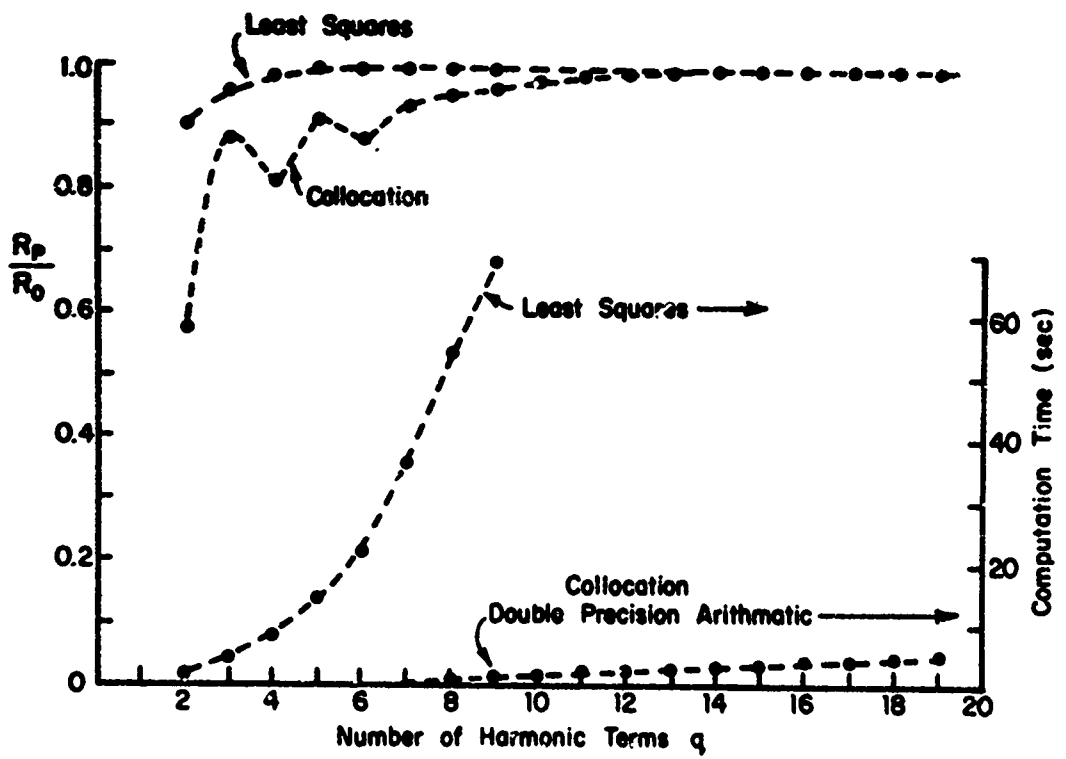


FIG. 1-4 COMPARISON OF THE LEAST SQUARES AND COLLOCATION SOLUTIONS FOR FOUR WIRES WITH SPACING  $c/a = 1.10$ .

collocation. Listings of the computer programs for both methods are in Appendix B.

## 2. Transverse Current Distributions

The number of harmonic terms used for the current distribution on a given system of conductors was determined by observing  $R_p/R_o$ . If increasing the number by two produced less than a 0.10% change in  $R_p/R_o$ , the number of terms was deemed sufficient. The normalized surface current densities  $g(\theta)$  for systems with 3, 4, 5 and 6 conductors and various spacings  $c/a$  are plotted in Figs. 1-5 through 1-8. The distributions for 2 conductors are not plotted, since they are identical to those in Fig. 1-3. In systems with three or more closely spaced cylinders there are both positive and negative currents on the surface of the outer conductors. These currents in opposite directions add nothing to the net current in the wire; they just increase the ohmic loss. When the spacing between cylinders is very close, currents on adjacent surfaces of two conductors tend toward equal values with opposite sign; for example: for 4 wires, spacing  $c/a = 1.1$ ,  $g(\pi) \doteq -2$  on cylinder 1, while on cylinder 2,  $g(\pi) \doteq +2$ .

## 3. The Additional Ohmic Resistance Per Unit Length Due to the Proximity Effect

Computed values of the additional ohmic resistance per unit length due to the proximity effect  $R_p/R_o$  for systems with various spacings  $c/a$  and up to eight conductors are presented in Fig. 1-9 and Table 1-1. Calculations of  $R_p/R_o$  were not made for extremely close spacings, i. e.

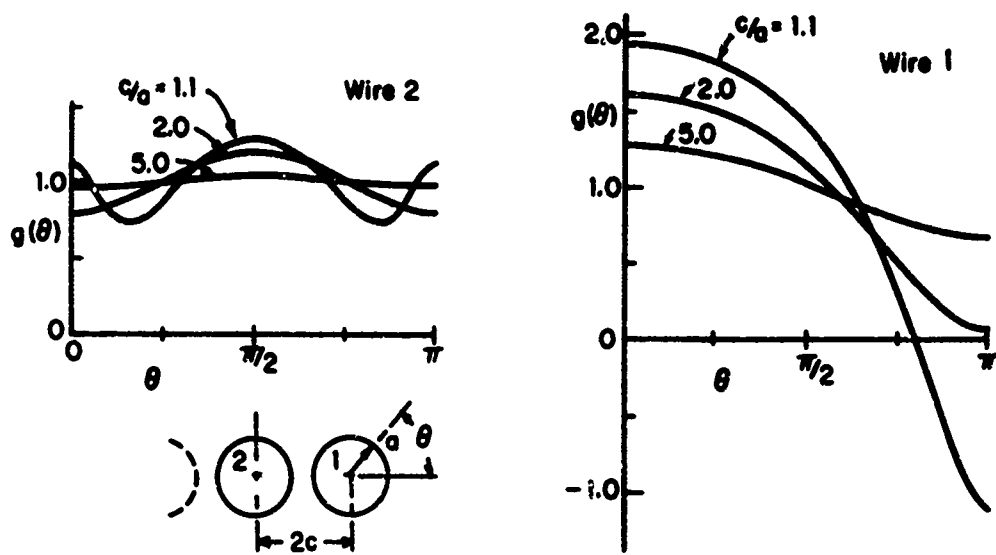


FIG. 1-5 NORMALIZED SURFACE CURRENT DISTRIBUTION FOR THREE WIRES

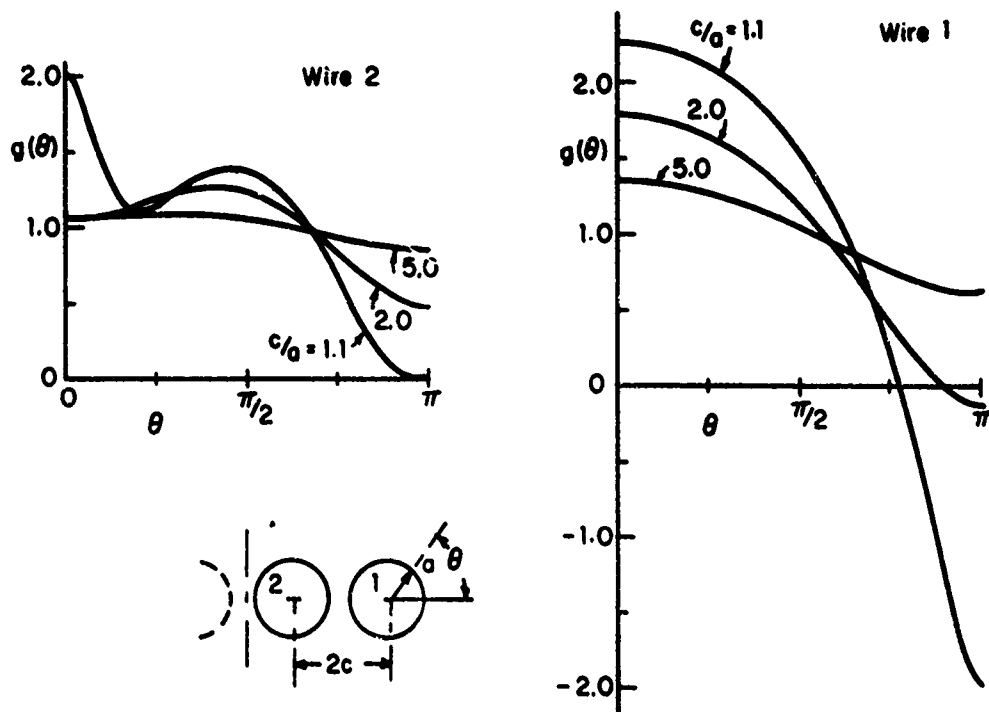


FIG. 1-6 NORMALIZED SURFACE CURRENT DISTRIBUTION FOR FOUR WIRES

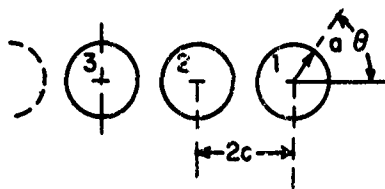
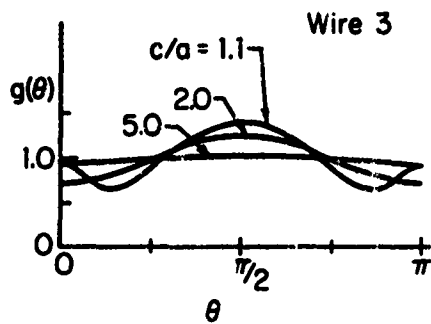
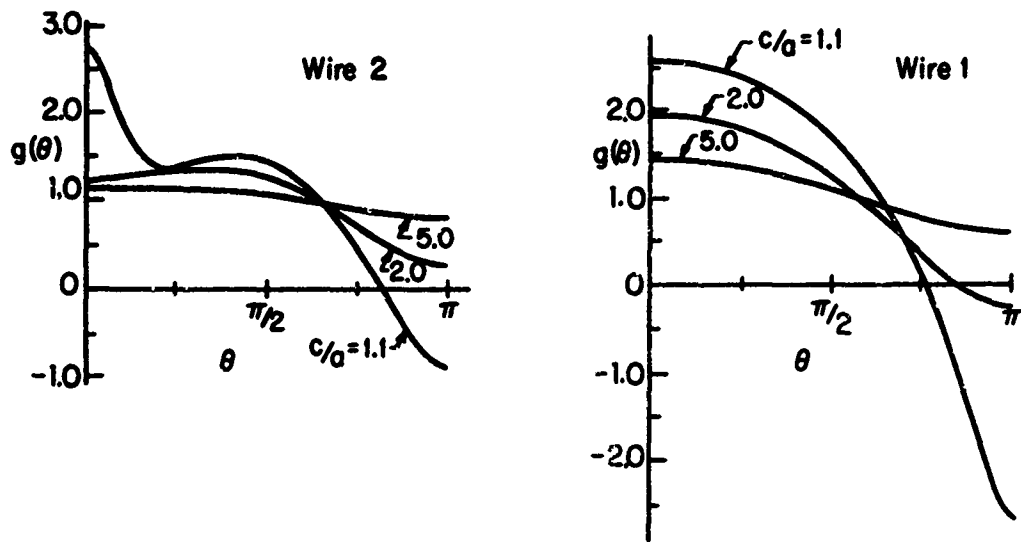


FIG.1-7 NORMALIZED SURFACE CURRENT DISTRIBUTION FOR FIVE WIRES

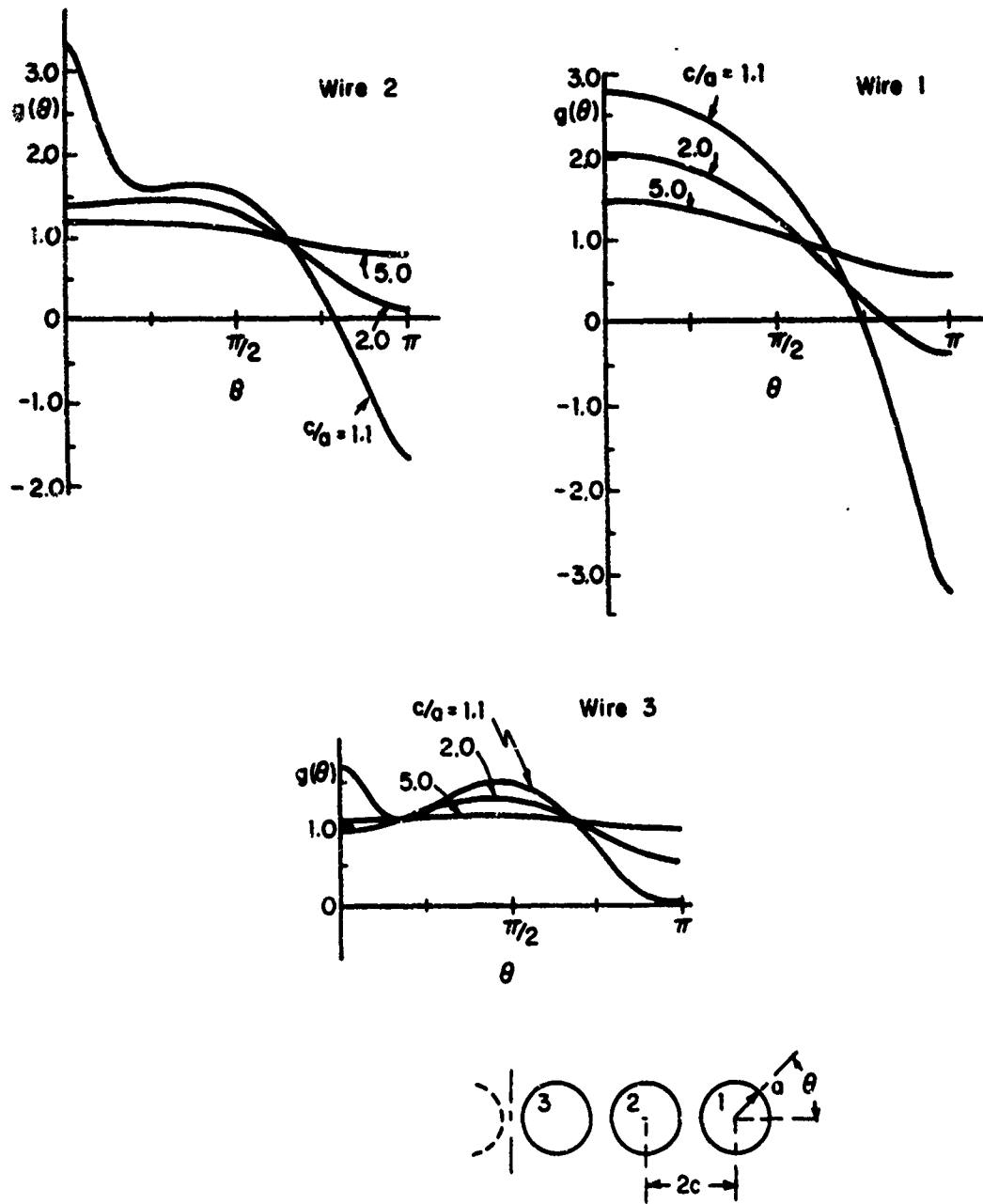


FIG.1-8 NORMALIZED SURFACE CURRENT DISTRIBUTION FOR SIX WIRES

Table 1-1. Normalized Additional Ohmic Resistance Per Unit Length  
Due to the Proximity Effect  $R_p/R_o$ .

Spacing $c/a$	Number of Conductors						
	2	3	4	5	6	7	8
1.00	0.333						
1.05	0.316	0.748	1.231				
1.10	0.299	0.643	0.996	1.347	1.689	2.020	2.340
1.15	0.284	0.580	0.868	1.142	1.400	1.693	1.872
1.20	0.268	0.531	0.777	1.002	1.210	1.401	1.577
1.25	0.254	0.491	0.704	0.896	1.068	1.224	1.365
1.30	0.240	0.455	0.644	0.809	0.956	1.086	1.203
1.40	0.214	0.395	0.546	0.674	0.784	0.880	0.965
1.50	0.191	0.346	0.470	0.572	0.658	0.732	0.796
1.60	0.173	0.305	0.408	0.492	0.561	0.620	0.670
1.70	0.155	0.270	0.353	0.428	0.485	0.532	0.573
1.80	0.141	0.241	0.316	0.375	0.423	0.462	0.495
1.90	0.128	0.216	0.281	0.332	0.372	0.405	0.433
2.00	0.116	0.195	0.252	0.295	0.330	0.358	0.392
2.20	0.098	0.161	0.205	0.239	0.265	0.286	0.304
2.40	0.032	0.135	0.170	0.197	0.217	0.234	0.247
2.50	0.077	0.124	0.156	0.180	0.198	0.213	0.225
2.60	0.071	0.114	0.144	0.165	0.182	0.195	0.206
2.80	0.061	0.098	0.123	0.141	0.154	0.165	0.174
3.00	0.054	0.085	0.106	0.121	0.133	0.142	0.150
3.50	0.040	0.062	0.077	0.087	0.095	0.101	0.106
4.00	0.031	0.048	0.058	0.066	0.072	0.076	0.080

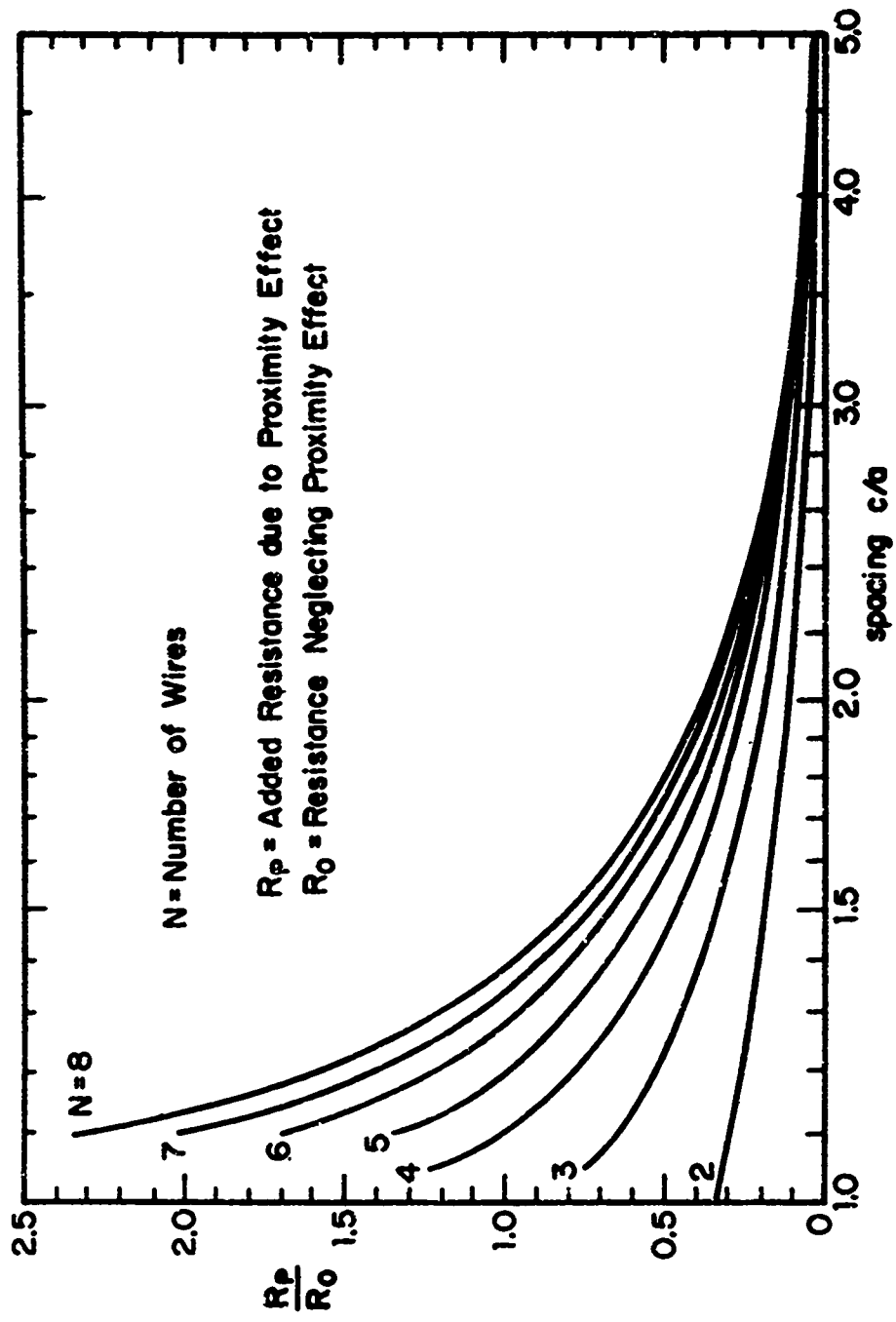


FIG. 1-9 THE ADDITIONAL OHMIC RESISTANCE PER UNIT LENGTH OF A SYSTEM OF PARALLEL WIRES DUE TO THE PROXIMITY EFFECT.

3 and 4 wires,  $c/a$  less than 1.05; 5 or more wires,  $c/a$  less than 1.10. The reason for this will be evident after a closer examination of the approximation already made.

In the limit as  $c/a$  approaches 1.0, the surface current develops large spikes at adjacent points on successive cylinders. This is illustrated for 3 wires with spacings  $c/a = 1.10, 1.05, \text{ and } 1.01$  in Fig. 1-10. For wires with finite conductivity, a change in the form of the current distribution in the radial direction is expected to accompany these areas of high current density. As a result, the radial decay rate will differ from the high frequency skin depth  $d_s$  in these regions. This is basically the same idea expressed in equation (1-22). Spikes in the surface current require high harmonic content ( $p$  large) which, from (1-22), require very small skin depths (high conductivity) for the high frequency skin effect approximation to be valid.

In Fig. 1-11 the resistance  $R_p/R_o$  is plotted against the number of harmonic terms used in the series representing the current. The coefficients  $a_{mp}$  obtained by either of the approximate methods, unlike the Fourier coefficients, are a function of the number of terms  $q$  used in the series. They approach the exact coefficients in the limit as  $q$  becomes large or, in terms of the resistance, as  $R_p/R_o$  converges to the limiting value. For this reason the coefficients used in constructing Fig. 1-11 are those found for the limiting value of  $R_p/R_o$ . From Fig. 1-11, 6 harmonic terms are sufficient to give  $R_p/R_o$  to within 1% of the limiting value for the minimum conductor spacings presented in Table 1-1. Using equation (1-22) with 6 harmonic terms, the high frequency skin effect approximation will be valid provided

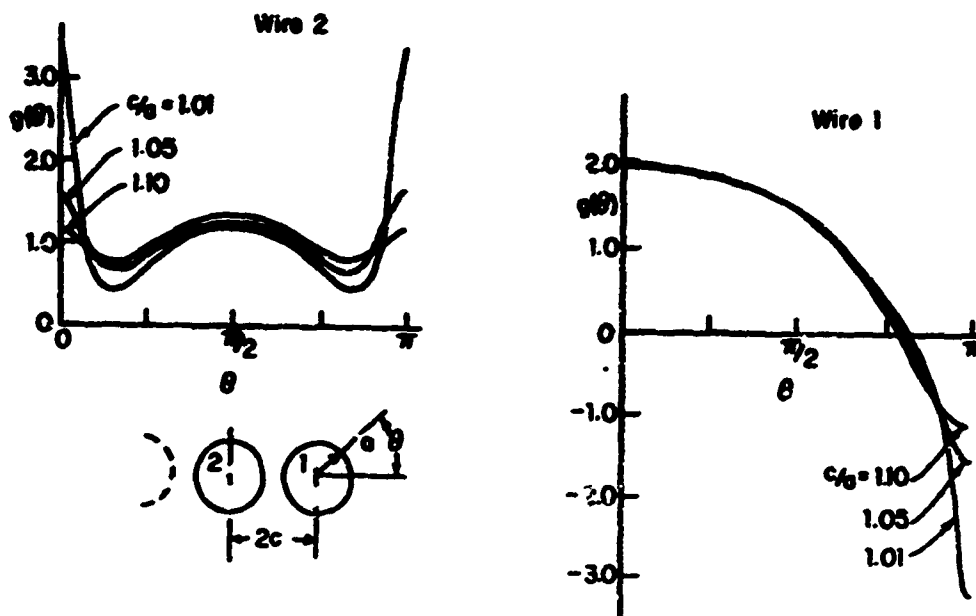


FIG. 1-10 NORMALIZED SURFACE CURRENT DISTRIBUTION FOR THREE WIRES WITH CLOSE SPACING.

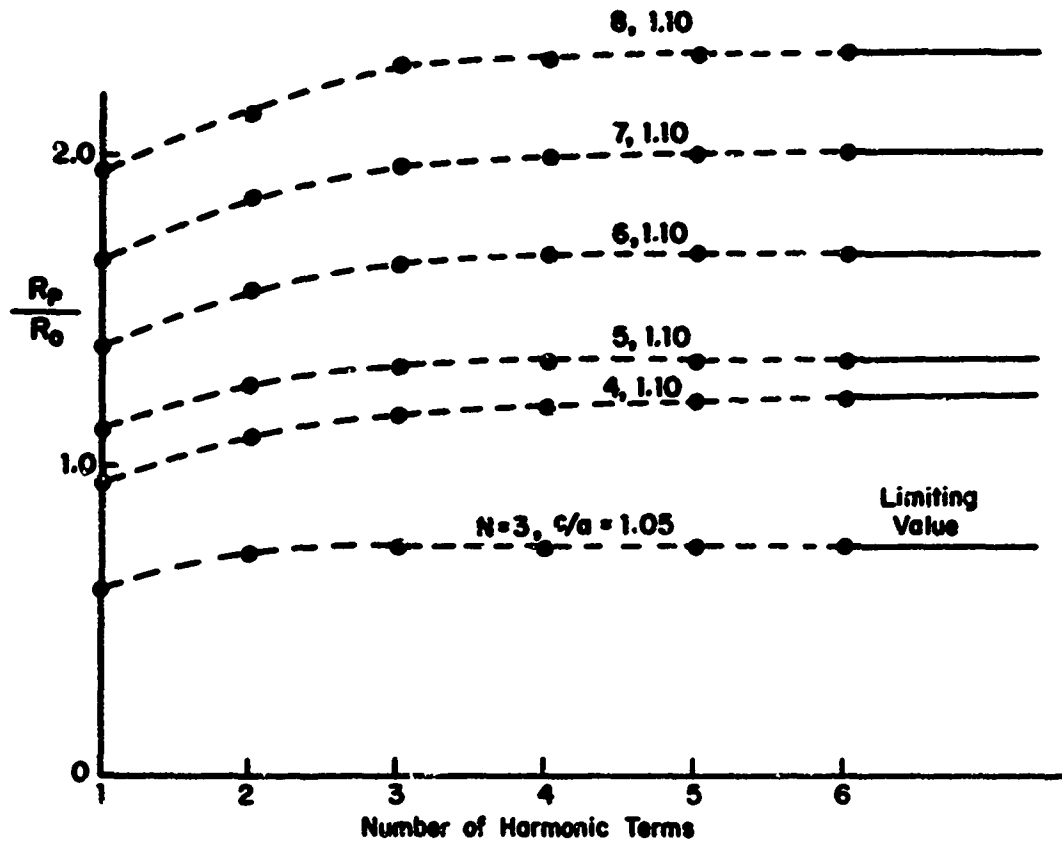


FIG. 1-11 THE RESISTANCE  $R_p/R_0$  AS A FUNCTION OF THE NUMBER OF HARMONIC TERMS USED TO REPRESENT THE CURRENT DISTRIBUTION ON EACH WIRE. THE SPACINGS  $c/a$  ARE THE MINIMUM VALUES PRESENTED IN TABLE 1-1.

$$a/d_s \gg 1 \tag{1-69a}$$

$$\frac{9\left(\frac{d_s}{a}\right)^2}{\left(1-9\frac{d_s}{a}\right)} \ll 1 \tag{1-69b}$$

These conditions are satisfied by most wire sizes used in practical antennas operating at frequencies above 1 MHz.; for example: 1/8 inch radius copper wire has the following values

Frequency (MHz.)	a/d <sub>s</sub>	$\frac{(3d_s/a)^2}{(1-9d_s/a)}$
1	34	1.1 x 10 <sup>-2</sup>
10	107	8.5 x 10 <sup>-4</sup>
100	340	8.0 x 10 <sup>-5</sup>

The failure of the skin effect approximation for extremely close conductor spacings places no serious restriction on the usefulness of the solution, since in practical applications the minimum spacing, determined by the thickness of the wire insulation, is usually within the range of values covered in Fig. 1-9 and Table 1-1.

#### 4. Comparison with the Work of Butterworth

As previously mentioned, Butterworth has calculated the ohmic resistance of systems of parallel wires. In this section two of his formulas, rewritten in the form  $R_p/R_o$ , are compared with the present

calculations of additional ohmic resistance due to the proximity effect (Fig. 1-9). The first graph in Fig. 1-12 is a comparison with Butterworth's "semi-empirical formula" which, for high frequencies, can be written as [10, p. 709, equation 53]

$$\frac{R_p}{R_o} \doteq \frac{1}{8} w_n (a/c)^4 + \frac{u_n (a/c)^2}{2(1 - \frac{1}{4} v_n (a/c)^2)^2} \quad (1-70)$$

where  $u_n$ ,  $v_n$ , and  $w_n$  are constants which depend on the number of conductors in the system. This formula gives results which are in fair agreement with the present calculations.

In the second graph of Fig. 1-12, the present theory is compared with another of Butterworth's formulas, one which is often found in handbooks on coil design [11], [13], and [14]. This formula is derived by making assumptions similar to those already discussed. Consider each conductor to be in a uniform magnetic field due to the other conductors. With (1-53) and (1-4), the power loss per unit length in the  $m^{\text{th}}$  conductor is

$$P_m \doteq \frac{I^2}{4\pi a} R^s \left[ 1 + \frac{1}{2} (a/c)^2 \left( \sum_{\substack{l=1 \\ l \neq m}}^n \frac{1}{(m-l)} \right)^2 \right] \text{ Watts/meter} \quad (1-71)$$

and the resulting ohmic resistance due to the proximity effect becomes

$$\frac{R_p}{R_o} \doteq \frac{1}{2} (a/c)^2 \left[ \sum_{m=1}^n \left( \sum_{\substack{l=1 \\ l \neq m}}^n \frac{1}{(m-l)} \right)^2 \right] \quad (1-72)$$

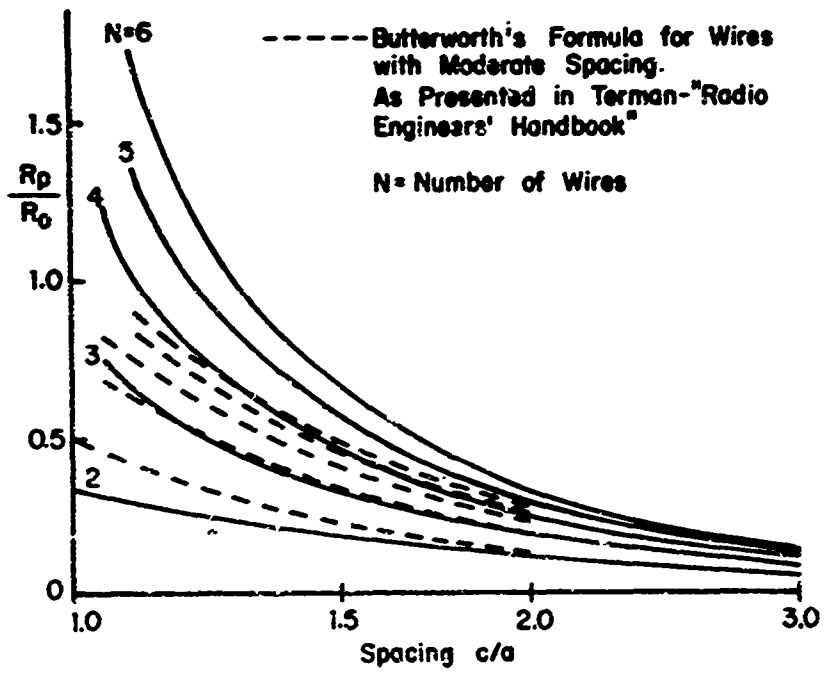
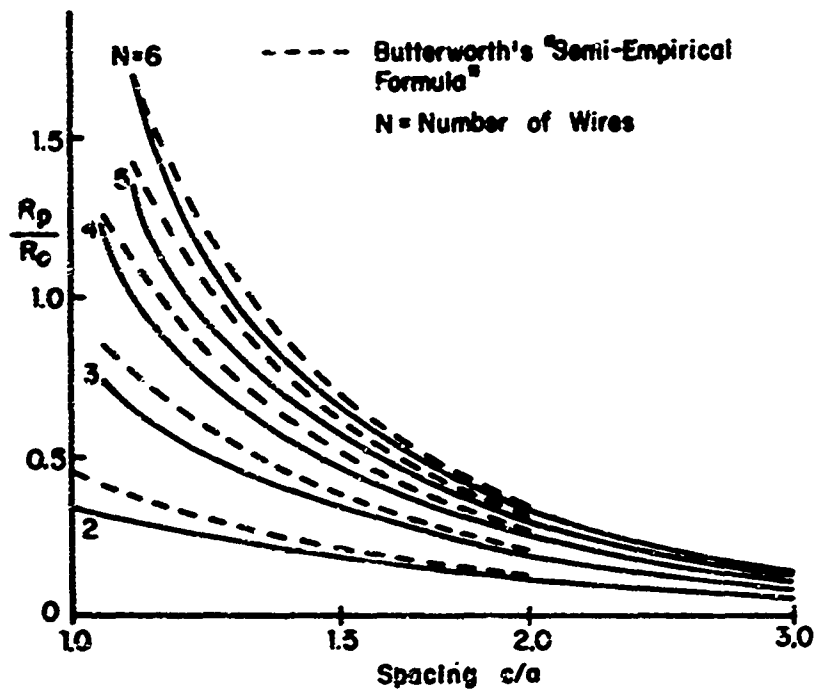


FIG.1-12 THE ADDITIONAL OHMIC RESISTANCE DUE TO THE PROXIMITY EFFECT-COMPARISON WITH BUTTERWORTH'S SOLUTIONS.

As seen in Fig. 1-12, this formula gives results which are obviously in error for spacings in the range  $1 \leq c/a \leq 2$ . It is applicable only in a region ( $c/a \gg 1$ ) where the proximity effect is of little interest, since values of  $R_p/R_o$  are small and fairly independent of the number of wires.

### 5. Optimum Conductor Spacing when the Cross Sectional Dimensions are Restricted

In certain applications a given number  $n$  of parallel, in-line conductors must fit within a specified length  $l$ ; see Fig. 1-13. It is of interest to ask for which wire radius  $a$ , or spacing  $c/a$ , is the resistance of the wires a minimum. If there were no proximity effect, making the radius of the wire as large as possible ( $a = l/2n$ ) would minimize the skin effect resistance. With the proximity effect present, increasing the wire radius increases the loss due to proximity and a minimum resistance point is reached where the decrease in skin effect loss is just balanced by an increase in proximity loss. In Fig. 1-13, the dimensionless quantity  $2\pi l R/nR^s$ , which is proportional to the ohmic resistance per unit length of the system of conductors, is plotted against the normalized wire radius  $a/l$ . The points of minimum resistance are clearly exhibited in Fig. 1-13 and the corresponding conductor spacings are listed in Table 1-2.

Number of Conductors $n$	$a/l$	$c/a$	$\frac{2\pi l R}{R^s}$
2	0.250	1.00	5.33
3	0.148	1.19	10.41
4	0.098	1.37	16.07
5	0.071	1.50	22.01
6	0.056	1.59	28.10
7	0.046	1.66	34.30
8	0.039	1.71	40.57

Table 1-2. Conductor Spacings for Minimum Resistance.

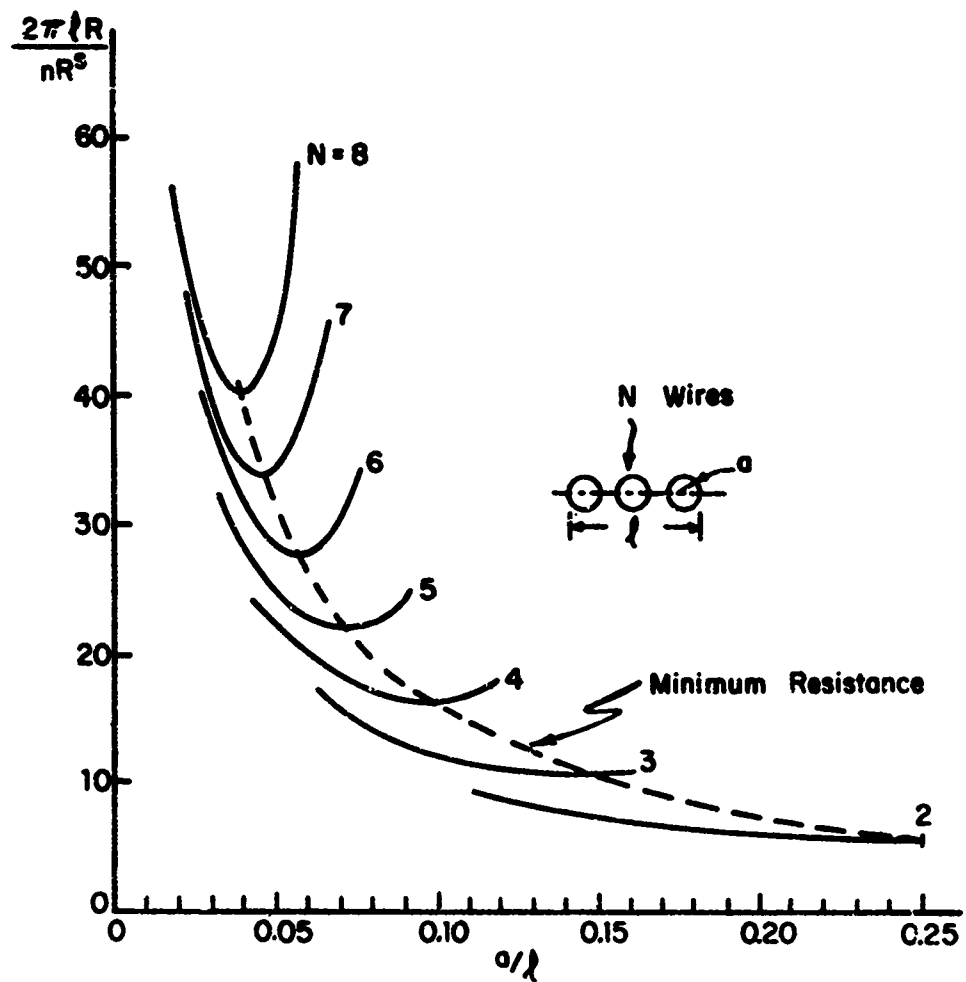


FIG. 1-13 THE OHMIC RESISTANCE AS A FUNCTION OF THE WIRE RADIUS  $a$  WITH THE DEPTH OF WINDING  $l$  FIXED

6. Conclusion

Systems of equally spaced, in-line conductors carrying equal currents in the same direction have been studied. A set of integral equations was formulated to determine the transverse distribution of axial current at high frequencies when the current is confined to a thin skin near the conductor surface. Using the integral equations, an approximate solution for the current in the form of a trigonometric series was obtained. For two wires, the approximate solution for the current showed good agreement with an exact expression obtained by a conformal mapping procedure.

With the current distribution determined, the high frequency resistance per unit length of the system was calculated for various numbers of conductors and spacings. The results of these calculations may be summarized qualitatively as follows:

i. For small numbers of conductors, the additional ohmic resistance due to the proximity effect  $R_p/R_o$  increases either with an increase in the number of conductors or with a decrease in the conductor spacing. This was checked for systems with up to eight wires and spacings as close as  $c/a = 1.1$ .

ii. For closely spaced conductors the additional ohmic resistance due to the proximity effect can be greater than the resistance of the isolated wires.

iii. When the cross sectional length  $l = 2a + (n-1)c$  of the group of conductors is restricted, there is a definite wire radius that will give a minimum resistance per unit length for the system.

Only cylinders carrying equal currents in the same direction were considered in this chapter. With a simple scaling of the harmonic terms on each conductor the present theory and associated computer codes could handle systems of wires with different net currents in each wire. Such a solution would be useful for making computations for multiwire transmission lines where the wires carry currents with equal magnitude but in opposite directions.

## SECTION II

### THE ELECTRICALLY SMALL MULTITURN LOOP ANTENNA

#### 1. Introduction

The single turn loop has been the subject of much investigation and from the practical standpoint adequate design data are available for this structure [28], [29]. The multiturn loop, with no restrictions on electrical size, has received much less attention. The solutions available are for the "one dimensional" current distribution and therefore, strictly speaking, only valid for loops with spacings between turns large compared to the wire diameter [30], [31].

In practical applications, the electrically small loop is often used because it has a desirable field pattern as compared to larger loops whose patterns have many lobes. The ohmic resistance of small loops is in general much larger than the radiation resistance, thus radiation efficiencies are very low and greatly dependent on the ohmic resistance. In an effort to increase the radiation efficiency multiturn structures are often used. The radiating properties (radiation resistance and field pattern) of electrically small single or multiturn loops are easily derived, either directly from the integral form of Maxwell's equations [28], [32] or as a limiting case of one on the more general analyses mentioned above. These methods are usually concerned with perfectly conducting wires and thus provide no information about ohmic loss of the antenna.

The ohmic resistance of a small loop is usually taken to be the same as that of an equivalent length of straight conductor. This assumption, although adequate for the single turn loop, is not for the multiturn case. In a multiturn loop, the distribution of current over the conductor cross section is determined by the same effects discussed in Chapter I - - proximity and skin effects. The increase in ohmic resistance due to the proximity effect, which is normally unimportant in large antennas, has a dramatic effect on calculations of the power radiated by electrically small transmitting loops.

## 2. Review of Small Loop Theory

The properties of electrically small loop antennas covered in the literature are briefly discussed below. For a more detailed discussion, see King [32] or King and Harrison [28].

The model chosen to represent the multiturn loop antenna is illustrated in Fig. 2-1. All turns of the loop are circular and lie in parallel planes. The straight segments of wire interconnecting the turns and the feed wires of the delta-function generator are short, parallel and closely spaced. These are assumed to have negligible ohmic resistance compared to that of the overall circuit, and to contribute negligibly to the radiation resistance since parallel segments carry equal and oppositely directed currents. The dimension  $2c$  is exaggerated in Fig. 2-1.

The multiturn loop with  $n$  turns will have essentially the same total current ( $I$ ) at any conductor cross section, provided

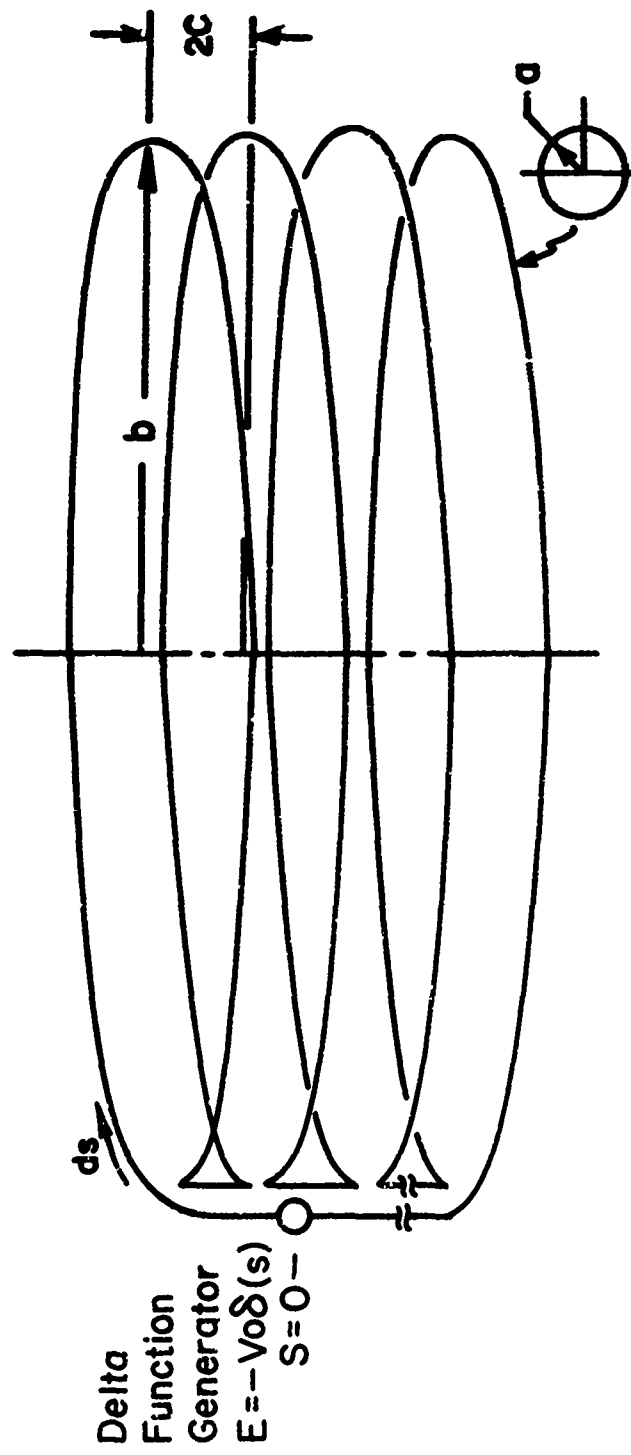


FIG. 2-1 MODEL FOR THE MULTITURN LOOP ANTENNA

the total length of the loop is much less than the free space wavelength at the operating frequency. More specifically,

$$I(s) \doteq I \quad (2-1)$$

when

$$\beta_0 nb \ll 1 \quad (2-2)$$

For this analysis, the following additional constraints are placed on the wire radius  $a$  and the turn spacing  $c$ .

$$a \ll b, \quad \beta_0 a \ll 1 \quad (2-3)$$

$$n^2 c^2 \ll b^2, \quad c > a \quad (2-4)$$

A real power equation expressed in terms of the scalar and vector potentials  $\phi$  and  $\vec{A}$  for the loop antenna is

$$\text{Re} \left( \int_V \vec{J} \cdot \vec{E}_\delta \, dv \right) = \text{Re} \left( \int_V \frac{J^2}{\sigma} \, dv - i\omega \int_V \vec{J} \cdot \vec{A} \, dv - i\omega \int_S \eta \phi \, ds \right) \quad (2-5)$$

where  $\vec{J}$  represents the free current density,  $\eta$  the free surface charge density,  $\sigma$  the conductivity of the antenna wire, and  $\vec{E}_\delta$  the electric field of the delta-function generator. The first three integrals are over the volume occupied by the loop conductor and generator while the fourth is over the surface of this volume. An  $e^{-i\omega t}$  time dependence is assumed.

Fig. 2-2 shows sections of two typical loop turns and the coordinates associated with them. Making use of (2-1), and assuming the transverse current distribution to be the same at any cross section, the current density on the  $m^{\text{th}}$  turn becomes

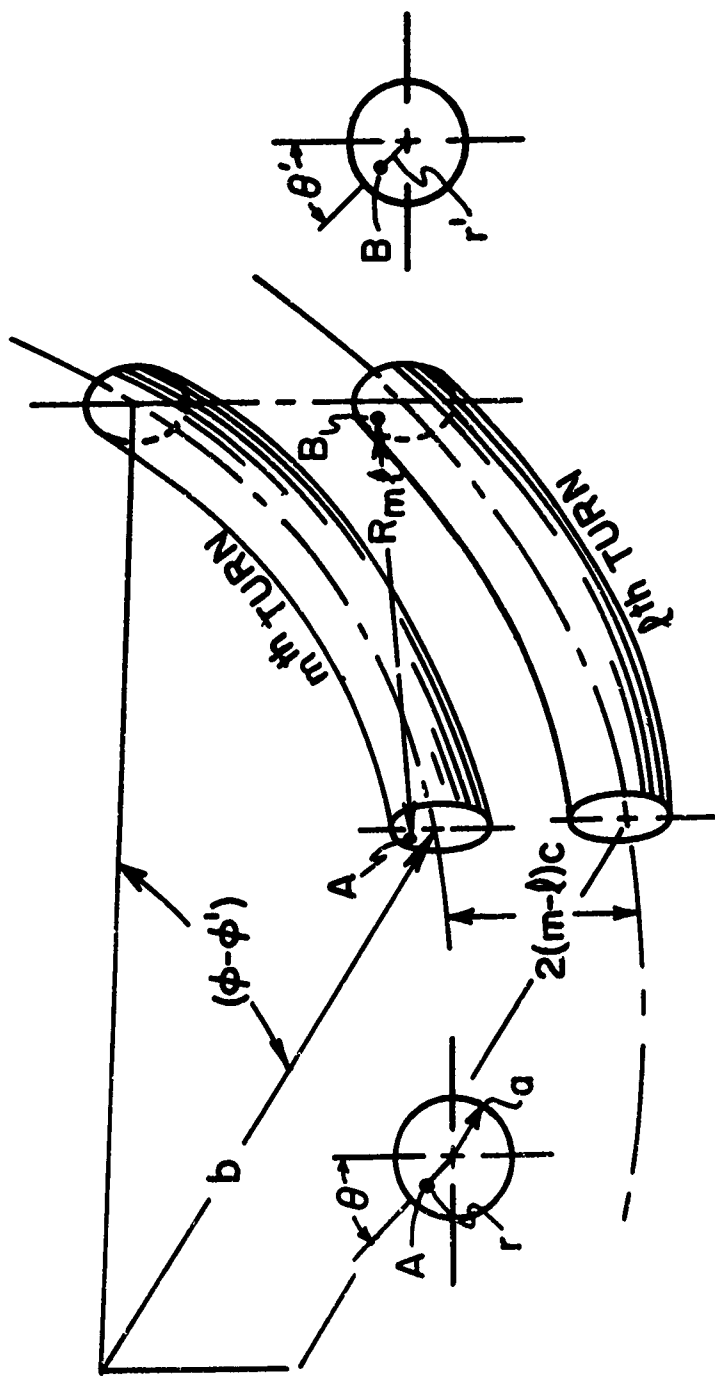


FIG. 2-2 SECTIONS OF TWO TYPICAL LOOP TURNS

$$\vec{J}_m(r, \theta, \varphi) = J_{m\varphi}(r, \theta) \hat{\varphi} \quad (2-6)$$

where

$$\int_{\theta=-\pi}^{\pi} \int_{r=0}^a J_m(r, a) r dr d\theta = I \quad (2-7)$$

The assumption of constant current also precludes the possibility of a charge accumulation on the loop turns. Therefore,

$$\eta = 0 \quad (2-8)$$

With (2-6), (2-7) and (2-8), and the definition of the delta-function generator

$$E_\delta = -V_o \delta(s) \quad (2-9)$$

(the distance  $s$  is shown in Fig. 2-1), (2-5) becomes

$$\begin{aligned} IV_o = & \sum_{m=1}^n \left\{ \frac{2\pi b}{\sigma} \int_{\theta=-\pi}^{\pi} \int_{r=0}^a J_{m\varphi}^2(r, a) r dr d\theta \right. \\ & \left. + \operatorname{Re} \left[ -i2\pi b w \int_{\theta=-\pi}^{\pi} \int_{r=0}^a J_{m\varphi}(r, a) A_{m\varphi}(r, \theta) r dr d\theta \right] \right\} \quad (2-10) \end{aligned}$$

$A_{m\varphi}$  is the component of the vector potential tangent to the axis of the conductor of the  $m^{\text{th}}$  turn.

Referring to Fig. 2-2, the vector potential at point A due to the current element at point B is

$$dA_{m\ell\varphi}(r, a, \varphi) = \frac{\mu_0 e^{i\beta_0 R_{m\ell}}}{4\pi R_{m\ell}} J_{\ell\varphi}(r', \theta') (b + r' \cos \phi') \cos(\theta - \theta') r' dr' d\theta' d\varphi' \quad (2-11)$$

where

$$R_{m\ell} = \left\{ 4b^2 \sin^2 [(\theta - \theta')/2] + 4(m-\ell)^2 c^2 + r^2 + r'^2 + 2rr' \cos(\phi - \varphi') \right\}^{\frac{1}{2}} \quad (2-12)$$

The vector potential at A due to the current in all turns is then

$$A_{m\varphi} = \frac{\mu_0}{4\pi} \sum_{\ell=1}^n \left[ \int_{\varphi'=-\pi}^{\pi} \int_{\theta'=-\pi}^{\pi} \int_{r'=0}^a J_{\ell\varphi}(r', \theta') \frac{e^{i\beta_0 R_{m\ell}}}{R_{m\ell}} \cos(\theta - \theta') (b + r' \cos \varphi') r' dr' d\theta' d\varphi' \right] \quad (2-13)$$

Introducing the condition on the conductor length described in (2-2), the exponential in the integrand of (2-13) is expanded in a power series in  $\beta_0 R_{m\ell}$ . Keeping the first two imaginary terms in this series yields

$$\text{Im} \left( e^{i\beta_0 R_{m\ell}} \right) = \beta_0 R_{m\ell} - \frac{\beta_0^3 R_{m\ell}^3}{6} \quad (2-14)$$

and the imaginary part of (2-13) becomes

$$\text{Im}(A_{m\varphi}) = \frac{\mu_0}{4\pi} \sum_{\ell=1}^n \left[ \int_{\varphi'=-\pi}^{\pi} \int_{\theta'=-\pi}^{\pi} \int_{r'=0}^a J_{\ell\varphi}(r', \theta') \left( \beta_0 - \frac{\beta_0^3 R_{m\ell}^2}{6} \right) \cos(\theta - \theta') (b + r' \cos \varphi') r' dr' d\theta' d\varphi' \right] \quad (2-15)$$

For the purpose of calculating the second integral in (2-10), the radiation term, and approximate value of the vector potential  $A_{m\varphi}$  is used. Subject to the restrictions on the conductor radius expressed in (2-3),  $A_{m\varphi}$  is approximately the vector potential that would exist on the surface of the wire with the loop current  $I$  located along the axis of the conductors. King [33] discusses the validity of this type of approximation when used in calculating the vector potential. With this simplification, (2-15) reduces to the following

$$\text{Im}(A_{m\varphi}) = \frac{\mu_0 I b}{4\pi} \sum_{\ell=1}^n \int_{\varphi'=-\pi}^{\pi} \frac{-\beta_0^3 R_{m\ell}^2}{6} \cos(\varphi - \varphi') d\varphi' \quad (2-16)$$

where

$$R_{m\ell} = \left\{ 4b^2 \sin^2 [(\theta - \theta')/2] + 4(m-\ell)^2 c^2 + a^2 \right\} \quad (2-17)$$

and (2-10) becomes

$$V_o = I \left\{ \sum_{m=1}^n \left[ \frac{2\pi b}{\sigma} \int_{\alpha=-\pi}^{\pi} \int_{r=0}^a \frac{J_{m\varphi}^2(r, \theta)}{I^2} r dr d\theta \right. \right. \\ \left. \left. + \frac{\mu_0 \beta_0^3 b^2}{12} \sum_{\ell=1}^n \int_{\varphi'=-\pi}^{\pi} -R_{m\ell}^2 \cos(\alpha - \theta') d\theta' \right] \right\} \quad (2-18)$$

Evaluating the second integral, (2-18) becomes

$$V_o = I \left\{ \sum_{m=1}^n \left[ \frac{2\pi b}{\sigma} \int_{\theta=-\pi}^{\pi} \int_{r=0}^a \frac{J_{m\phi}^2(r, \theta)}{I^2} r dr d\theta \right] + 20\pi^2 n^2 \beta_o^4 b^4 \right\}$$

$$= I \left[ R_{Ohmic} + R_{Rad.} \right] \quad (2-19)$$

where the two terms on the right hand side of the equation are identified as the ohmic and radiation resistances.

The radiation efficiency of the n turn loop is now

$$E_A = \frac{R_{Rad.}}{R_{Rad.} + R_{Ohmic}} = \frac{20\pi^2 n^2 \beta_o^4 b^4}{20\pi^2 n^2 \beta_o^4 b^4 + R_{Ohmic}} \quad (2-20)$$

This simple form is a consequence of the constant current assumption which makes the ohmic and radiation resistances appear as circuit elements in series.

### 3. Transverse Current Distributions

To evaluate the expression (2-20) for the radiation efficiency the transverse current distribution is needed. If the skin effect approximation applies,  $a/ds \gg 1$ , the ohmic resistance term in equation (2-20) can be replaced by

$$\sum_{m=1}^n \left[ \frac{2\pi b}{\sigma} \int_{\theta=-\pi}^{\pi} \int_{r=0}^a \frac{J_{m\phi}^2(r, \theta)}{I^2} r dr d\theta \right] = \frac{bR^s}{2\pi a} \sum_{m=1}^n \int_{\theta=-\pi}^{\pi} g_{m\phi}^2(\theta) d\theta \quad (2-21)$$

where  $g_{m\phi}(\theta)$  is normalized surface current density on an equivalent perfectly conducting loop.

Using a procedure similar to that in section I-3, the transverse current distribution  $g_{m\phi}(\theta)$  can be derived. The integral for the vector potential component  $\vec{A}_\phi$  at a point  $(r, \theta, \phi)$  just off the surface of the  $m^{\text{th}}$  turn is

$$A_{m\phi}(r, \theta, \phi) = \frac{\mu_0 I b}{8\pi^2} \int_{\phi'=-\pi}^{\pi} \int_{\theta'=-\pi}^{\pi} \sum_{l=1}^n \left[ \frac{g_l(\theta') e^{i\beta_0 R_{ml}}}{R_{ml}} \cos(\phi - \phi') \right] d\theta' d\phi' \quad (2-22)$$

where

$$R_{ml} = \left\{ [ 2b^2 + 4(m-l)^2 c^2 + r^2 + a^2 + 4(m-l)c(r \cos\theta - a \cos\theta') - 2b(r \sin\theta + a \sin\theta') - 2ar \cos\theta \cos\theta' ] - 2[(b - r \sin\theta)(b - a \sin\theta') \cos(\phi - \phi')] \right\}^{\frac{1}{2}} = \left\{ q^2 - p \cos(\phi - \phi') \right\}^{\frac{1}{2}} \quad (2-23)$$

with the condition (2-23) is small compared to unity. Dropping terms of this order, (2-22) becomes

$$A_{m\phi}(r, \theta, \phi) = \frac{\mu_0 I b}{8\pi^2} \int_{\phi'=-\pi}^{\pi} \int_{\theta'=-\pi}^{\pi} \sum_{l=1}^n \left[ \frac{g_l(\theta') \cos(\phi - \phi')}{[q - p \cos(\phi - \phi')]^{\frac{1}{2}}} \right] d\theta' d\phi' \quad (2-24)$$

This is equivalent to considering the quasistatic fields as the primary factor in determining the transverse current distribution. The integration with respect to  $\phi'$  may be expressed in the form

$$A_{m\varphi}(r, \theta, \varphi) = \frac{\mu_0 I b}{8\pi^2} \int_{\theta'=-\pi}^{\pi} \sum_{\ell=1}^n \left\{ \frac{4p}{\sqrt{p+q}} g_{\ell}(\theta') \left[ K'(k) - \frac{(p-q)}{q} E(k) \right] \right\} d\theta' \quad (2-25)$$

where  $K$  and  $E$  are the complete elliptic integrals of the first and second kind [34]. The modulus  $k$  and complimentary modulus  $k'$  of the elliptic integrals are

$$k = \sqrt{\frac{2p}{p+q}} \quad (2-26a)$$

$$(k')^2 = 1 - k^2 \quad (2-26b)$$

Subject to the restrictions imposed in (2-3) and (2-4)

$$(k')^2 = \left( \frac{r_{m\ell}}{2b} \right)^2 \left[ 1 + O\left(\frac{a}{b}\right) + O\left(\frac{(m-\ell)^2 c^2}{b^2}\right) + \dots \right] \approx \left( \frac{r_{m\ell}}{2b} \right)^2 \quad (2-27)$$

where

$$r_{m\ell} = \left[ 4(m-\ell)^2 c^2 + a^2 + r^2 + 4(m-\ell)c(r \cos \theta - a \cos \theta') - 2ar \cos(\theta - \theta') \right]^{\frac{1}{2}} \quad (2-28)$$

Since  $r_{m\ell}$  is of the order of  $2(m-\ell)c$ ,  $(k')^2$  is a small quantity

$$(k')^2 = O\left(\frac{(m-\ell)c}{b}\right)^2 \ll 1 \quad (2-29)$$

and the power series representations for  $K$  and  $E$  are useful [35].

$$K = \mu_0 I + \frac{\mu_0 I}{4} k'^2 + \frac{9}{6} \left( -\frac{7}{6} \right) k'^4 + \dots \quad (2-30a)$$

$$E = 1 + \frac{1}{2} \left( \mu_0 - \frac{1}{2} \right) k'^2 + \frac{3}{16} \left( \mu_0 - \frac{13}{12} \right) k'^4 + \dots \quad (2-30b)$$

$$\Lambda = \ln \left( \frac{b}{k'r} \right) \quad (2-30c)$$

Substituting the above series into (2-25) and dropping all terms small compared to unity  $a/b$ ,  $(r_1-1)^2 c^2/b^2$  or less, the integral for the vector potential becomes

$$A_{m\phi}(r, \theta, \phi) = \frac{\mu_0 I}{8\pi} \left\{ -2 \int_{\theta'=-\pi}^{\pi} \sum_{\ell=1}^n \left[ g_{\ell}(\theta') \ln(r_{m\ell}) \right] \cos \ell \theta' + 4\pi n \left[ \ln(8b) - z \right] \right\} \quad (2-31)$$

Except for a term with only  $z$  dependence and an additive constant, this expression is the same as that for  $A_{mz}(r, \theta, z)$  in the equivalent system of parallel, straight conductors, equation (2-30).

Due to the symmetry already assumed in this problem, only the  $A_{m\phi}$  component of the vector potential is involved in the expression for the surface current density,  $g_m(\theta)$ .

$$g_m(\theta) = \frac{-2\pi a}{\mu_0 I} \left. \frac{2A_{m\phi}(r, \theta, \phi)}{2r} \right|_{r=a} \quad (2-32)$$

With (2-31) substituted into (2-32), the resulting equation for the current density is identical to that for the straight conductors (1-39).

Subject to the inequalities presented in equations (2-2), (2-3) and (2-4), the transverse current distributions on the loop turns

and the ohmic resistance per unit length are the same as those for a system of parallel, straight conductors which have the same wire radius and spacing.

#### 4. Radiation Efficiency

With the results of the last section and equation (2-20), the radiation efficiency of an  $n$  turn electrically small loop is

$$E_A = \frac{20 \pi^2 n^2 \beta_o^4 b^4}{20 \pi^2 n^2 \beta_o^4 b^4 + n R^2 \left(\frac{b}{a}\right) \left(1 + \frac{R_p}{R_o}\right)} \quad (2-33)$$

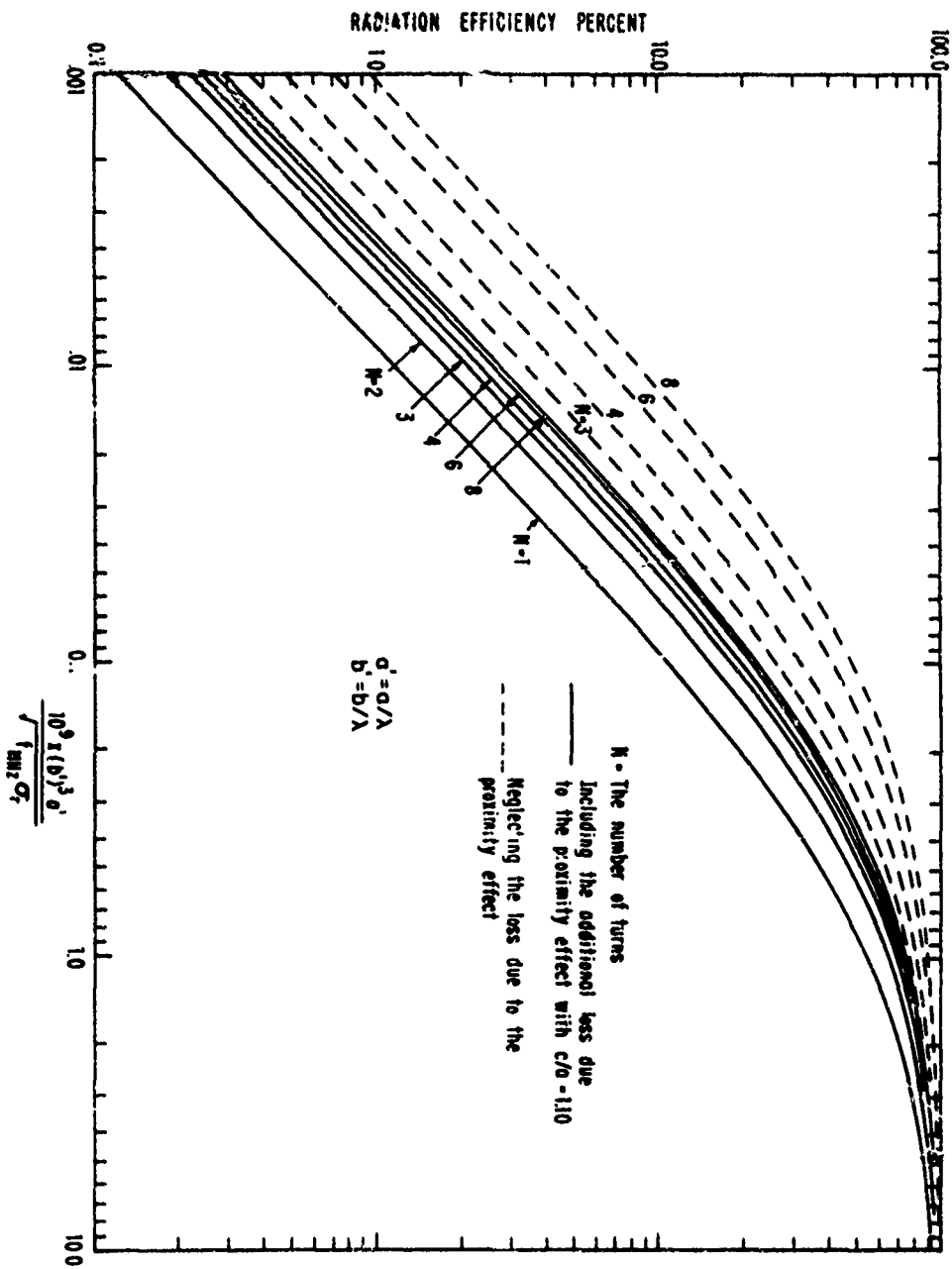
Rearranging terms, the efficiency becomes

$$E_A = \frac{1}{1 + \frac{8.48 \times 10^{-10} \sqrt{f_{\text{MHz}} \sigma_r}}{n (b')^3 a'}} \left(1 + \frac{R_p}{R_o}\right) \quad (2-34)$$

where  $a'$  and  $b'$  are the radius of the wire and the radius of the loop normalized to the free space wavelength,  $f_{\text{MHz}}$  is the frequency in megahertz, and  $\sigma_r$  is the ratio of the conductivity of the loop wire to that of copper ( $\sigma_{\text{Cu}} = 5.8 \times 10^7 / \text{ohm-m}$ ). In Fig. 2-3, the efficiency is plotted as a function of the dimensionless quantity  $(b')^3 a' / \sqrt{f_{\text{MHz}} \sigma_r}$  and the number of turns. The dashed lines are for no loss due to proximity ( $R_p/R_o = 0$ ) while the solid lines include the proximity effect for a spacing  $c/a = 1.10$ . For most practical applications, these two lines will give an upper and lower bound on the efficiency obtainable with various turn spacings.

Neglecting the proximity effect can lead to large errors in the calculation of radiation efficiency. For example, from Fig.

FIG. 2-3 RADIATION EFFICIENCY OF ELECTRICALLY SMALL LOOPS



2-3, without the proximity effect, the calculated efficiency of a three turn loop can be larger than the actual efficiency of an eight turn loop of the same size with close conductor spacing ( $c/a = 1.10$ ). When the loop is used as a transmitting antenna the radiated power is directly proportional to the radiation efficiency. Neglecting the proximity effect can make the computed efficiency for a small loop in error by a factor of two or larger; thus errors in the calculation of radiated power can be as large as one hundred percent.

In some applications a constraint is placed on the volume the loop antenna can occupy. If the depth of winding  $l$  is restricted to a value much smaller than the diameter of the loop ( $l \ll b$ , see Fig. 2-4) the results of section I-5 can be used to optimize the efficiency. With no proximity effect, the maximum efficiency is obtained when  $a = l/2n$  and is independent of the number of turns  $n$ .

$$E_A = \frac{l}{1 + \frac{1.70 \times 10^{-9} \sqrt{f \text{ MHz } \sigma_r}}{(b')^3 l}} \quad (2-35)$$

If the proximity effect is included, the antenna has optimum efficiency when the turn spacings are those presented in Table I-2

$$E_A = \frac{l}{1 + \frac{8.48 \times 10^{-10} \sqrt{f \text{ MHz } \sigma_r}}{n(b')^3 l'} \left( \frac{2\pi l R}{R^8} \right)} \quad (2-36)$$

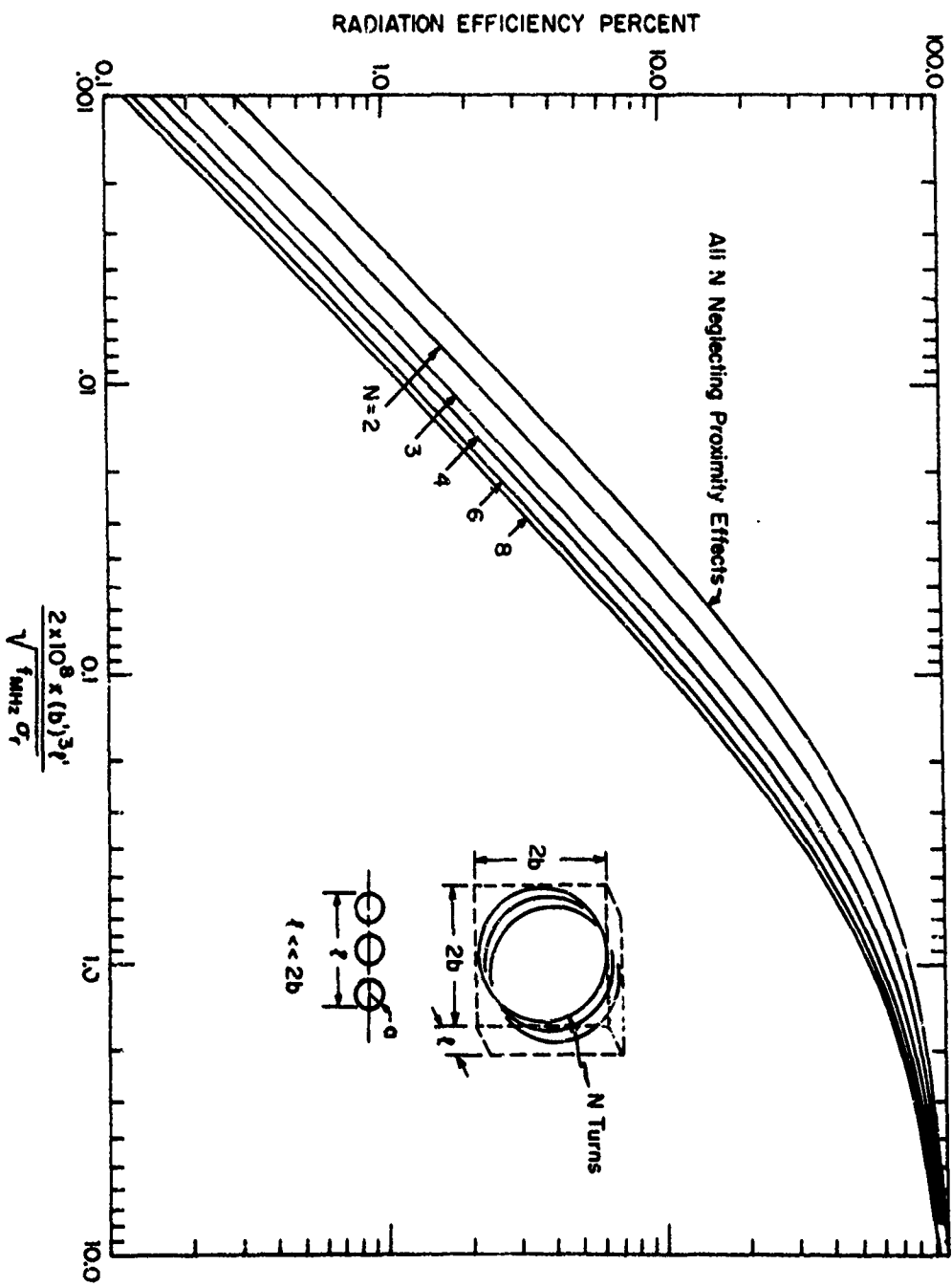


FIG. 2-4 RADIATION EFFICIENCY OF ELECTRICALLY SMALL MULTITURN LOOPS IN A CONFINED VOLUME (2b x 2b x l) FOR OPTIMUM WIRE RADIUS

where  $l' = l/\lambda$  and  $(2\pi lR/R^3)$  is the value given in Table 1-2.

Both equations (2-35) and (2-36) are graphed in Fig. 2-4.

As the number of turns is increased, the term  $\frac{1}{n} \left( \frac{2\pi lR}{R^3} \right)$  in (2-36) increases, causing a decrease in the efficiency.

With the antenna restricted to a volume of this shape, it is better, then, to optimize the wire size rather than to increase the number of loop turns. At a first glance, this last statement seems contrary to the common notion that increasing the number of loop turns increases the radiation efficiency. It must be kept in mind that one usually speaks of increasing the number of turns while keeping the wire radius and spacing constant, something which is impossible to do when the depth of winding  $l$  is also fixed.

Power is usually supplied to electrically small antennas through a suitable matching network. The components in the matching network often introduce losses as large as the ohmic loss of the antenna. The overall radiation efficiency of the antenna-matching network combination is then

$$E = E_A \cdot E_M \quad (2-37)$$

where  $E_A$  and  $E_M$  are the efficiency of the antenna and matching network individually. In this chapter, only  $E_A$  is considered; for a discussion of matching network efficiency, see Wheeler [36].

## 5. Conclusion

The analysis in this chapter has shown that the results obtained for the ohmic resistance per unit length of a system of straight wires are applicable to the electrically small multiturn loop when the depth of winding of the loop is small compared to the loop radius,  $(nc)^2 \ll b^2$ . Two separate calculations of the radiation efficiency of small multiturn loops were made: the first includes the added resistance due to the close proximity of turns and the second neglects all proximity losses, i. e. considers the ohmic resistance of the loop to be the same as that for an equivalent length of straight conductor. A comparison of the results for these two cases indicates that the proximity effect is an important factor in making accurate calculations of radiation efficiency, especially for loops whose efficiency is below 10%.

The problem of optimizing the radiation efficiency of an electrically small loop confined to a fixed volume was also examined. The special case of a circular, multiturn loop restricted to a volume whose depth is small compared to the loop radius ( $l \ll b$ ) was treated. For this geometry there is an optimum wire radius which gives maximum radiation efficiency for a given number of loop turns. With the optimum wire radius used for each number of turns, the radiation efficiency was found to decrease with an increase in the number of turns, indicating that, from the efficiency standpoint, it is better to optimize the wire radius than to increase the number of turns.

The change in the transverse distribution of current due to the proximity effect will also alter the loop inductance. The inductance of the loop, however, does not have to be known to a high degree of accuracy in most applications, since it is usually made to resonate with a variable capacitance in a matching network.

## SECTION III

### EXPERIMENTAL INVESTIGATION

#### I. Description of Experimental Apparatus

To verify the results of Section I, experimental apparatus was constructed for measuring the transverse distribution of current on a system of parallel round wires, see Figs. 3-1 and 3-2. The parallel wires are modelled by 34" long copper tubes interconnected with wire braids so that they carry equal currents in the same direction. A 100 Watt, 100 KHz transmitter drives a current of the order of 1-2 Amps. through the model, which for matching purposes is fed in series with a 50 Ohm load. The current distribution is measured by sampling the transverse magnetic field with a small loop probe mounted on one of the tubes. This tube has plugs fitted with beryllium copper finger stock at both ends; these maintain electrical contact as the tube is rotated (Fig. 3-3 ). The voltage at the terminals of the loop probe is amplified and metered using a General Radio model 1232-A Tuned Amplifier and Null Detector.

At 100 KHz the  $1\frac{1}{4}$ " copper pipes are about 200 skin depths in diameter; thus the axial currents are confined to a thin layer near the outside of the tube. The tubes are also about 20 skin depths thick, so they are electrically equivalent to solid conductors.

To maximize the angular resolution of the measured current distribution, the radial dimension of the loop probe

*Preceding page blank*

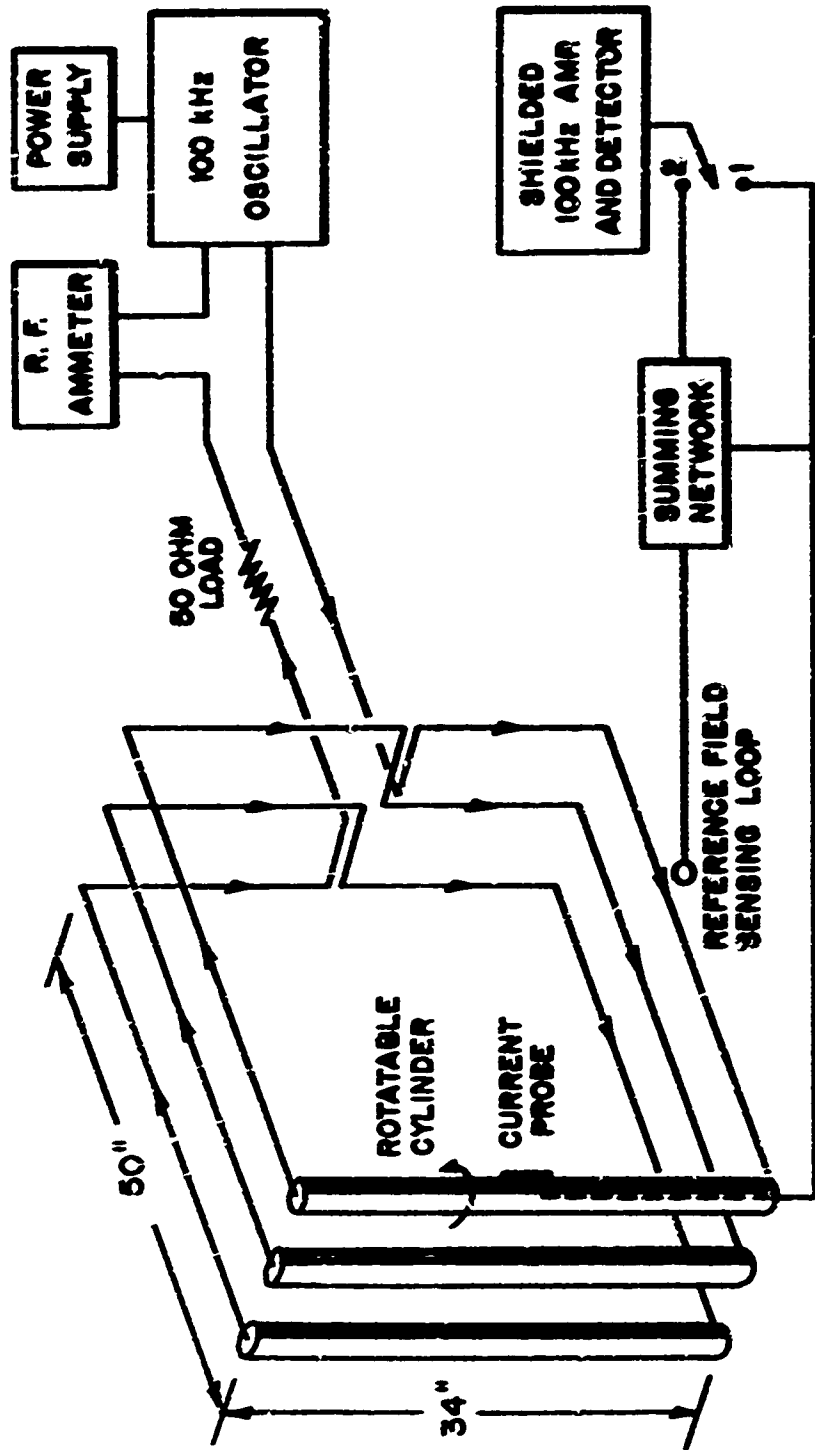
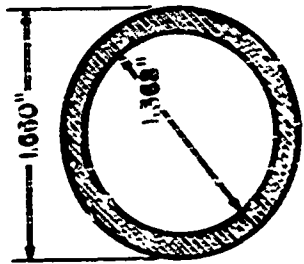


FIG. 3-1 BLOCK DIAGRAM OF THE CURRENT MEASURING EQUIPMENT



FIG. 3-2 CURRENT MEASURING EQUIPMENT



CYLINDER CROSS SECTION



FIG. 3-3 DETAIL OF ROTATABLE CYLINDER

was made as small as possible (0.050"). Since the fields are fairly uniform over small lengths near the center of the tube, the axial dimension of the loop could be a few inches long. Using the theory of Whiteside and King [37] the voltage at the terminals of the rectangular loop when the tube carries a total current of one Ampere is

$$|V| = 3.95 \times 10^{-3} l_r l_a \left[ \frac{(R_L^4 - X_0^2 R_L^2)^{\frac{1}{2}}}{R_L^2 + X_0^2} \right] \frac{\text{Volts}}{\text{Amp.}} \quad (3-1)$$

$$X_0 = 6.38 \times 10^{-3} \left\{ 2 l_r \ln \left[ \frac{4 l_r l_a}{r(l_r + D)} \right] + l_a \ln \left[ \frac{4 l_r l_a}{r(l_r + D)} \right] + 2(r - D - l_a - 2 l_r) \right\} \quad (3-2)$$

where  $l_r$ ,  $l_a$  are the radial and axial dimensions of the loop in inches,  $r$  the loop wire radius in inches, and  $R_L$  the load impedance at the probe terminals which is about 50 K Ohms for the G. R.

1232-A. From ( 3-1 ), the 3" x 0.050" loop probe constructed of 28 gage wire provides a 0.6 m volt/Amp signal. This is more than adequate for metering on the G. R. 1232-A, since it has a maximum sensitivity of 10  $\mu$  Volts for a full scale deflection at 100 KHz. For rigidity a polyfoam support was placed between the loop and the tube (see Fig. 3-3 ).

Initial measurements indicated that the metering circuit was picking up a very strong signal induced by the large loop formed by the tubes and interconnecting wires. To eliminate this interference, the meter was completely enclosed in a

copper box and all cables used were doubly shielded.

The G. R. 1232-A Tuned Amplifier and Null Detector was calibrated at 100 KHz using a pair of Hewlett Packard precision attenuators as a standard. Fig. 3-4b is a schematic of the circuit used for the calibration. The linear scale meter reading is plotted against the attenuator setting in Fig. 3-4a. The small vertical lines indicate the experimentally determined points; a  $\pm$  unit reading error is assumed. The solid line was constructed by fitting polynomials to the experimental points over three ranges. The polynomials in the form used to correct the experimental data are

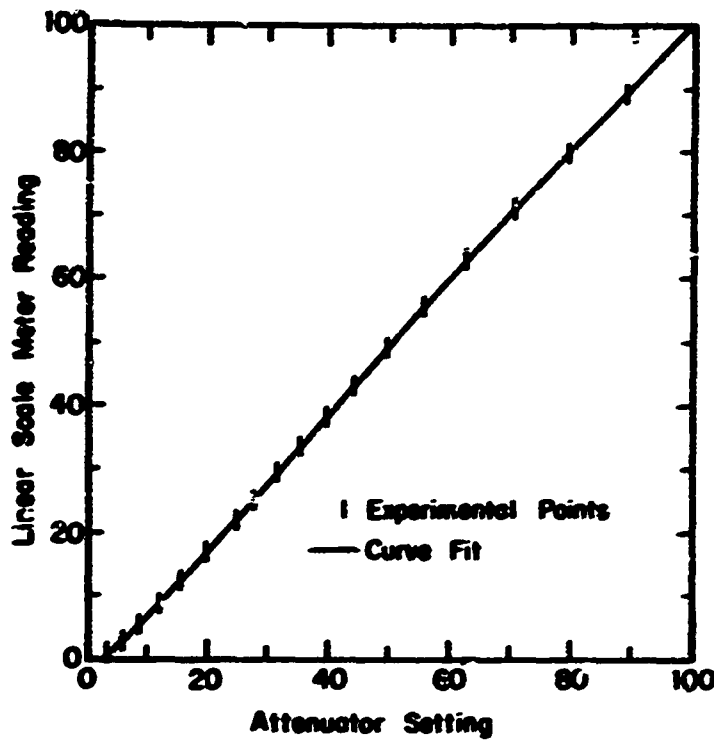
$$V'_m = V_m, \quad 63 \leq V_m \leq 100 \quad (3-3a)$$

$$V'_m = V_m + 3.5 - 4.8 \times 10^{-2}(V_m - 16) - 5.7 \times 10^{-4}(V_m - 16)^2, \quad 16 < V_m < 63 \quad (3-3b)$$

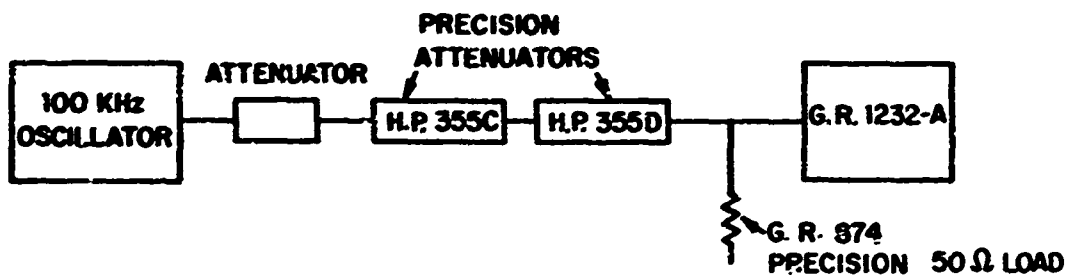
$$V'_m = V_m + 3.5, \quad 0 \leq V_m \leq 16 \quad (3-3c)$$

where  $V_m$  is the meter reading and  $V'_m$  the corrected meter reading. This correction is apparently only a function of the meter circuitry and not the linear amplifier section of the instrument, since the same correction applies over a 40dB. range of amplifier gain.

Since the theory predicts both positive and negative currents on closely spaced tubes, a method was devised to experimentally verify a  $180^\circ$  phase shift in the current density. Referring to Fig. 3-1, a small ferrite loaded loop is used to sample the field of the large loop formed by the tubes and the interconnecting wires. This reference signal is added to the signal from the current probe



(a) CALIBRATION CURVE



(b) SCHEMATIC OF CALIBRATION CIRCUIT

FIG. 3-4 CALIBRATION OF THE G.R. 1232-A TUNED AMPLIFIER AND NULL DETECTOR

in a resistive summing network and then metered. The phase of the current on the tube is determined by noting if the signal from the current probe adds to or subtracts from the reference signal.

## 2. Correction for Interconnecting Wires

In addition to the net currents in the tubes, three other current elements influence the current distribution on the tube cross section. They are currents in the horizontal and vertical interconnecting wires and negative line currents which represent the absence of a continuation of the axial current beyond the ends of the tube. Referring to Fig. 3-5, these currents can be treated as filamentary elements since each is at a distance from the probe which is large compared to the tube radius ( $s = 20a$ ,  $w = 60a$ ). As a result, their effect on the transverse distribution of current is additive in the sense that it may be subtracted from the measured data to obtain results for direct comparison with the theoretical distributions.

The vector potential at a point  $(r, \theta, z)$  near the center of the  $m^{\text{th}}$  tube is

$$\vec{A}_m(r, \theta, z) = \hat{z} A_{mz} + \hat{y} A_{my} = \hat{z} \left\{ \frac{-\mu_0 I}{4\pi} \int_{\theta'=\pi}^{\pi} \sum_{\ell=1}^n \left[ g'_{\ell c}(\theta') \ln(r_{m\ell}') \right] d\theta' d'z + A'_{mz}(z) \frac{-\mu_0 I}{2\pi} \int_{z'=0}^s \sum_{\ell=1}^n \frac{1}{R_{m\ell}} dz' - \frac{\mu_0 I}{2\pi} \int_{z'=s}^{\infty} \sum_{\ell=1}^n \frac{1}{R_{m\ell^2}} dz' \right\} + \hat{y} \left\{ \frac{\mu_0 I}{4\pi} \int_{y=0}^w \sum_{\ell=1}^n \left[ \frac{1}{R_{m\ell^3}} - \frac{1}{R_{m\ell^4}} \right] dy \right\} \quad (3-4)$$

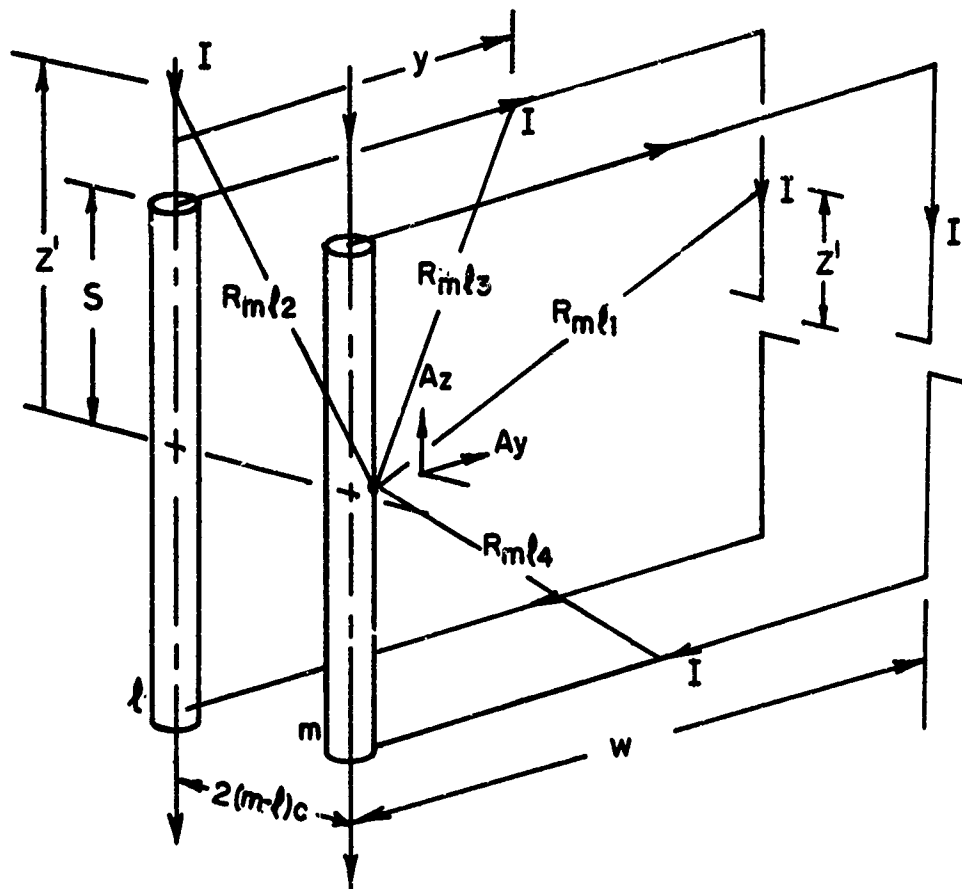


FIG. 3-5 INTERCONNECTING WIRES USED IN THE EXPERIMENTAL MODEL

$$R_{m\ell 1} = [(w-r\sin\theta)^2 + (2(m-\ell)c + r \cos\theta)^2 + (z-z')^2]^{\frac{1}{2}} \quad (3-5)$$

$$R_{m\ell 2} = [(z'-z)^2 + (z(m-\ell)c + r \cos\theta)^2 + (r \sin\theta)^2]^{\frac{1}{2}} \quad (3-6)$$

$$R_{m\ell 3} = [(s-z)^2 + (z(m-\ell)c + r \cos\theta)^2 + (y-r \sin\theta)^2]^{\frac{1}{2}} \quad (3-7)$$

$$R_{m\ell 4} = [(s+z)^2 + (2(m-\ell)c + r \cos\theta)^2 + (y-r \sin\theta)^2]^{\frac{1}{2}} \quad (3-8)$$

$g_{mc}(\theta)$  is the normalized surface current density induced in the cylinders by the three external current elements. It is the term which must be subtracted from the measured current for comparison with theory.

The following boundary condition relates  $A_m$  and  $g_{mc}$ .

$$g_{mc}(\theta) = \frac{-2\pi a}{\mu_0 I} \left[ \frac{2A_{mz}}{2r} - \sin\theta \frac{2A_{my}}{2z} \right]_{\substack{r=a \\ z=0}} \quad (3-9)$$

Substituting (3-4) into (3-9) yields

$$g_{mc}(\theta) = \frac{1}{2\pi} \left\{ \lim_{\tau \rightarrow i} \int_{\theta' = -\pi}^{\pi} \frac{g_{mc}(\theta') [\tau - \cos(\theta - \theta')]}{\tau^2 + 1 - 2\tau \cos(\theta - \theta')} d\theta' \right. \\ \left. + \int_{\theta' = -\pi}^{\pi} \sum_{\substack{\ell=1 \\ \ell=m}}^n K_{m,\ell}(\theta, \theta') g_{\ell c}(\theta') d\theta' \right\} - \left(\frac{a}{w^2}\right) \left(a/w + 2(m-\ell)(c/w) \right. \\ \left. \cos\theta - \sin\theta \right) \int_{z'=0}^s \sum_{\ell=1}^n \frac{1}{\left(\frac{r'}{m\ell 1}\right)^3} dz' - \left(\frac{a}{s^2}\right) \left(a/s + 2(m-\ell)(c/s) \cos\theta \right) \\ \int_{z'=s}^{\infty} \sum_{\ell=1}^n \frac{1}{\left(\frac{r'}{m\ell 2}\right)^3} dz' + \left(\frac{a}{s}\right) \sin\theta \int_{y=0}^w \sum_{\ell=1}^n \frac{1}{\left(\frac{r'}{m\ell 3}\right)^3} dy \quad (3-10)$$

where

$$r'_{m,l} = [ (1-(a/w)\sin\theta)^2 + (2(m-l)(c/w) + (a/w)\cos\theta)^2 + (z'/w)^2 ]^{\frac{1}{2}} \quad (3-11)$$

$$r'_{m,l2} = [ (z'/s)^2 + (2(m-l)(c/s) + (a/s)\cos\theta)^2 + (a/s)^2(\sin\theta)^2 ]^{\frac{1}{2}} \quad (3-12)$$

$$r'_{m,l3} = [ 1 + (2(m-l)(c/s) + (a/s)\cos\theta)^2 + (y/s - (a/s)\sin\theta)^2 ]^{\frac{1}{2}} \quad (3-13)$$

The first integral in (3-10) was evaluated in section I-3; the other integrals are a standard form [19, p. 50, 200.03]. Performing these integrations, (3-10) becomes

$$g_{mc}(\theta) = \frac{1}{\pi} \int_{\theta'=\pi}^{\pi} \sum_{\substack{l=1 \\ l \neq m}}^n K_{m,l}(\theta, \theta') g_{lc}(\theta') d\theta' - 2(a/w)(s/w) \sum_{l=1}^n \frac{(a/w + 2(m-l)(c/w) \cos\theta - \sin\theta)}{[ (1-(a/w)\sin\theta)^2 + (2(m-l)(c/w) + (a/w)\cos\theta)^2 ] [ (1-(a/w)\sin\theta)^2 + (2(m-l)(c/w) + (a/w)\cos\theta)^2 + (s/w)^2 ]^{\frac{1}{2}}} - 2(a/s) \sum_{l=1}^n \frac{(a/s + 2(m-l)(c/s) \cos\theta)}{[ (2(m-l)(c/s) + (a/s) \cos\theta)^2 + (a/s)^2 (\sin\theta)^2 ]} \left\{ 1 - \frac{1}{[ 1 + (2(m-l)(c/s) + (a/s)\cos\theta)^2 + (a/s)^2 ]} + 2(a/s)\sin\theta \sum_{l=1}^n \frac{1}{[ 1 + (2(m-l)(c/s) + (a/s)\cos\theta)^2 ]} \right\} + \left\{ \frac{(w/s)(1 - (a/w)\sin\theta)}{[ 1 + (w/s)^2 (1-(a/w)\sin\theta)^2 + (2(m-l)(c/s) + (a/s)\cos\theta)^2 ]^{\frac{1}{2}}} + \frac{(a/s)\sin\theta}{[ 1 + (2(m-l)(c/s) + (a/s)\cos\theta)^2 + (a/s)^2 (\sin\theta)^2 ]^{\frac{1}{2}}} \right\} \quad (3-14)$$

When terms of order  $(a/s)^2$  or less are dropped, equation (3-14) reduces to

$$\begin{aligned}
 g_{mc}(\theta) = & \frac{1}{\pi} \int_{\alpha'=-\pi}^{\pi} \sum_{\substack{l=1 \\ l \neq m}}^n K_{m,l}(\theta;\theta') g_{lc}(\theta') d\alpha' + 2(a/s) \sum_{l=1}^n \\
 & \left. \frac{1}{[1 + (s/w)^2 + 4(m-l)^2(c/w)^2]^{\frac{1}{2}}} \left\{ \frac{(s/w)^2 [\sin\theta - 2(m-l)(c/w)\cos\theta]}{[1 + 4(m-l)^2(c/w)^2]} \right. \right. \\
 & \left. \left. + \frac{\sin\theta}{[1 + 4(m-l)^2(c/s)^2]} \right\} - 2(a/s) \sum_{l=1}^n \frac{(a/s + 2(m-l)(c/s)\cos\theta)}{[(a/s)^2 + 4(m-l)^2(c/s)^2]} \right. \\
 & \left. \frac{1}{[1 + 4(m-l)(c/s)(a/s)]} \left\{ 1 - \frac{1}{[1 + 4(m-l)^2(c/s)^2]^{\frac{1}{2}}} \right\} \right. \quad (3-15)
 \end{aligned}$$

If the interaction between the induced currents on the tubes is ignored, that is, each tube is considered as isolated from the others, the integral in (3-15) disappears, and a first order approximation for the current results.

$$\begin{aligned}
 g_{mc}(\theta) = & 2(a/s) \sum_{l=1}^n \frac{1}{[1 + (s/w)^2 + 4(m-l)^2(c/w)^2]^{\frac{1}{2}}} \\
 & \left\{ \frac{(s/w)^2 [\sin\theta - 2(m-l)(c/w)\cos\theta]}{[1 + 4(m-l)^2(c/w)^2]} + \frac{\sin\theta}{[1 + 4(m-l)^2(c/s)^2]} \right\} \\
 & - 2(a/s) \sum_{l=1}^n \frac{(a/s + 2(m-l)(c/s)\cos\theta)}{[(a/s)^2 + 4(m-l)^2(c/s)^2 + 4(m-l)(c/s)(a/s)\cos\theta]}
 \end{aligned}$$

$$\left\{ 1 - \frac{1}{[1 + 4(m-l)^2 (c/s)^2]^{\frac{1}{2}}} \right\} \quad (3-16)$$

The three terms in (3-16) are due to the currents in the vertical interconnecting wires, horizontal interconnecting wires and axial tube extensions, respectively. The currents induced by the horizontal wires are the major factors since they are about  $(w/s)^2 \approx 10$  times greater than those due to the vertical wires and, for large spacings  $(c/s) = 1$ , at least 3 times greater than those due to the tube extensions.

To solve for the current in the complete expression (3-15), which includes interactions between tubes, a trigonometric series is postulated for  $g_{mc}$  (6). Since the average value of  $g_{mc}(\theta)$  is zero and it is not symmetric about the lines  $0:\pi$  or  $\pi/2 : 3\pi/2$ , the series has no constant term and contains both sine and cosine terms.

$$g_{mc}(\theta) = \sum_{p=1}^q [ a_{mcp} \cos(p\theta) + b_{mcp} \sin(p\theta) ] \quad (3-17)$$

Substituting (3-17) into (3-15), the following results are obtained

$$\begin{aligned} & \sum_{p=1}^q a_{mcp} \left[ -\cos(p\theta) + \frac{(-1)^p}{\pi} \int_{\theta'=-\pi}^{\pi} \overset{n \text{ even}}{K(\theta, \theta')} \cos(p\theta') d\theta' \right] \\ & + \sum_{p=1}^q b_{mcp} \left[ -\sin(p\theta) - \frac{(-1)^p}{\pi} \int_{\theta'=-\pi}^{\pi} K(\theta, \theta') \sin(p\theta') d\theta' \right] \end{aligned}$$

$\begin{matrix} m, n+1-m \\ m, n+1-m \end{matrix}$

$$\begin{aligned}
 & + \sum_{\substack{k=1 \\ k \neq m}}^{n/2} \sum_{p=1}^q a_{kcp} \left\{ \frac{1}{\pi} \int_{-\pi}^{\pi} [K_{m,2}(\theta, \theta') + (-1)^p K_{m, n+1-k}(\theta, \theta')] \cos(p\theta') d\theta' \right\} \\
 & + \sum_{\substack{k=1 \\ k \neq m}}^{n/2} \sum_{p=1}^q b_{kcp} \left\{ \frac{1}{\pi} \int_{-\pi}^{\pi} [K_{m,2}(\theta, \theta') - (-1)^p K_{m, n+1-k}(\theta, \theta')] \sin(p\theta') d\theta' \right\} \\
 & = -2(a/s) \sum_{k=1}^n \frac{1}{[1 + (s/w)^2 + 4(m-k)^2 (c/w)^2]^{\frac{1}{2}}} \left\{ \frac{(s/w)^2 [\sin \theta - 2(m-k)(c/w) \cos \theta]}{[1 + 4(m-k)^2 (c/w)^2]} \right. \\
 & \left. + \frac{\sin \theta}{[1 + 4(m-k)^2 (c/s)^2]} \right\} + 2(a/s) \sum_{k=1}^n \frac{(a/s + 2(m-k)(c/s) \cos \theta}{[(a/s)^2 + 4(m-k)^2 (c/s)^2 + 4(m-k)(c/s)]} \\
 & \frac{(a/s) \cos \theta}{(a/s) \cos \theta} \left\{ 1 - \frac{1}{[1 + 4(m-k)^2 (c/s)^2]} \right\} \tag{3-18}
 \end{aligned}$$

$m = 1, 2, \dots, n/2$

n odd

$$\sum_{p=1}^q a_{mcp} \left[ -\cos \begin{cases} p\theta, & m \neq (n+1)/2 \\ 2p\theta, & m = (n+1)/2 \end{cases} \right] + \frac{(-1)^p}{\pi} h(m) \int_{\theta'=-\pi}^{\pi}$$

$$K(\theta, \theta') \cos(p\theta') d\theta' \Big] + \sum_{p=1}^q b_{mcp} \left[ -\sin \theta \begin{cases} p\theta, & m \neq (n+1)/2 \\ 2(p+1)\theta, & m = (n+1)/2 \end{cases} \right]$$

$$\begin{aligned}
 & - \frac{(-1)^p}{\pi} h(m) \int_{\theta'=-\pi}^{\pi} K(\theta, \theta')_{m, n+l-m} \sin(p\theta') d\theta' \Big] + \sum_{\substack{l=1 \\ l \neq m}}^{(n-1)/2} \sum_{p=1}^q a_{lp} \\
 & \left\{ \frac{1}{\pi} \int_{\theta'=-\pi}^{\pi} [K(\theta, \theta')_{m, l} + (-1)^p K(\theta, \theta')_{m, n+l-l}] \cos(p\theta') d\theta' \right\} + \sum_{\substack{l=1 \\ l \neq m}}^{(n-1)/2} \sum_{p=1}^q b_{lcp} \\
 & \left\{ \frac{1}{\pi} \int_{\theta'=-\pi}^{\pi} [K(\theta, \theta')_{m, l} - (-1)^p K(\theta, \theta')_{m, n+l-l}] \sin(p\theta') d\theta' \right\} + \sum_{p=1}^q \frac{a_{n+l}}{2} c_p \\
 & \left[ \frac{h(m)}{\pi} \int_{\theta'=-\pi}^{\pi} K(\theta, \theta')_{m, (n+l)/2} \cos(2p\theta') d\theta' \right] + \sum_{p=1}^q \frac{b_{m+l}}{2} c_p \left[ \frac{h(m)}{\pi} \int_{\theta'=-\pi}^{\pi}
 \end{aligned}$$

$$K(\theta, \theta')_{m, (n+l)/2} \sin(2p+1)\theta' d\theta' \Big] = -2(a/s) \sum_{l=1}^n \frac{1}{[1 + (s/w)^2 + 4(m-l)^2 (c/w)^2]^{\frac{1}{2}}}$$

$$\left\{ \frac{(s/w)^2 [\sin\theta - 2(m-l)(c/w) \cos\theta]}{[1 + 4(m-l)^2 (c/w)^2]} + \frac{\sin\theta}{[1 + 4(m-l)^2 (c/s)^2]} \right\}$$

$$+ 2(a/s) \sum_{l=1}^n \frac{(a/s + 2(m-l)(c/s) \cos\theta)}{[(a/s)^2 + 4(m-l)^2 (c/s)^2 + 4(m-l)(c/s)(a/s) \cos\theta]}$$

$$\left\{ 1 - \frac{1}{[1 + 4(m-l)^2 (c/s)^2]^{\frac{1}{2}}} \right\}$$

$$m = 1, 2, \dots, (n+1)/2$$

The definite integrals which appear in (3-18) and (3-19) can be represented by two forms. The integrals containing  $\cos(p\theta)$  terms are the same as the integrals denoted by  $I(\alpha, m-1, p)$  in section 3-5 and evaluated in Appendix A. The integrals involving  $\sin(p\theta)$  terms are of the form

$$I'(\alpha, m-1, p) = \frac{1}{\pi} \int_{\alpha'=-\pi}^{\pi} \frac{[1 + 2(m-1)(c/a)\cos\theta - (c/a)^2 \cos^2\theta]}{[4(m-1)^2(c/a)^2 + 2 + 4(m-1)(c/a)\cos\alpha + \sin\alpha \sin\alpha'] \sin(p\theta) d\theta} \\ - \{4(m-1)(c/a) + 2 \cos(\theta')\} \cos\theta' - 2 \sin\theta \sin\theta' \} \\ p = 1, 2, \dots \quad (3-20)$$

An evaluation of this integral is in Appendix C, the results of which are

$$I'(\theta, m-1, p) = \frac{1}{(1-s^2)(-s)^{p+1}} [A's^2 + B's + C'] \quad (3-21a)$$

where

$$s = (4(m-1)^2(c/a)^2 + 1 + 4(m-1)(c/a) \cos\theta)^{\frac{1}{2}} \quad (3-21b)$$

$$A' = \sin(\alpha - (p-1)\frac{\pi}{2}) \quad (3-21c)$$

$$B' = -2(1 + 2(m-1)(c/a) \cos\alpha; \sin(p\frac{\pi}{2})) \quad (3-21d)$$

$$C' = -\sin(\theta + (p+1)\frac{\pi}{2}) \quad (3-21e)$$

$$\theta = \left\{ \begin{array}{l} \pi - \tan^{-1} \left( \frac{\sin\theta}{2(m-1)(c/a) + \cos\theta} \right), \quad (m-1) = 1, 2, \dots \\ \tan^{-1} \left( \frac{-\sin\theta}{2(m-1)(c/a) + \cos\theta} \right), \quad (m-1) = -1, -2, \dots \end{array} \right\} \quad (3-21f)$$

The principle value of  $\tan^{-1}$  is used in (3-21f).

With (3-2i), the system of equations (3-18) for the case  $n$  even becomes

$$\sum_{p=1}^q a_{mcp} [-\cos(p\theta) + (-i)^p I(\theta, 2m-n-1, p)] + \sum_{\substack{l=1 \\ l \neq m}}^{n/2} \sum_{p=1}^q a_{lcp} [I(\theta, m-l, p) + (-i)^p I(\theta, m+l-n-1, p)] + \sum_{p=1}^q b_{mcp} [-\sin(p\theta) - (-i)^p I'(\theta, 2m-n-1, p)] + \sum_{\substack{l=1 \\ l \neq m}}^{n/2} \sum_{p=1}^q b_{lcp} [I'(\theta, m-l, p) - (-i)^p I'(\theta, m+l-n-1, p)] = -2(a/s) \sum_{l=1}^n$$

$$\frac{1}{[1 + (s/w)^2 + 4(m-l)^2(c/w)^2]^{\frac{1}{2}}} \left\{ \frac{(s/w)^2 [\sin\theta - 2(m-l)(c/w) \cos\theta]}{[1 + 4(m-l)^2(c/w)^2]} + \frac{\sin\theta}{[1 + 4(m-l)^2(c/s)^2]} \right\} + 2(a/s) \sum_{l=1}^n \frac{(a/s + 2(m-l)(c/s) \cos\theta)}{[(a/s)^2 + 4(m-l)^2(c/s)^2]} - \frac{4(m-l)(c/s)(a/s) \cos\theta}{[1 + 4(m-l)^2(c/s)^2]^{\frac{1}{2}}}$$

$m = 1, 2, \dots, n/2$

Similar results are obtained for the case  $n$  odd. Formula (3-22) represents a set of  $n/2$  equations relating the  $q_n$  unknowns. This system of equations can be solved by either of the two approximate methods discussed in section I-5, methods of collocation and least squares.

Appendix D contains a listing of a computer program which solves for the coefficients  $a_{mcp}$  and  $b_{mcp}$  by the method of collocation. The  $q_n$  matching points in the interval  $0 \leq \theta \leq 2\pi$  are chosen as

$$\theta_k = k \left( \frac{2\pi}{q+1} \right), \quad k = 1, 2 \dots q \quad (3-23)$$

on all cylinders except the center cylinder in a system with  $n$  odd where the points are

$$\theta_k = -\left( \frac{2k-1}{2} \right) \left( \frac{q}{q+1} \right), \quad k = 1, 2 \dots q \quad (3-24)$$

Examples of the correction currents  $g_{mc}$  are plotted in Fig. 3-6. Both the full correction current (3-17) and the first order correction current (3-15) are shown. A comparison of the two curves indicates that the interaction between induced currents on the tubes must be included in any accurate expression for the correction current.

### 3. Results of the Measurements

Current distributions were measured on systems with up to six cylinders and spacings ranging from  $c/a = 1.10$  to  $c/a = 2.50$ . After correcting for meter calibration, the measured values were normalized. The procedure for normalizing was first to measure

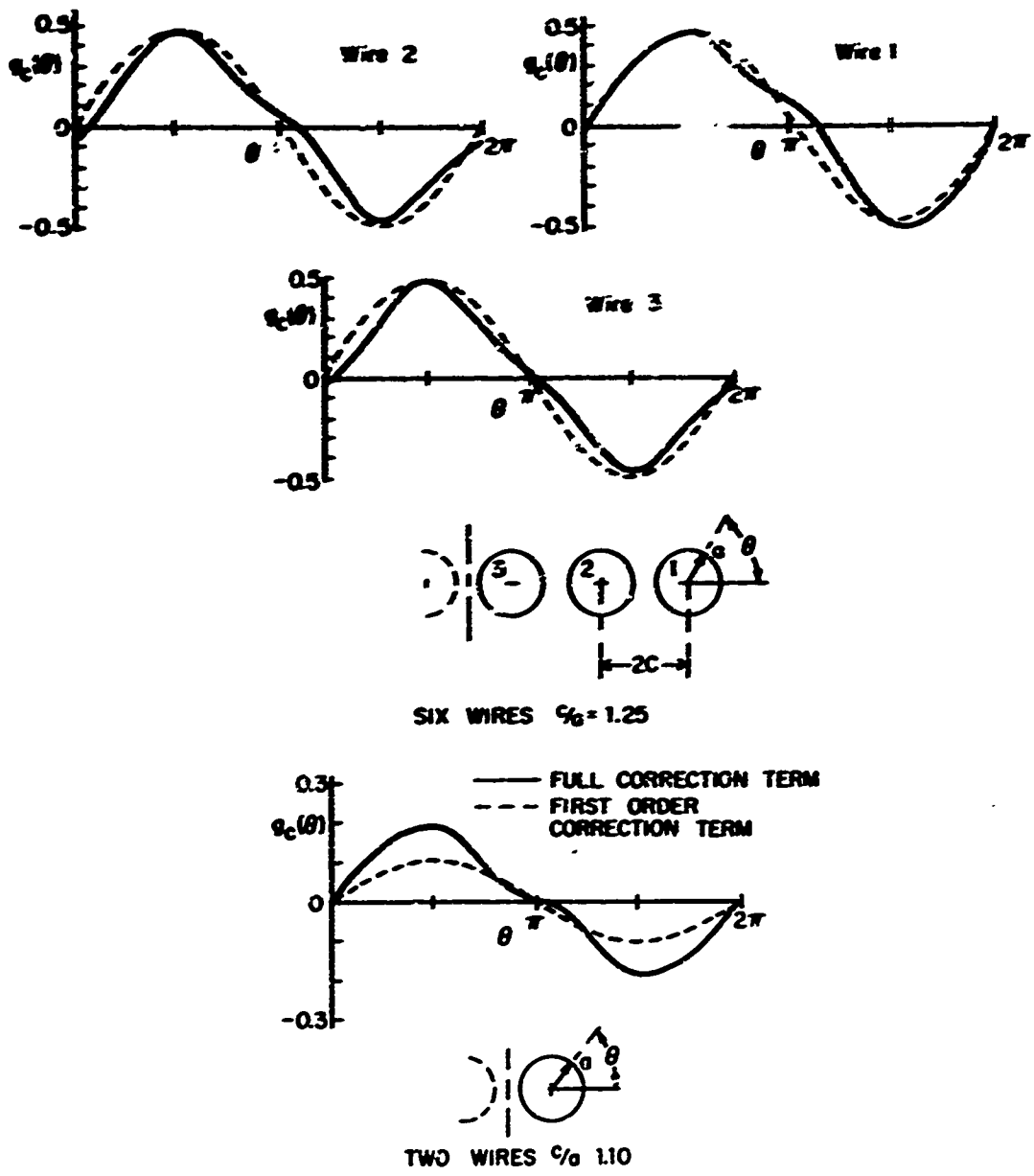


FIG. 3-6 NORMALIZED CURRENTS FOR THE CORRECTION TERM

the current distribution on the system of conductors with the meter gain held constant and a known current flowing through the model. The system of conductors was then replaced by a single conductor and the current distribution measured with the meter gain and current through the model the same as in the previous measurement. The normalized currents on the multiwire system were obtained by dividing the measured currents by the average value of the measured currents on the single cylinder.

The measured currents, with the correction current  $g_{mc}$  subtracted out after they were normalized, are compared with the theoretical distributions in Figs. 3-7 to 3-11. The circles about the measured points indicate the range of error ( $\pm 2$  scale units) associated with the repeatability of the measurements. The measurements are in good agreement with the theory.

The minimum spacings used in making the measurements were restricted to  $c/a = 1.10$  for two wires and  $c/a = 1.25$  for three or more wires. For three or more wires, the currents at adjacent points on consecutive cylinders are quite large when the spacings are small. The radial dimension  $l_r$  of the loop probe is a significant fraction of the distance between cylinders; for example, when  $c/a = 1.10$  the gap between the cylinders is only three times as large as  $l_r$ . As a result, the loop responds to the currents on both cylinders giving an erroneous interpretation of the current density. The problem is not as severe for two wires since the currents at adjacent points on the two cylinders approach zero as  $c/a$  goes to 1.

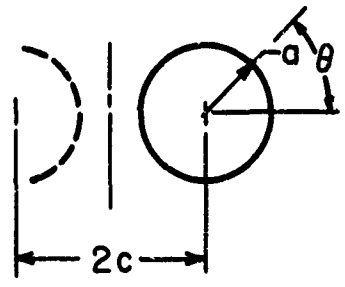
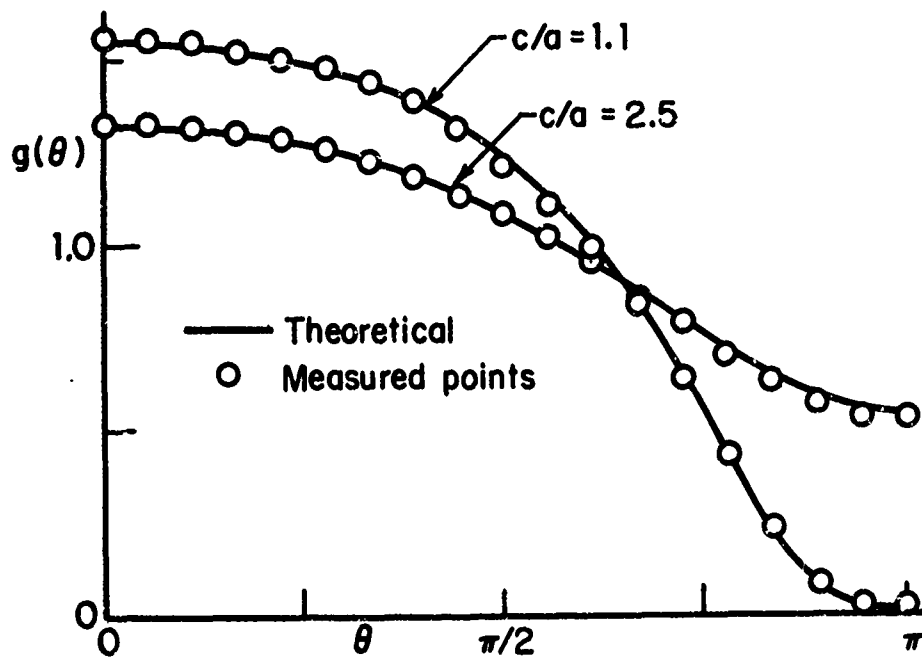


FIG. 3-7 MEASURED AND THEORETICAL SURFACE CURRENT DISTRIBUTIONS FOR TWO WIRES

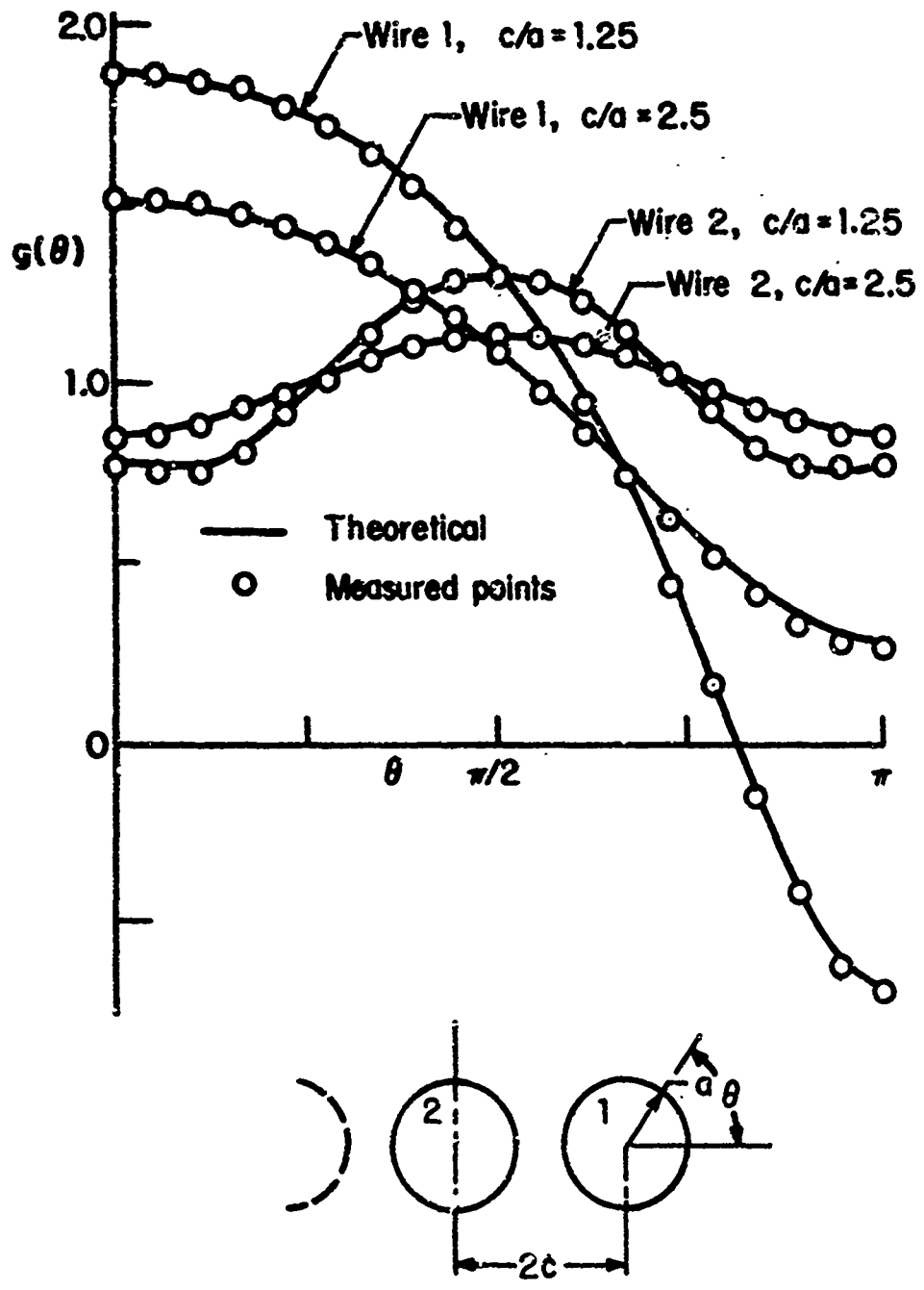


FIG. 3-8 MEASURED AND THEORETICAL SURFACE CURRENT DISTRIBUTIONS FOR THREE WIRES

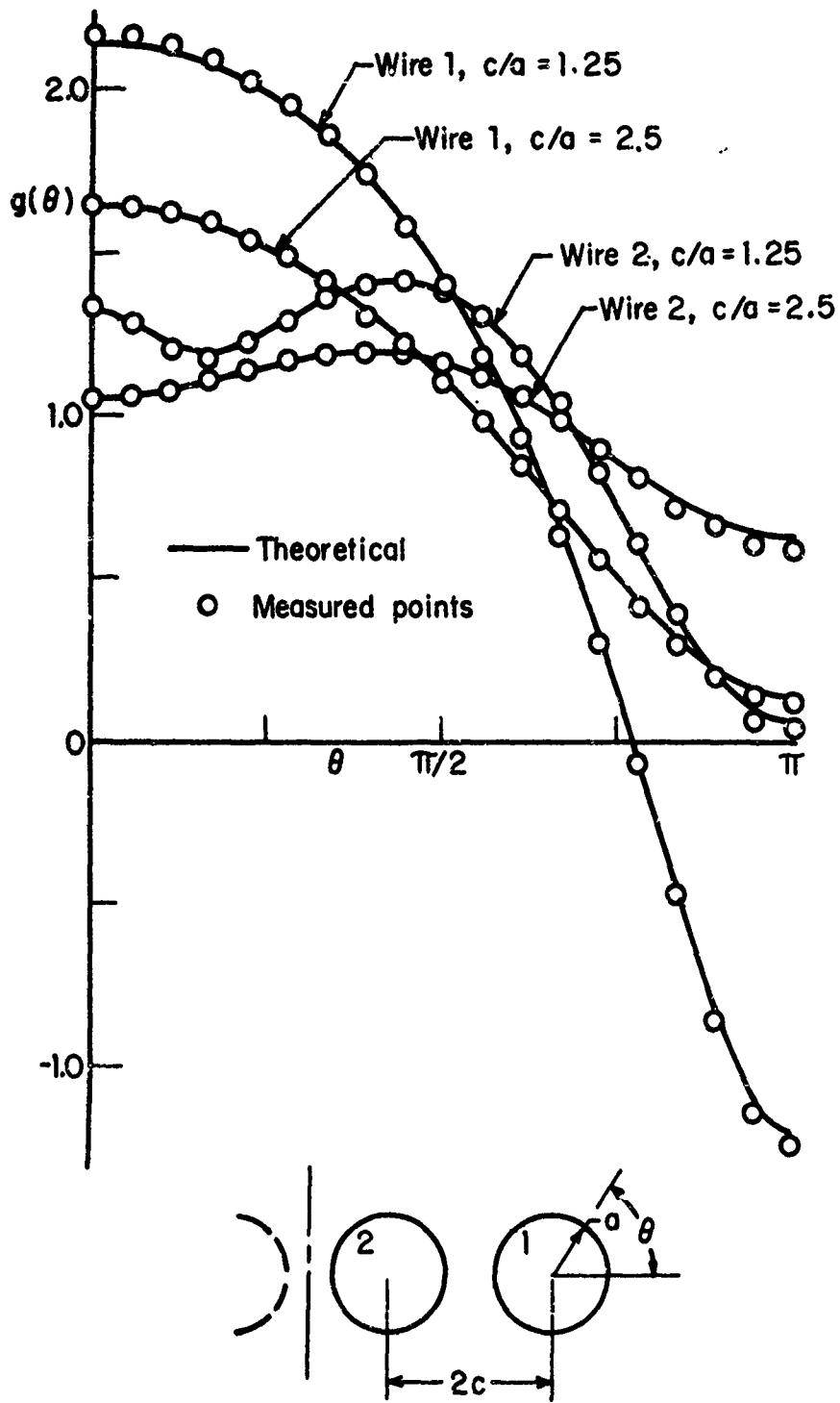


FIG. 3-9 MEASURED AND THEORETICAL SURFACE CURRENT DISTRIBUTIONS FOR FOUR WIRES

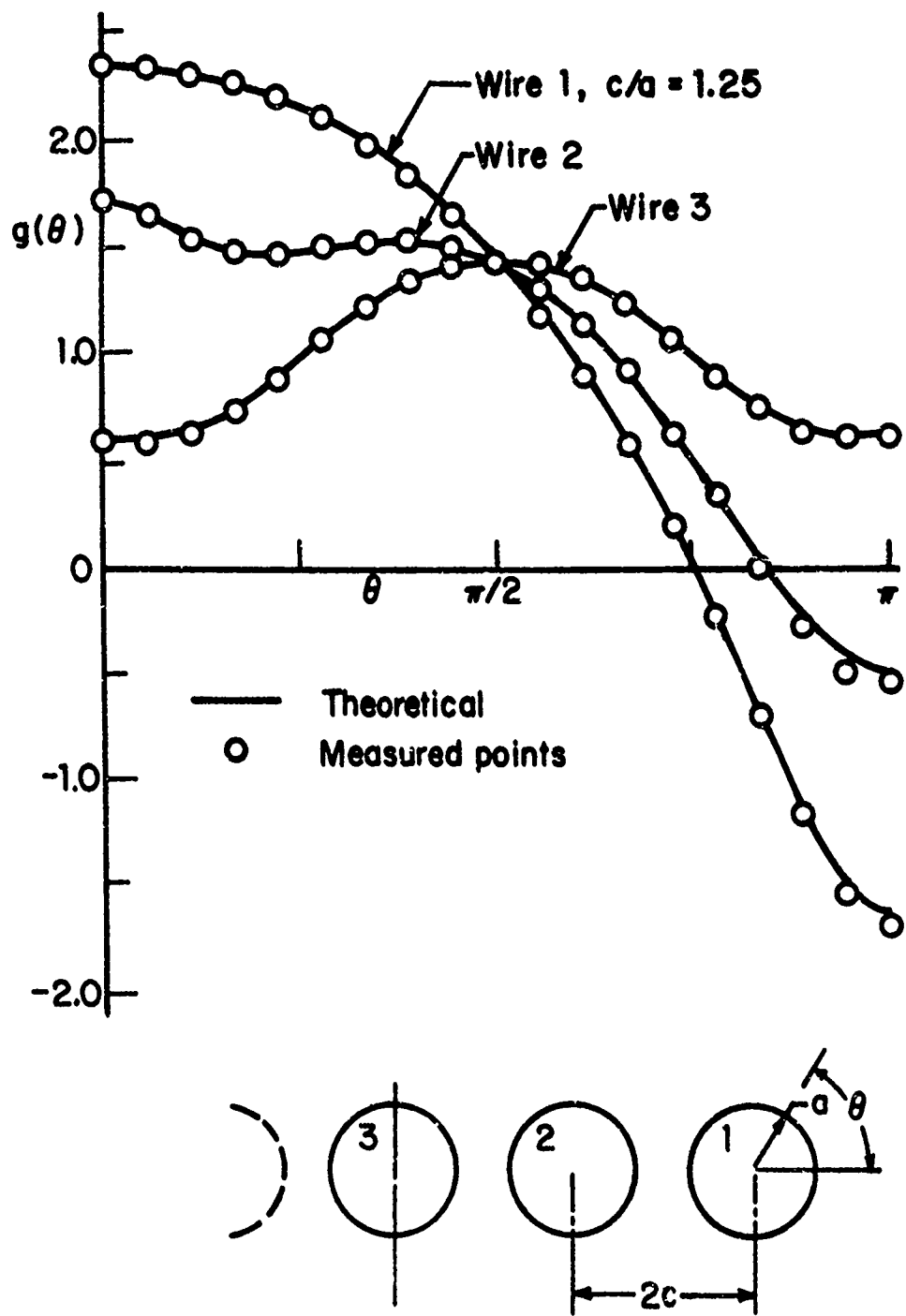


FIG. 3-10 MEASURED AND THEORETICAL SURFACE CURRENT DISTRIBUTIONS FOR FIVE WIRES

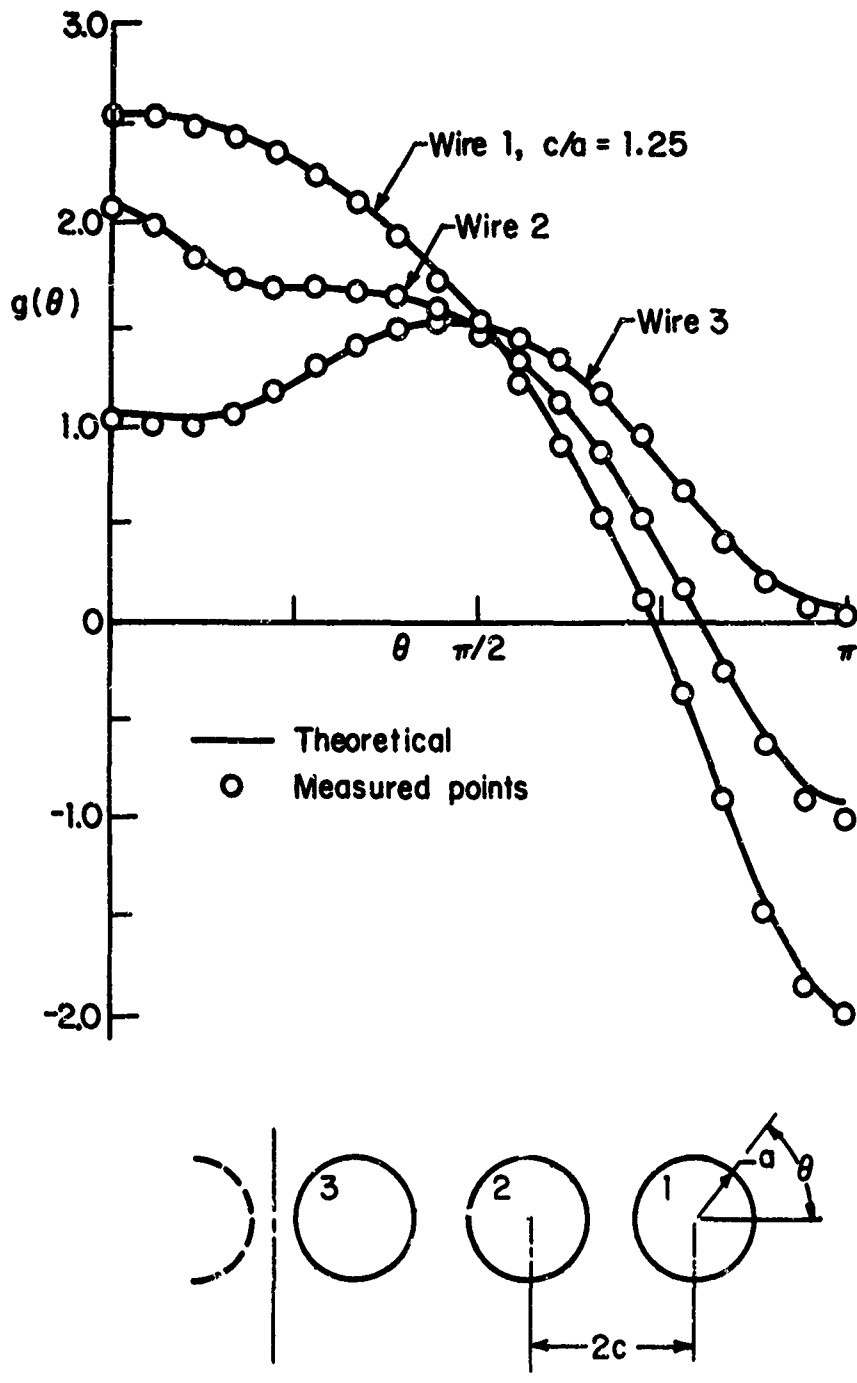


FIG. 3-11 MEASURED AND THEORETICAL SURFACE CURRENT DISTRIBUTIONS FOR SIX WIRES

4. Conclusion

An experimental apparatus was constructed to measure the transverse distribution of current on systems of parallel conductors. After correcting the measured data for equipment calibration and extraneous sources, good correlation between theoretical and experimental current distributions was obtained.

Acknowledgement

The author wishes to thank Mr. Victor Richard of the Microwave Physics Branch, Ballistic Research Laboratories, U. S. Army Aberdeen Proving Ground for his interest in and support of this project.

## Appendix A

Evaluation of the Integral  $I(\theta, m-l, p)$ 

$$I(\alpha, m-l, p) = \frac{1}{\pi} \int_{\theta'=-\pi}^{\pi} \frac{[1 + 2(m-l)(c/a) \cos\theta - \cos(\alpha-\alpha')] \cos(p\alpha') d\alpha'}{[4(m-l)^2 (c/a)^2 + 2 + 4(m-l)(c/a) \cos\alpha - (4(m-l)(c/a) + 2 \cos\theta) \cos\theta' - 2 \sin\theta \sin\theta']} \quad (\text{A-1})$$

Using the trigonometric identity  $\cos(A+B) = \cos A \cos B - \sin A \sin B$  to combine the  $\cos\theta'$  and  $\sin\theta'$  terms, the denominator of the integrand becomes

$$D = r_{m\ell} = s^2 + 1 + 2s \cos(\theta' + \psi) \quad (\text{A-2})$$

where

$$S = (4(m-l)^2 (c/a)^2 + 1 + 4(m-l)(c/a) \cos\alpha)^{\frac{1}{2}} \quad (\text{A-3a})$$

$$\psi = \left\{ \begin{array}{l} \pi - \tan^{-1} \frac{\sin\alpha}{2(m-l)(c/a) + \cos\theta} \quad , (m-l) = 1, 2, \dots \\ \tan^{-1} \frac{-\sin\theta}{2(m-l)(c/a) + \cos\theta} \quad , (m-l) = -1, -2, \dots \end{array} \right\} \quad (\text{A-3b})$$

The principal value of  $\tan^{-1}$  is used in (A-3b). The quantities  $s$  and  $\psi$  are identified with the geometry of the system in Fig. A-1. Applying standard trigonometric identities the numerator of the integrand is expanded, giving

$$N = \frac{1}{2} \left\{ -A \cos[(p-l)(\theta' + \psi)] + B \cos[p(\theta' + \psi)] - C \cos[(p+l)(\theta' + \psi)] - E \sin[(p-l)(\theta' + \psi)] + F \sin[p(\theta' + \psi)] - G \sin[(p+l)(\theta' + \psi)] \right\} \quad (\text{A-4})$$

where

$$A = \cos(\theta - (p-1)\psi) \tag{A-5a}$$

$$B = 2(1 + 2(m-l)(c/a) \cos\alpha) \cos(p\psi) \tag{A-5b}$$

$$C = \cos(\theta + (p+1)\psi) \tag{A-5c}$$

$$E = \sin(\theta - (p-1)\psi) \tag{A-5d}$$

$$F = 2(1 + 2(m-l)(c/a) \cos\alpha) \sin(p\psi) \tag{A-5e}$$

$$G = \sin(\theta + (p+1)\psi) \tag{A-5f}$$

In terms of the new variable  $\xi = (\alpha + \psi)$  equation (A-1) is

$$I(\theta, m-l, p) = \frac{1}{2\pi} \int_{\xi=-\pi}^{\pi} \frac{-A \cos[(p-1)\xi] + B \cos[p\xi] - C \cos[(p+1)\xi] + E \sin[p\xi] - F \sin[(p+1)\xi]}{s^2 + 1 + 2s \cos(\xi)} d\xi \tag{A-6}$$

The  $\sin[(\ )\xi]$  terms integrate to zero and the remaining terms are in the form of a definite integral which is readily evaluated [19, p. 219, 858.536]

$$\int_{\xi=0}^{2\pi} \frac{\cos(p\xi)}{1 + H \cos \xi} d\xi = \begin{cases} \frac{2\pi [\sqrt{1-H^2} - 1]^p}{H^p \sqrt{1-H^2}} & , p = 1, 2, \dots \\ \frac{2\pi}{(1-H^2)^{3/2}} & , p = 0 \end{cases} \tag{A-7}$$

Substituting (A-7) in (A-6) and rearranging,  $I(\theta, m-l, p)$  becomes

$$I(\theta, m-l, p) = \begin{cases} \frac{1}{(1-s^2)(-s)^{p+1}} [As^2 + Bs + C], & p = 1, 2, \dots \\ \frac{-1}{s(1-s^2)} [Bs + 2C], & p = 0 \end{cases} \tag{A-8}$$

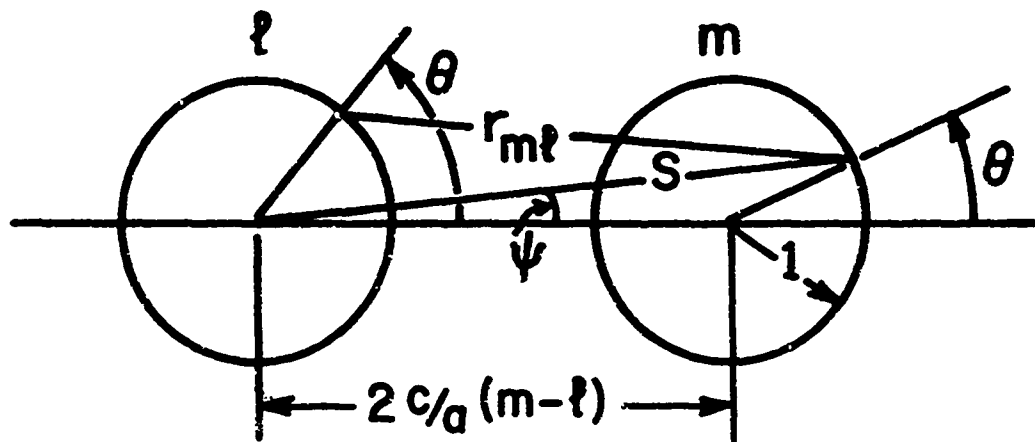


FIG. A-1

## Appendix B

## Listings of Computer Programs

This appendix contains two computer programs written in Fortran IV language for use on the I. B. M. 360/65 computer. Both programs compute the coefficients  $a_{mp}$  of the trigonometric series for the normalized surface current densities,  $g_m$ , and the normalized resistance per unit length,  $R/R_0$ . The input/output formats for both programs are identical and specify the following parameters: the number of conductors  $n$ , the number of harmonics  $q$ , and the spacing  $c/a$ .

Preceding page blank

```

C FORTRAN IV PROGRAM FOR SOLUTION BY THE METHOD OF COLLOCATION
C
C
C THIS PROGRAM USES THE METHOD OF COLLOCATION TO SOLVE A SYSTEM OF EQUATIONS
C FOR THE COEFFICIENTS OF TRIGONOMETRIC SERIES. THE SERIES REPRESENT THE
C NORMALIZED SURFACE CURRENT DENSITY ON EACH WIRE IN A SYSTEM OF NW EQUALLY
C SPACED, PARALLEL, PERFECTLY CONDUCTING WIRES. USING THIS CURRENT AN
C APPROXIMATE VALUE OF THE NORMALIZED HIGH FREQUENCY RESISTANCE OF THE SYSTEM
C IS CALCULATED. THE NUMBER OF HARMONIC TERMS USED TO DESCRIBE THE CURRENT ON
C EACH WIRE IS NH. THE RATIO CA IS EQUIVALENT TO THE SPACING BETWEEN WIRE
C CENTERS DIVIDED BY THE WIRE DIAMETER. FOR NW WIRES AND NH HARMONICS THE
C SIZE OF THE MATRIX T(I,J) MUST BE AT LEAST AS LARGE AS (NW1*NH+1,NW1*NH)
C WHERE NW1=NW/2 FOR NW EVEN AND NW1=(NW+1)/2 FOR NW ODD.
      LOGICAL LSGLVE
      DOUBLE PRECISION PI,THETA,SEP,CA,SOURCE,T,SWIN
      COMMON THETA,SEP,PI/MATRIX/T(48,49)
      WRITE(6,1)
1  FORMAT(1H1)
      PI=3.14159265358979300
2  READ(5,3) NW,NH,CA
3  FORMAT(11,3X,12,3X,05.3)
      WRITE(6,4) NW,CA,NH
4  FORMAT(//35X11,21H WIRES, SPACING CA=,F6.3,4H', ,12,10H HARMON
      ICS)
      NW20=(2*NW+1+(-1)**(NW+1))/4
      NW2E=(2*NW-1+(-1)**NW)/4
      NSIZE=NW2C*NH
      NAUG=NH*NW20+1
      DO 14 L=1,NH
      NR1=(NW20-1)*NH+L
C SETTING COLLOCATION POINTS
      THETA=PI*(DFLOAT(L))/(DFLOAT(NH+1))
      IF(2*(NH/2).NE.NH.AND.L.LE.(NH+1)/2) THETA=PI*FLOAT(L)/FLOAT(NH+2)
      IF(2*(NH/2).NE.NH.AND.L.GT.(NH+1)/2) THETA=PI*FLUAT(L+1)/FLUAT(NH+
      L2)
      DO 14 P=L,NR1,NH
      NRW=1+(M-L)/NH
      IF (NW20.EQ.NW2E) GO TO 5
      IF (NRW.EQ.NW20) THETA=THETA/2.000
5  NSW=1
      N1=NH
      DO 14 N=1,NAUG
      IF (N.EQ.NAUG) GO TO 11
      IF (N-N1) 7,7,6
6  N1=N1+NH
      NSW=NSW+1
7  NSH=N-NH*(NSW-1)
      IF (NRW.EQ.NSW) GO TO 9
      SEP=CA*DFLOAT(NSW-NRW)
      IF ((2*NSW).EQ.(NW+1)) GO TO 8
      T(M,N)=-SWIN(NSH)
      SEP=CA*DFLOAT(NH+1-NSW-NRW)
      T(M,N)=T(M,N)-(-1.000)**NSH*SWIN(NSH)
      GO TO 14
8  T(M,N)=-SWIN(2*NSH)
      GO TO 14
9  IF ((2*NSW).EQ.(NW+1)) GO TO 10
      SEP=CA*DFLOAT(NH+1-2*NRW)
      T(M,N)=(DCOS(DFLOAT(NSH)*THETA))/2.000-(-1.000)**NSH*SWIN(NSH)

```

```

      GO TO 14
10  T(M,N)={DCOS(CFLOAT(2*NSH)*THETA)}/2.000
      GO TO 14
11  SOURCE=0.000
      NSELFH=0
      DO 12 LD1=1,NW2E
          SEP=CA*CFLOAT(NW+1-LD1-NRW)
          SOURCE=SOURCE+SWIN(NSELFH)
12  CONTINUE
      DO 13 LD2=1,NW2O
          IF (LD2.EQ.NRW) GO TO 13
          SEP=CA*CFLOAT(LD2-NRW)
          SOURCE=SOURCE+SWIN(NSELFH)
13  CONTINUE
      T(M,N)=SOURCE
14  CONTINUE
15  IF(LSOLVE(NSIZE)) GO TO 24
C   CALCULATING THE NORMALIZED RESISTANCE
      RESN=1.0
      NCS=NW2E*NH
      DO 16 NC=1,NCS
          RESN=RESN+((T(NC,NAUG))**2)/FLCAT(NW)
16  CONTINUE
      IF (NW2O.EQ.NW2E) GO TO 18
      NDB=NCS+1
      DO 17 ND=ND0,NSIZE
          RESN=RESN+((T(NC,NAUG))**2)/FLCAT(2*NW)
17  CONTINUE
18  WRITE(6,19) RESN
19  FORMAT(/40X23H NORMALIZED RESISTANCE ,F7.4)
      WRITE(6,20)
20  FORMAT(/40X31H-THE HARMONIC COEFFICIENTS ARE-)
      DO 23 L=1,NW2C
          M=NH*(L-1)+1
          N=NH*L
          WRITE(6,21) L
21  FORMAT(51X6H WIRE ,I1)
          WRITE(6,22) (T(I,NAUG),I=M,N)
22  FORMAT (5X,12F10.5)
23  CONTINUE
      GO TO 26
24  WRITE(6,25)
25  FORMAT(/53H THE T MATRIX IS SINGULAR. NO UNIQUE SOLUTION EXISTS.)
26  GO TO 2
27  STOP
      END
C   THIS FUNCTION SUBROUTINE EVALUATES THE ANALYTIC EXPRESSION FOR THE DEFINITE
C   INTEGRAL SWIN.
      DOUBLE PRECISION FUNCTION SWIN(IHAR)
      DOUBLE PRECISION THETA,SEP,PI,T,CA,PSI,H,B,C,E,G
      COMMON THETA,SEP,PI
50  IF (SEP) 51,55,52
51  PSI=DATAN(DSIN(THETA)/(-2.000*SEP-DCOS(THETA)))
      GO TO 53
52  PSI=PI-DATAN(DSIN(THETA)/(2.000*SEP+DCOS(THETA)))
53  S=DSQRT(4.000*(SEP)**2-1.000+4.000*SEP*DCOS(THETA))
      A=0.500*DCOS(THETA-PSI*DFLOAT(IHAR-1))
      B=(1.000+2.000*SEP*DCOS(THETA))*DCOS(PSI*DFLOAT(IHAR))
      C=0.500*DCOS(THETA+PSI*DFLOAT(IHAR+1))
      IF (IHAR.EQ.0) GO TO 54
      SWIN=(A*(S**2)+B*S+C)/((1.000-S**2)*(-S)**(IHAR+1))

```

100

```
GO TO 55
54 SUM=(E+S*2.000000)/(S*51.000-S*021)
55 RETURN
END

C THIS FUNCTION SUBROUTINE SOLVES A SYSTEM OF N LINEAR EQUATIONS IN N UNKNOWN
E BY USING GAUSSIAN ELIMINATION WITH COLUMN PIVOTING.
LOGICAL FUNCTION LSOLVE(N)
DOUBLE PRECISION SEP,PI,T,SUM,TEMP,TOLER
COMMON /MATRIX/II(40,40)

60 SUM=0.000
DO 61 I=1,N
DO 61 J=1,N
61 SUM=SUM+ABS(II(I,J))
TOLER=(SUM/DFLOAT(N)**2)*1.0E-12
NPI=N-1
NM=N-1
DO 66 K=1,NPI
KPI=K+1
TEMP=ABS(T(K,K))
ITEMP=K
DO 62 I=KPI,N
IF (ABS(T(I,K))>.LE.TEMP) GO TO 62
TEMP=ABS(T(I,K))
ITEMP=I
62 CONTINUE
IF (ITEMP>.LE.TOLER) GO TO 70
IF (ITEMP<EQ.K) GO TO 64
DO 63 I=K,NPI
TEMP=T(K,I)
T(K,I)=T(ITEMP,I)
63 T(ITEMP,I)=TEMP
DO 65 I=KPI,N
T(I,K)=T(I,K)/T(K,K)
DO 65 J=KPI,NPI
65 T(I,J)=T(I,J)-T(I,K)*T(K,J)
66 CONTINUE
IF (ABS(T(N,N))>.LE.TOLER) GO TO 70
T(N,NPI)=T(N,NPI)/T(N,N)
DO 66 I=1,NM:
K=N-I
DO 67 J=1,I
L=NPI-J
67 T(K,NPI)=T(K,NPI)-T(K,L)*T(L,NPI)
68 T(K,NPI)=T(K,NPI)/T(K,K)
69 LSOLVE=.FALSE.
GO TO 71
70 LSOLVE=.TRUE.
71 RETURN
END
```

```

C FORTRAN IV PROGRAM FOR SOLUTION BY THE METHOD OF LEAST SQUARES
C
C
C THIS PROGRAM USES THE METHOD OF LEAST SQUARES TO SOLVE A SYSTEM OF EQUATIONS
C FOR THE COEFFICIENTS OF TRIGONOMETRIC SERIES. THE SERIES REPRESENT THE
C NORMALIZED SURFACE CURRENT DENSITY ON EACH WIRE IN A SYSTEM OF NW EQUALLY
C SPACED, PARALLEL, PERFECTLY CONDUCTING WIRES. USING THIS CURRENT AN
C APPROXIMATE VALUE OF THE NORMALIZED HIGH FREQUENCY RESISTANCE OF THE SYSTEM
C IS CALCULATED. THE NUMBER OF HARMONIC TERMS USED TO DESCRIBE THE CURRENT ON
C EACH WIRE IS NH. THE RATIO CA IS EQUIVALENT TO THE SPACING BETWEEN WIRE
C CENTERS DIVIDED BY THE WIRE DIAMETER. FOR NW WIRES AND NH HARMONICS THE
C SIZE OF THE MATRIX T(I,J) MUST BE AT LEAST AS LARGE AS T(NW1*NH+1,NW1*NH)
C WHERE NW1=NW/2 FOR NW EVEN AND NW1=(NW+1)/2 FOR NW ODD.
  LOGICAL LSOLVE
  EXTERNAL F1,F2,F3,F4,F5
  COMMON PI,CA,SEPSIM,SEPMUT,SEPMIM/MATRIX/T(20,29)//NW20,NW2E,NRW,J
  1,NSWH,NSWH2,NW
  WRITE(6,1)
  1 FORMAT(1H1)
  PI=3.141593
  2 READ(5,3) NW,NH,CA
  3 FORMAT(11,3X,12,3X,F5.3)
  WRITE(6,4)NW,CA,NH
  4 FORMAT(///35X11,21H WIRES, SPACING CA=,F6.3,4H, ,12,10H HARMON
  1ICS)
  NW20=(2*NW+1+(-1)**(NW+1))/4
  NW2E=(2*NW-1+(-1)**NW)/4
  NSIZE=NW20*NH
  NAUG=NSIZE+1
  DO 10 NRW=1,NW20
  SEPSIM=CA*FLOAT(NW+1-2*NRW)
  DO 10 J=1,NH
  NRW=(NRW-1)*NH+J
  DO 9 NSW=1,NW20
  SEPMUT=CA*FLOAT(NSW-NRW)
  SEPMIM=CA*FLUAT(NW+1-NSW-NRW)
  DO 9 NSWH=1,NH
  NSWH2=2*NSWH
  NCOL=(NSW-1)*NH+NSWH
  DEL=0.0
  J1=J
  IF(NW20.NE.NW2E.AND.NRW.EQ.NW20) J1=2*J1
  IF(J.EC.NSWH) DEL=PI/8.0
  IF(NRW.EQ.NW20.AND.NW2E.NE.NW20) GO TO 7
  IF(NRW.EQ.NSW) GO TO 6
  IF(NSW.EQ.NW20.AND.NW2E.NE.NW20) GO TO 5
  T(NRCW,NCOL)=-ALSQI(J,NSWH,F1)
  GO TO 9
  5 T(NRCW,NCOL)=-ALSQI(J,NSWH2,F2)
  GO TO 9
  6 T(NRCW,NCOL)=DEL-0.5*ALSQI(J,NSWH,F3)
  GO TO 9
  7 IF(NRW.EQ.NSW) GO TO 8
  T(NRCW,NCOL)=-0.5*ALSQI(J1,NSWH,F4)
  GO TO 9
  8 T(NRCW,NCOL)=DEL
  9 CONTINUE
  T(NRCW,NAUG)=ALSQI(J1,J,F5)
  10 CONTINUE

```

102

```
IF(LSOLVE(NSIZE)) GO TO 19
WRITE(6,11)
11 FORMAT(/40X31H-THE HARMONIC COEFFICIENTS ARE-)
DO 14 L=1,NW20
M=NH*(L-1)+1
N=NH*L
WRITE(6,12) L
12 FORMAT(21X6H WIRE ,11)
WRITE(6,13) (T(I,NAUG),I=M,N)
13 FORMAT(5X,12F10.5)
14 CONTINUE
C CALCULATING THE NORMALIZED RESISTANCE
RESN=1.0
NCS=NH2E*NH
DO 15 NC=1,NCS
RESN=RESN+((T(NC,NAUG))**2)/FLCAT(NH)
15 CONTINUE
IF(NH2E.EQ.NW20) GO TO 17
NCS=NCS+1
DO 16 ND=NCS,NSIZE
RESN=RESN+((T(ND,NAUG))**2)/FLCAT(2*NH)
16 CONTINUE
17 WRITE(6,18) RESN
18 FORMAT(/40X23H NORMALIZED RESISTANCE ,F7.4)
GO TO 21
19 WRITE(6,20)
20 FORMAT(/53H THE T MATRIX IS SINGULAR. NO UNIQUE SOLUTION EXISTS.)
21 GO TO 2
22 STOP
END)
C THIS FUNCTION SUBROUTINE EVALUATES THE DEFINITE INTEGRALS WHICH ARISE IN THE
C ELEMENTS OF THE MATRIX T.
FUNCTION ALSQI(J,NSWH,F)
EXTERNAL F1,F2,F3,F4,F5
COMMON PI
MP=MAX0(J,NSWH)
THETA1=0.0
THETA2=PI/(2.0*FLOAT(MP))
THETA3=PI-THETA2
DTHETA=2.0*THETA2
ALSQI=0.0
DO 30 IP=1,MP
ALSQI=ALSQI+GAUSS6(THETA1,THETA2,F)
THETA1=THETA2
30 THETA2=THETA2+DTHETA
ALSQI=ALSQI+GAUSS6(THETA3,PI,F)
RETURN
END
C F1, F2, F3, F4 AND F5 ARE AUXILIARY FUNCTION SUBROUTINES USED TO SIMPLIFY THE
C INTEGRANDS OF THE DEFINITE INTEGRALS WHICH ARE EVALUATED NUMERICALLY.
FUNCTION F1(THETA)
COMMON PI,CA,SEPSIM,SEPMUT,SEPMIM,NW20,NW2E,NRW,J,NSWH,NSWH2,NW
F1=(0.5*CCS(FLOAT(J)*THETA)-(-1.0)**J*SINTGL(THETA,SEPSIM,J))*(SIN
1 IGL(THETA,SEPMUT,NSWH) +(-1.0)**NSWH*SINTGL(THETA,SEPMIM,NSWH))
RETURN
END
FUNCTION F2(THETA)
COMMON PI,CA,SEPSIM,SEPMUT,SEPMIM,NW2C,NW2E,NRW,J,NSWH,NSWH2,NW
F2=(0.5*CCS(FLOAT(J)*THETA)-(-1.0)**J*SINTGL(THETA,SEPSIM,J))*(SIN
1 IGL(THETA,SEPMUT,NSWH2))
RETURN
```

```

END
FUNCTION F3(THETA)
COMMON PI,CA,SEPSIM,SEPMUT,SEPPIM,NW20,NW2E,NRW,J,NSWH,NSWH2,NW
F3=(-1.0)**J*SINTGL(THETA,SEPSIM,J)*COS(FLOAT(NSWH)*THETA)+(-1.0)*
1*NSWH*SINTGL(THETA,SEPSIM,NSWH)*COS(FLOAT(J)*THETA)-2.0*(-1.0)**(J
1+NSWH)*SINTGL(THETA,SEPSIM,J)*SINTGL(THETA,SEPSIM,NSWH)
RETURN
END
FUNCTION F4(THETA)
COMMON PI,CA,SEPSIM,SEPMUT,SEPPIM,NW20,NW2E,NRW,J,NSWH,NSWH2,NW
F4=COS(2.0*FLCAT(J)*THETA)*(SINTGL(THETA,SEPMUT,NSWH)+(-1.0)**NSWH
1*SINTGL(THETA,SEPPIM,NSWH))
RETURN
END
FUNCTION F5(THETA)
COMMON PI,CA,SEPSIM,SEPMUT,SEPPIM,NW20,NW2E,NRW,J,NSWH,NSWH2,NW
ZERU=0.0
NULL=0
F5=ZERU
DO 40 K=1,NW2E
SEPMUT=CA*FLOAT(K-NRW)
SEPPIM=CA*FLOAT(NW+1-K-NRW)
IF(K.EQ.NRW) GO TO 40
F5=F5+SINTGL(THETA,SEPMUT,NULL)+SINTGL(THETA,SEPPIM,NULL)
40 CONTINUE
SEPMUT=CA*FLOAT(NW20-NRW)
IF(NW20.NE.NW2E.AND.NRW.NE.NW20) F5=(F5+SINTGL(THETA,SEPMUT,NULL)+
1SINTGL(THETA,SEPSIM,NULL))*(0.5*CCS(FLOAT(J)*THETA)-(-1.0)**J*SINT
1GL(THETA,SEPSIM,J))
IF(NW20.EQ.NW2E) F5=(F5+SINTGL(THETA,SEPSIM,NULL))*(0.5*COS(FLOAT(
1J)*THETA)-(-1.0)**J*SINTGL(THETA,SEPSIM,J))
IF(NW20.NE.NW2E.AND.NRW.EQ.NW20) F5=F5*(0.5*COS(FLOAT(J)*2.0*THETA
1))
RETURN
END
C THIS FUNCTION SUBROUTINE EVALUATES THE ANALYTIC EXPRESSION FOR THE DEFINITE
C INTEGRAL SINTGL.
FUNCTION SINTGL(THETA,SEP,IHAR)
COMMON PI
50 IF (SEP) 51,55,52
51 PSI=ATAN(SIN(THETA)/(-2.0*SEP-COS(THETA)))
GO TO 53
52 PSI=PI-ATAN(SIN(THETA)/(2.0*SEP+COS(THETA)))
53 S=SQRT(4.0*(SEP)**2+1.0+4.0*SEP*COS(THETA))
A=0.5*CCS(THETA-PSI*FLUAT(IHAR-1))
B=(1.0+2.0*SEP*COS(THETA))*COS(PSI*FLUAT(IHAR))
C=0.5*CCS(THETA+PSI*FLUAT(IHAR+1))
IF (IHAR.EQ.0) GO TO 54
SINTGL=(A*(S**2)+B*S+C)/((1.0-S**2)*(-S)**(IHAR+1))
GO TO 55
54 SINTGL=-{(B*S+2.0*C)/(S*(1.0-S**2))}
55 RETURN
END
C GAUSS6 IS A FUNCTION SUBROUTINE WHICH COMPUTES AN APPROXIMATE VALUE OF THE
C INTEGRAL OF F(X) OVER THE INTERVAL FROM X=XL TO X=XU. EVALUATION IS DONE BY
C MEANS OF A 6- POINT GAUSS QUADRATURE FORMULA.
FUNCTION GAUSS6(XL,XU,F)
A=.5*(XU+XL)
B=XU-XL
C=.4662348*B
GAUSS6=.08566225*(F(A+C)+F(A-C))

```

```

C=.3306047*B
GAUSS6=GAUSS6+.1803808*(F(A+C)+F(A-C))
C=.1193096*B
GAUSS6=B*(GAUSS6+.2339570*(F(A+C)+F(A-C)))
RETURN
END

```

C THIS FUNCTION SUBROUTINE SOLVES A SYSTEM OF N LINEAR EQUATIONS IN N UNKNOWNNS  
L BY USING GAUSSIAN ELIMINATION WITH COLUMN PIVOTING.

```

LOGICAL FUNCTION LSOLVE(N)
COMMON /MATRIX/A(28,24)
60 SUM=0.0
DO 61 I=1,N
DO 61 J=1,N
61 SUM=SUM+ABS(A(I,J))
TOLER=(SUM/FLGAT(N)**2)*1.0E-6
NPI=N+1
NMI=N-1
DO 66 K=1,NMI
KPI=K+1
TEMP=ABS(A(K,K))
ITEMP=K
DO 62 I=KPI,N
IF (ABS(A(I,K)).LE.TEMP) GO TO 62
TEMP=ABS(A(I,K))
ITEMP=I
62 CONTINUE
IF (TEMP.LE.TOLER) GO TO 70
IF (ITEMP.EQ.K) GO TO 64
DO 63 I=K,NPI
TEMP=A(K,I)
A(K,I)=A(ITEMP,I)
63 A(ITEMP,I)=TEMP
64 DO 65 I=KPI,N
A(I,K)=A(I,K)/A(K,K)
DO 65 J=KPI,NPI
65 A(I,J)=A(I,J)-A(I,K)*A(K,J)
66 CONTINUE
IF (ABS(A(N,N)).LE.TOLER) GO TO 70
A(N,NPI)=A(N,NPI)/A(N,N)
DO 68 I=1,NMI
K=N-I
DO 67 J=1,I
L=NPI-J
67 A(K,NPI)=A(K,NPI)-A(K,L)*A(L,NPI)
68 A(K,NPI)=A(K,NPI)/A(K,K)
69 LSOLVE=.FALSE.
GO TO 71
70 LSOLVE=.TRUE.
71 RETURN
END

```

Appendix C

Evaluation of the Integral  $I'(\theta, m-1, p)$

$$I'(\theta, m-1, p) = \frac{1}{\pi} \int_{\alpha' = -\pi}^{\pi} \frac{[1 + 2(m-1)(c/a) \cos \alpha - (\cos \theta \cos \alpha') + \sin \alpha \sin \theta'] \sin(p\theta') d\alpha'}{[4(m-1)^2 (c/a)^2 + 2 + 4(m-1)(c/a) \cos \alpha - (4(m-1)(c/a) + 2 \cos \alpha) \cos \alpha' - 2 \sin \alpha \sin \alpha']} \quad (C-1)$$

The evaluation of  $I'(\alpha, m-1, p)$  closely follows that for  $I(\alpha, m-1, p)$  carried out in Appendix A. Using standard trigonometric identities the numerator and denominator of the integrand are rewritten as

$$N = \frac{1}{2} \left\{ -A' \cos[(p-1)(\alpha' + \psi)] + B' \cos[p(\alpha' + \psi)] - C' \cos[(p+1)(\alpha' + \psi)] - E' \sin[(p-1)(\theta' + \psi)] + F' \sin[p(\theta' + \psi)] - G' \sin[(p+1)(\alpha' + \psi)] \right\}$$

$$D = s^2 + 1 + 2s \cos(\theta' + \psi) \quad (C-2)$$

where

$$A' = \sin(\alpha - (p-1)\psi) \quad (C-2a)$$

$$B' = -2(1 + 2(m-1)(c/a) \cos \alpha) \sin(p\psi) \quad (C-2b)$$

$$C' = -\sin(\theta + (p+1)\psi) \quad (C-2c)$$

$$E' = \cos(\xi - (p-1)\psi) \quad (C-2d)$$

$$F' = 2(1 + 2l \cos \theta) \cos(p\psi) \quad (C-2e)$$

$$G' = \cos(\alpha + (p+1)\psi) \quad (C-2f)$$

$$s = s^2 + 1 + 2s \cos(\theta' + \psi) \quad (C-3a)$$

$$\psi = \left\{ \begin{array}{l} \pi - \tan^{-1} \left( \frac{\sin \theta}{2(m-l)(c/a) + \cos \theta} \right), \quad (m-l) = 1, 2, \dots \\ \tan^{-1} \left( \frac{-\sin \theta}{2(m-l)(c/a) + \cos \theta} \right), \quad (m-l) = -1, -2, \dots \end{array} \right\} \quad (C-3b)$$

The principle value of  $\tan^{-1}$  is used in (C-3b).

With equations (C-2), (C-3) and the new variable  $\xi = (\alpha' + \psi)$

(C-1) becomes

$$I'(\alpha, m-l, p) = \frac{1}{2\pi} \int_{\xi=-\pi}^{\pi} \frac{-A \cos[(p-l)\xi] + B \cos[p\xi]}{s^2 + 1 + 2s \cos(\xi)} \underline{- C \cos[(p-l)\xi] + E \sin[p\xi] - F \sin[(p+l)\xi]} da' \quad (C-4)$$

The  $\sin[(\ )\xi]$  terms integrate to zero and the remaining terms

are in the form of a definite integral which is evaluated in Appendix .

A, equation (A-7). With these integrations performed  $I'(\alpha, m-l, p)$  is

$$I'(\alpha, m-l, p) = \frac{1}{(1-s^2)(-s)^{p+1}} [A's^2 + B's + C'], \quad p = 1, 2, \dots \quad (C-5)$$

107

## Appendix D

### Listing of Computer Program

This appendix contains a computer program written in Fortran IV language for use on the I. B. M. 360/65 computer. The program computes the coefficients  $a_{mcp}$  and  $b_{mcp}$  of the trigonometric series for the normalized correction current densities  $g_{mc}$ .

108

```

C FORTRAN IV PROGRAM FOR CALCULATING THE CURRENT DISTRIBUTIONS CAUSED
C BY INTERCONNECTING WIRES IN THE EXPERIMENTAL MODEL.
C
C THIS PROGRAM USES THE METHOD OF COLLOCATION TO SOLVE A SYSTEM OF
C EQUATIONS FOR THE COEFFICIENTS OF TRIGONOMETRIC SERIES. THE SERIES
C REPRESENT THE NORMALIZED SURFACE CURRENT DENSITY ON EACH WIRE IN
C SYSTEM OF NW WIRES. THE NUMBER OF HARMONIC TERMS USED TO DESCRIBE
C THE CURRENT ON EACH WIRE IS NH. THE RATIO CA IS EQUIVALENT TO THE
C SPACING BETWEEN WIRE CENTERS DIVIDED BY THE WIRE DIAMETER. THE
C NORMALIZED DIMENSIONS CAH2 AND CHL2 ARE THE TUBE RADIUS DIVIDED BY
C THE TUBE HALF HEIGHT AND THE TUBE HALF HEIGHT DIVIDED BY THE LENGTH
C OF THE INTERCONNECTING WIRES.
C LOGICAL LINECN
COMMON THETA,SEP,PI/MATRIX/A(36,37)
WRITE(6,1)
1 FORMAT(1+1)
PI=3.141593
CAH2=0.0+8645
CHL2=0.3+0824
2 READ(5,3) NW,NH,CA
3 FORMAT(11,3X,12,3X,F5.3)
WRITE(6,4) NW,CA,NH
4 FORMAT(//35X11,21H WIRES, SPACING CA=,F5.3,4H, ,12,10H HARMON
1ICS)
NW21=(2*NW+1+(-1)**(NW+1))/4
NW2=(2*NW-1+(-1)**NW)/4
NSIZE=NW21*NH
NAUG=NH*NW21+1
DO 17 L=1,NH
NR1=(NW21-1)*NH+L
C SETTING COLLOCATION POINTS
THETA=PI*2.0*(FLOAT(L))/(FLOAT(NH+1))
DO 17 M=L,NR1,NH
NRW=1+(M-L)/NH
IF (NW21.EQ.NW2) GO TO 5
IF(NRW.EQ.NW21) THETA=(THETA-PI)/2.0
IF(THETA.LE.0.0) THETA=2.0*PI+THETA
5 NSW=1
N1=NH
DO 17 N=L,NAUG
IF (N.EQ.NAUG) GO TO 15
IF (N-N1) 7,7,6
6 N1=N1+NH
NSW=NSW+1
7 NSH=N-NH*(NSW-1)
IF(N.EQ.2*(N/2)) NSH=NSH/2
IF(N.EQ.2*(N/2)) NSH=(NSH+1)/2
IF (NRW.EQ.NSW) GO TO 11
SEP=CA*FLOAT(NSW-NRW)
IF ((2*NSW).EQ.(NW+1)) GO TO 9
IF(2*(N/2).EQ.N) GO TO 8
A(M,N)=-A1NE(NSH)
SEP=CA*FLOAT(NW+1-NSW-NRW)
A(M,N)=A(M,N)-(-1.0)**NSH*A1NE(NSH)
GO TO 17
8 A(M,N)=-A1NES(NSH)
SEP=CA*FLOAT(NW+1-NSW-NRW)
A(M,N)=A(M,N)+(-1.0)**NSH*A1NES(NSH)

```

```

GO TO 17
9 IF(2*(N/2).EQ.%) GO TO 10
  A(M,N)=-AINE(2*NSH)
  GO TO 17
10 A(M,N)=-AINES(2*NSH-1)
  GO TO 17
11 IF ((2*NSH).EQ.(NH+1)) GO TO 13
  SEP=CA*FLOAT(NH+1-2*NRW)
  IF(2*(N/2).EQ.N) GO TO 12
  A(M,N)=(COS(FLJAT(NSH)*THETA))/2.0-(-1.0)**NSH*AINE(NSH)
  GO TO 17
12 A(M,N)=(SIN(FLOAT(NSH)*THETA))/2.0+(-1.0)**NSH*AINES(NSH)
  GO TO 17
13 IF(2*(N/2).EQ.N) GO TO 14
  A(M,N)=(COS(FLOAT(2*VSH)*THETA))/2.0
  GO TO 17
14 A(M,N)=(SIN(FLOAT(2*VSH-1)*THETA))/2.0
  GO TO 17
15 SOURCE=0.0
  DO 16 LD1=1,NW
  SEP=CA*FLJAT(LD1-NRW)
  SOURC1 = (CAH2/SQRT(1.0+(CHL2)**2+4.0*(SEP*CAH2*CHL2)**2))*((C
  HL2)**2*(SIN(THETA)-2.0*SEP*CAH2*CHL2*COS(THETA))/(1.0+4.0*(SEP*CA
  H2*CHL2)**2)+SIN(THETA)/(1.0+4.0*(SEP*CAH2)**2))-((1.0+2.0*SEP*COS
  1(THETA))/(1.0+4.0*SEP**2+4.0*SEP*COS(THETA)))*(1.0-1.0/SQRT(1.0+4.
  10*(CAH2)**2*SEP**2))
  SOURCE=SOURCE+SOURC1
16 CONTINUE
  A(M,N)=SOURCE
17 CONTINUE
18 IF (LINEJN(NSIZE)) GO TO 23
  WRITE(6,19)
19 FORMAT(/'OX31H-THE HARMONIC COEFFICIENTS ARE-')
  DO 22 L=1,NW21
  M=NH*(L-1)+1
  N=NH*L
  WRITE(6,20) L
20 FORMAT(51X6H WIRE ,11)
  WRITE(6,21)(A(I,NAUG),I=M,N)
21 FORMAT(5X,12F10.5)
22 CONTINUE
  GO TO 25
23 WRITE(6,24)
24 FORMAT(/'53H THE A MATRIX IS SINGULAR. NO UNIQUE SOLUTION EXISTS. ')
25 GO TO 2
26 STOP
  END
C THIS FUNCTION SUBROUTINE EVALJATES THE ANALYTIC EXPRESSION FOR THE
C DEFINITE INTEGRAL AINE.
  FUNCTION AINE(IHAR)
  COMMON THETA,SEP,PI/MATRIX/A(36,37)
50 IF(SEP) 51,54,52
51 IF(THETA.LE.PI) PSI=-ATAN(SIN(THETA)/(-2.0*SEP-COS(THETA)))
  IF(THETA.GE.PI) PSI=ATAN(-SIN(THETA)/(-2.0*SEP-COS(THETA)))
  GO TO 53
52 IF(THETA.LE.PI) PSI=PI+ATAN(SIN(THETA)/(2.0*SEP+COS(THETA)))
  IF(THETA.GE.PI) PSI=PI-ATAN(-SIN(THETA)/(2.0*SEP+COS(THETA)))
53 H=(1.0+2.0*SEP*COS(THETA))*COS(PSI*FLOAT(IHAR+1))
  B=-0.5*CJS(THETA-PSI*FLOAT(IHAR+1))
  C=-0.5*CJS(THETA+PSI*FLOAT(IHAR-1))
  E=4.0*(SEP)**2+2.0+4.0*SEP*COS(THETA)

```

```

F=(2.0*(E-1.0)**0.5)/E
G=((1.0-F**2)**0.5-1.0)/F
AINE=(G**2*(IHAR-1))*(H*G+B*(G**2)+C)/(E*((1.0-F**2)**0.5))
54 RETURN
END
C THIS FUNCTION SUBROUTINE EVALUATES THE ANALYTIC EXPRESSION FOR THE
C DEFINITE INTEGRAL AINES.
FUNCTION AINES(IHAR)
COMMON THETA,SEP,PI/MATRIX/A(36,37)
80 IF(SEP) $1,84,82
81 IF(THETA.LE.PI) PSI=-ATAN(SIN(THETA)/(-2.0*SEP-COS(THETA)))
IF(THETA.GE.PI) PSI=ATAN(-SIN(THETA)/(-2.0*SEP-COS(THETA)))
GO TO 83
82 IF(THETA.LE.PI) PSI=PI+ATAN(SIN(THETA)/(2.0*SEP+COS(THETA)))
IF(THETA.GE.PI) PSI=PI-ATAN(-SIN(THETA)/(2.0*SEP+COS(THETA)))
83 H1=(1.0+2.0*SEP*COS(THETA))*SIN(PSI*FLOAT(IHAR))
B1=-0.5*SIN(PSI*FLOAT(IHAR+1)-THETA)
C1=-0.5*SIN(PSI*FLOAT(IHAR-1)+THETA)
E=4.0*(SEP)**2+2.0+4.0*SEP*COS(THETA)
F=(2.0*(E-1.0)**0.5)/E
G=((1.0-F**2)**0.5-1.0)/F
AINES=(G**2*(IHAR-1))*(H1*G+B1*(G**2)+C1)/(E*((1.0-F**2)**0.5))
84 RETURN
END
C THIS FUNCTION SUBROUTINE SOLVES A SYSTEM OF N LINEAR EQUATIONS IN
C N UNKNOWN BY USING GAUSSIAN ELIMINATION WITH COLUMN PIVOTING.
LOGICAL FUNCTION LINEQN(N)
COMMON THETA,SEP,PI/MATRIX/A(36,37)
80 SUM=0.0
DO 61 I=1,N
DO 61 J=1,N
61 SUM=SUM+A(I,J)
TOLER=(SUM/FLOAT(N)**2)*1.0E-6
NP1=N+1
NM1=N-1
DO 66 K=1,NM1
KP1=K+1
TEMP=ABS(A(K,K))
ITEMP=K
DO 62 I=KP1,N
IF (ABS(A(I,K)).LE.TEMP) GJ TO 62
TEMP=ABS(A(I,K))
ITEMP=I
62 CONTINUE
IF (TEMP.LE.TOLER) GJ TO 70
IF (ITEMP.EQ.K) GO TO 64
DO 63 I=K,NP1
TEMP=A(K,I)
A(K,I)=A(ITEMP,I)
63 A(ITEMP,I)=TEMP
64 DO 65 I=KP1,N
A(I,K)=A(I,K)/A(K,K)
DO 65 J=KP1,NP1
65 A(I,J)=A(I,J)-A(I,K)*A(K,J)
66 CONTINUE
IF(ABS(A(N,N)).LE.TOLER) GJ TO 70
A(N,NP1)=A(N,NP1)/A(N,N)
DO 68 I=1,NM1
K=N-I
DO 67 J=1,I
L=NP1-J
67 A(K,NP1)=A(K,NP1)-A(K,L)*A(L,NP1)
68 A(K,NP1)=A(K,NP1)/A(K,K)
69 LINEQN=.FALSE.
GO TO 71
70 LINEQN=.TRUE.
71 RETURN
END

```

## REFERENCES

- [1] R. W. P. King, Fundamental Electromagnetic Theory, Dover Publications, New York, Chapter 5, 1963.
- [2] S. Ramo, J. R. Whinnery and T. VanDuzer, Fields and Waves in Communication Electronics, John Wiley and Sons, New York, Chapter 5, 1965, pp. 286-303.
- [3] H. A. Wheeler, "Formulas for the Skin Effect", Proc. I. R. E., 30:412-424, 1942.
- [4] A. E. Kennelly, F. A. Laws, and P. H. Pierce, "Experimental Researches on Skin Effect in Conductors", Trans. A. I. E. E., 34: 1953-2018, 1915.
- [5] A. E. Kennelly, H. A. Affel, "Skin-Effect Resistance Measurements of Conductors to 100 Kilocycles", Proc. I. R. E., 4:523-574, 1916.
- [6] J. R. Carson, "Wave Propagation over Parallel Wires: The Proximity Effect", Phil. Mag., Ser. 6, 41:607-633, 1921.
- [7] H. B. Dwight, "Skin Effect and Proximity Effect in Tubular Conductors", Trans. A. I. E. E., 41:189-198, 1922.
- [8] H. B. Dwight, "Proximity Effect in Wires and Thin Tubes", Trans. A. I. E. E., 42: 850-859, 1923.
- [9] S. Butterworth, "Eddy Current Losses in Cylindrical Conductors with Special Application to Alternating-Current Resistance of Short Coils", Phil. Trans. Roy. Soc. (London), 222A: 57-100, 1921.
- [10] S. Butterworth, "On the Alternating Current Resistance of Solenoidal Coils", Proc. Roy. Soc. (London), 107: 693-715, 1925.
- [11] S. Butterworth, "Effective Resistance of Inductive Coils at Radio Frequencies", Experimental Wireless and Wireless Engineer, 3: 203-210, 309-316, 417-424, 483-492, 1926.
- [12] B. B. Austin, "Effective Resistance of Inductive Coils at Radio Frequency", Experimental Wireless and Wireless Engineer, 11: 12-16, 1934.
- [13] F. E. Terman, Radio Engineers Handbook, McGraw Hill, New York, 1943, pp. 74-83.
- [14] E. C. Snelling, Soft Ferrites--Properties and Applications, C. R. C. Press, Cleveland, Ohio, Chapter 11, 1969.

- [15] R. G. Medhurst, "High Frequency Resistance and Self Capacitance of Single-Layer Solenoids", Wireless Engineer, 24, 281: 35-43, 24, 282: 88-92, 1947.
- [16] G. S. Smith, "The Radiation Efficiency of Electrically Small Multiturn Loop Antennas", Technical Report No. 612, Cruft Laboratory, Harvard University, Cambridge, Mass., June, 1976.
- [17] M. Abramowitz and I. A. Stegun, Handbook of Mathematical Functions, Dover Publications, New York, Chapters 16 and 17, 1968.
- [18] A. E. Sanderson, "Effect of Surface Roughness on Propagation of the Transverse Electromagnetic Mode", Thesis, Harvard University, 1969.
- [19] H. B. Dwight, Tables of Integrals and Other Mathematical Data, Macmillan Co., New York, 1961.
- [20] F. J. W. Whipple, "Equal Parallel Cylindrical Conductors in Electrical Problems", Roy. Soc. Proc., A 96: 465-475, 1920.
- [21] H. Poritsky, "The Field Due to Two Equally Charged Parallel Combining Cylinders", J. Math. and Phys., 11: 213-217, 1932.
- [22] E. P. Adams, "Electrical Distributions on Cylindrical Conductors", Ann. Philos. Soc. Proc. (Philadelphia), 75: 11-70, 1935.
- [23] P. M. Morse and H. Feshbach, Methods of Theoretical Physics, McGraw Hill, New York, 1953, pp. 427-433, 485-490, 1233-1243.
- [24] Jahnke, Emde, and Lösch, Tables of Higher Functions, McGraw Hill, New York, Chapter 6, 1960.
- [25] F. B. Hildebrand, Methods of Applied Mathematics, Prentice Hall, Englewood Cliffs, N.J., Chapter 4, Sec. 4.15-4.19, 1952.
- [26] D. G. M. Anderson, Unpublished Lecture Notes for Applied Mathematics 21, Harvard University, 1970.
- [27] I. B. M., System/360 Scientific Subroutine Package, I. B. M., New York, 1968, p. 300.
- [28] R. W. P. King and C. W. Harrison, Jr., Antennas and Waves, M. I. T. Press, Cambridge, Massachusetts, Chapters 9 and 10, 1969.
- [29] R. E. Harrington, Field Computations by Moment Methods, Macmillan Co., New York, 1968.

- [30] T. Padhi, "Theory of Coil Antennas", Radio Science, 69D: 997-1001, 1965.
- [31] G.A. Richards, "Reaction Formulation and Numerical Results for Multiturn Loop Antennas and Arrays", Thesis, Ohio State University, 1976.
- [32] R. W. P. King, Fundamental Electromagnetic Theory, Dover Publications, New York, Chapter 6, 1963.
- [33] R. W. P. King, The Theory of Linear Antennas, Harvard University Press, Cambridge, Massachusetts, Chapter 1, Sec. 7, 1956.
- [34] D. Bierens DeHaar, Nouvelles Tables D'Integrales Defines, G. E. Stechert Co., New York, 1939, p. 89.
- [35] Janke, Emde, and Losch, Tables of Higher Functions, McGraw Hill, New York, 1960, p. 62.
- [36] H.A. Wheeler, "Fundamental Limitations of Small Antennas", I.R.E. Proc., 35: 1479-1484, 1947.
- [37] H. Whiteside and R. W. P. King, "The Loop Antenna as a Probe", I.E.E. Transactions on Antennas and Propagation, May 1964, pp. 291-297.